INERT GAS WELDMENT EFFECTS STUDY

Phase II Report

27 January 1966 — 27 June 1966

D2-23647-5

Welding Development Laboratory

George C. Marshall Space Flight Center
NASA/MSFC
Huntsville, Alabama 35812

Contract NAS 8-20168

Aerospace Group
Quality Control Research Section
THE BOEING COMPANY
Seattle, Washington

PREPARED BY W. Evan Strobelt

APPROVED BY [signature]

APPROVED BY J Mueller

CONTENTS

ILLUSTRATIONS

ILLUSTRATIONS (Cont.)

ILLUSTRATIONS (Cont.)

ILLUSTRATIONS (Cont.)

ABSTRACT

This report describes the work performed in the second phase of a NASA-sponsored program to establish a quantitative relationship between weldment defects and atmospheric contamination in the inert shielding gas medium.

The metal studied in this program was 0.25-inch 2219-T87 aluminum alloy welded in the horizontal position by the tungsten inert gas shielding process. A uniform weld schedule, simulating production conditions, was used for all weldments; the gases (oxygen, nitrogen, hydrogen, and water vapor) were varied from a low level (commercially pure helium) to 1000 parts per million (ppm) according to a statistically designed program plan. The levels of contamination additions were controlled with a time-of-flight mass spectrometer by sampling the shielding gas at the weld cup near the fusion zone.

The quantitative effects of the gas contaminants present in the weld shielding envelope on weldment quality were evaluated in terms of: (1) magnitude, frequency, and distribution of porosity; (2) fatigue life; and (3) tensile properties. Contamination effects were studied with each gas individually and in various combinations.

From the program results it has been determined that all of the gases studied have an effect on weld quality. Hydrogen and water vapor were found to be the major gases contributing to porosity. Nitrogen and oxygen in general did not cause porosity and were found to reduce the effects caused by hydrogen and water vapor under most conditions. The low levels of porosity occurring during contamination-free conditions were not influenced significantly by the addition of nitrogen or oxygen. Results of the mixed-gas reactions were complex and did not necessarily follow the aforementioned trends.

Mathematical relationships were developed for calculation of a weld quality resulting from a specific contamination condition. Quantitative relationships were developed in terms of mass flow of the gas contamination per unit time, per unit quantity of weld material formed. This value was then related to specific weldment characteristics.

Mechanical properties (fatigue and tensile analysis) were related to gas contamination, although quantitative correlations were limited by the sensitivity and repeatability of the two examination methods.

Two additional studies were conducted in Phase II to broaden the scope of the program by determining the effects of: (1) backup gas contamination, and (2) helium flow rate variation on weldment quality. These tests established that neither backup gas nor helim flow-rate changes have significant effects on weldment quality using controlled environmental conditions. The test eliminated the backup gas and helium flow as variables in the program and further identified the contamination problem as related to the production situation.

INTRODUCTION

The production of Aerospace vehicles, such as the Saturn V, has necessitated the improvement of reliability in many of the fabrication processes. Welding of aluminum alloys, one of the most important methods of fabrication, has the problem of achieving the required high reliability, particularly with respect to the reduction and control of porosity in weldments. As a part of the integrated NASA program to quantitatively define welding parameters for ultimate resolution of the aluminum welding problem, Boeing is conducting a study of the role of shielding gas contamination on weldment quality.

The experimental program was designed to simulate gas contamination conditions that would be experienced during production welding. Atmosphere influx and impurities in the helium shielding gas were simulated by the additions of oxygen, nitrogen, and water vapor. Hydrogen was also studied because many gases or materials entering the shielding zone will decompose in the arc and form atomic hydrogen. A standard production weld schedule was established for all weldment test panels with the major variables being the gaseous additions.

The experimental evaluation was geared primarily to the porosity problem. Porosity was evaluated by: (1) radiographic analysis for size, frequency, and distribution, and (2) metallographic and gravimetric methods to determine the actual percentages. In addition, mechanical testing was performed to determine variations in tensile and fatigue properties resulting from the gas/metal reactions.

In Phase I, procedures and experimental methods were established. The results of Phase I are contained in Boeing document D2-23647-4, dated November 1, 1965. Only improvements or variations in experimental or evaluation methods will be included in this report, with the major context being devoted to a description of test results and the conclusion drawn from the program.

This report is presented in five sections: (1) equipment procedures and material preparation; (2) weldment evaluation procedures; (3) statistical program weld specimen evaluation and results; (4) conclusions; and (5) recommendation for additional studies.

EQUIPMENT, PROCEDURES, AND MATERIAL PREPARATION

EXPERIMENTAL TEST EQUIPMENT

The test equipment used to prepare the Phase II weldments is shown in Figure 1. The system (see schematic in Figure 2) included an atmosphere control chamber, a weld control unit, a time-of-flight mass spectrometer, and a gas flow control panel. In operation, a test panel was placed in the weld fixture, the chamber was evacuated and backfilled with helium, the desired impurities were introduced into the backup and weld cup and the weld was made while continuously measuring the contamination levels during the process. Excellent weld quality repeatability was obtained under these carefully controlled environmental conditions.

MATERIAL EVALUATION

The preliminary examination and analysis of the Phase II 2219-T87 aluminum plate is given in the preweld data sheet, Figure 3. A comparison between the Phase I and Phase II materials is given in Figure 4, in which several differences were observed. A preliminary material qualification experiment was conducted with two panels each from Phase I and Phase II materials. One panel was prepared using helium only and one using hydrogen from each of the material lots. These tests indicated that the materials were comparable from a weldability and gas effects standpoint; therefore, it was concluded that the Phase II material was acceptable for use in the program.

TOOLING

An O-ring sealed backing bar design was used throughout the program. In the Phase II study a "tough pitch" copper base bar having the thermal and electrical conductivity of the electrolytic copper previously used in Phase I and the hardness of Mallory 3 grade was used for the contact tooling. The purpose of this change was to reduce tooling deformation caused by clamping pressure and high temperature, while also accelerating the weld bead solidification. A design change in the inlet portion of the backing bar was made to improve the gas flow characteristics at low pressure and reduce the amount of scrapped start-end material.

An improved silicone rubber compound, Dow Corning 1255, which is softer and has higher resistance to temperature and abrasion, was incorporated into the backing bar. Recessed grooves to accommodate copper tubing for water cooling were machined on the outer edges of the bar, on the back side. The purpose of the cooling was to maintain a uniform panel temperature during the welding to reduce undercut occurrence, especially in the last few inches of the weld.

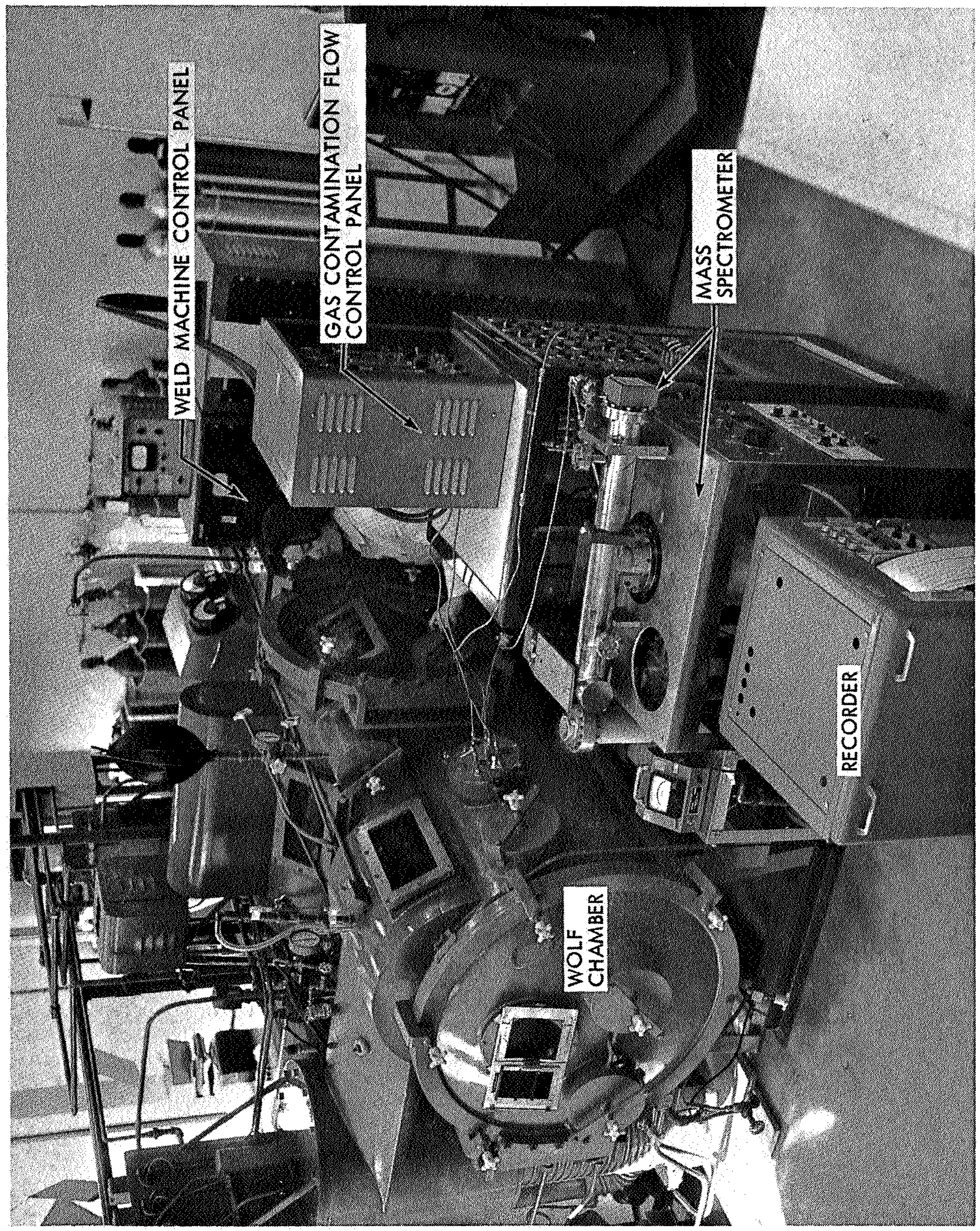

Figure 1: ATMOSPHERIC CONTROL CHAMBER AND ANALYTICAL MEASUREMENT EQUIPMENT

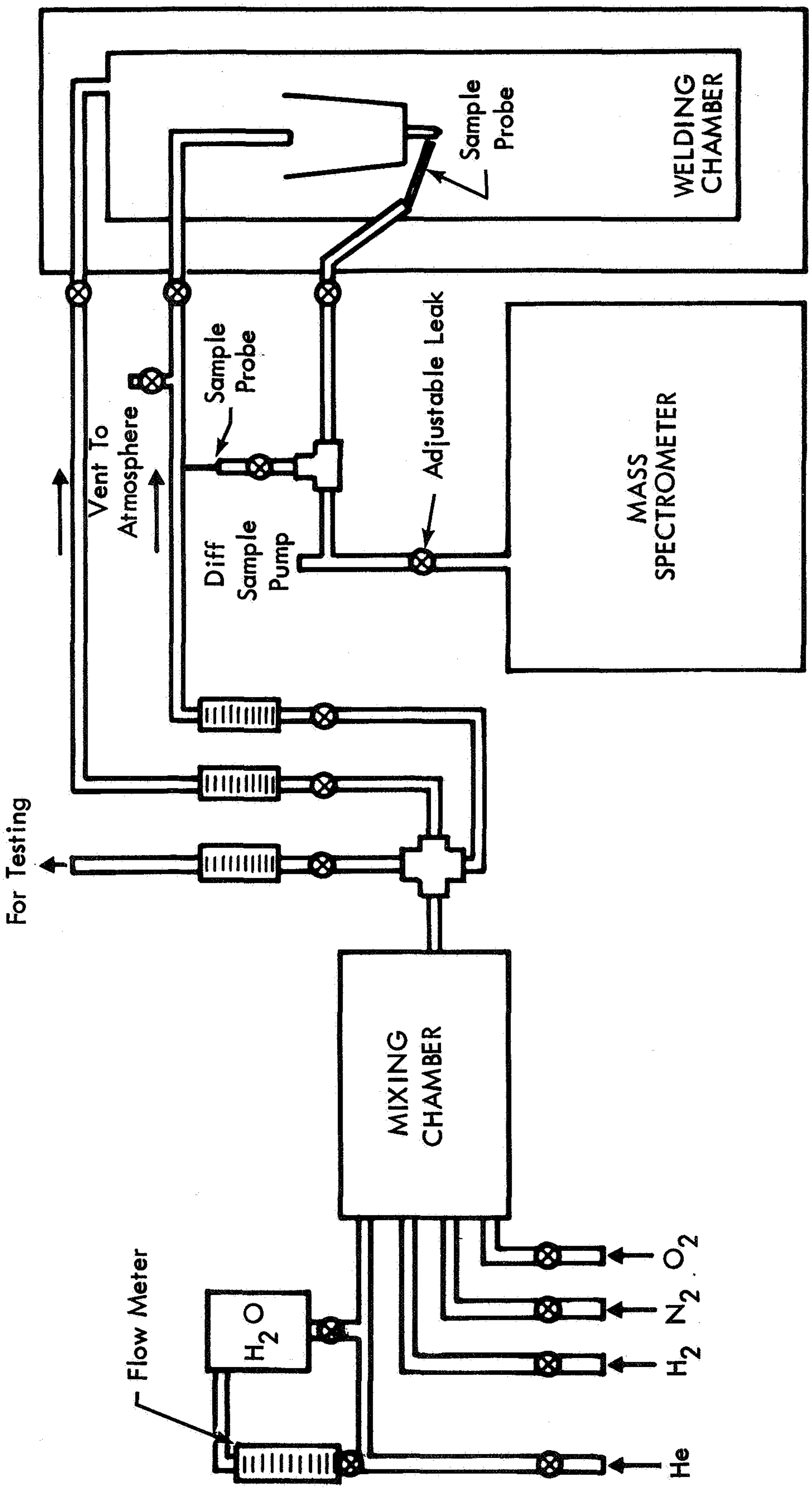

Figure 2 : GAS FLOW CONTROL & MEASUREMENT SYSTEM

PRE-WELD MATERIAL EVALUATION DATA SHEET
(INERT GAS EFFECTS STUDY)

DATE ______
MATERIAL Al 2219-T87
SHEET NO. 8-17
VENDOR REYNOLDS
HEAT # EE51389-1

WELDMENT PANEL CUT PATTERN

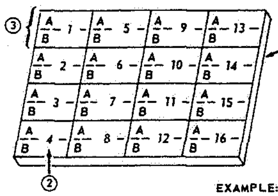

CODE FOR FINISHED WELDMENT PANEL

① ② ③ ④ ⑤
X — XX — XX — XXX — XX

① SHEET NO.
② WELDMENT PANEL NO.
③ MATCHING PAIRS
④ BOEING MFG. CALENDAR DATE
⑤ MFG. SEQUENCE DURING ANY ONE DATE

EXAMPLE: 1-01-717-01 = PANEL NO. 1, FROM SHEET NO. 1, 1ST PANEL WELDED ON 717

CHEMICAL ANALYSIS %

	Plate	Filler Wire
Cu	6.40	5.8 -6.8
Mn	0.32	0.20-0.40
Si	0.11	0.05-0.15
V	0.086	0.20
Zn	0.06	0.10
Ti	0.06	0.10-0.20
Fe	0.18	0.30
Mg	0.012	0.02
Zr	0.14	0.10-0.25
Al	Bal	

METALLURGICAL TEST DATA

ASTM GRAIN SIZE 5-6
MICROHARDNESS R_{HB} 81-82.5
Q.C. Support Lab Report 2-4891-3-204
P.O. N-679600-6843

TENSILE TEST DATA

	LONGITUDINAL TENSILE STRENGTH	TRANSVERSE TENSILE STRENGTH
ULTIMATE	70.3-71.3 KSI	70.9-71.5 KSI
YIELD 0.2% OFFSET	57.4-57.8 KSI	55.7-57.2 KSI
ELONGATION IN 0.5 IN.	16-24%	16-22%
IN 1.0 IN.	15-16.5%	14-16%
IN 2.0 IN.	10.5-11.5%	10-11.5%

BEND DUCTILITY TEST DATA

	LONGITUDINAL	TRANSVERSE
GAGE	Omitted from Ø II Study	
BEND RADIUS		
SPAN		
LOAD RATE		
SHEAR STRENGTH		
BEND ANGLE		

MACHINING HISTORY Layout, steel stamp I.D., saw per layout, mill abutting edges square, chem clean per BAC 5764 Method I

INSPECTION Engineering Acceptance

REMARKS & OBSERVATION

Material examination per BMS-7-105C. Filler wire same spool used for Phase I.

BOEING NO. ______ PAGE →

PRE-WELD MATERIAL EVALUATION DATA SHEET
(INERT GAS EFFECTS STUDY)

CALIBRATION DATA MACHINE NO. ______ SHOP ______

AMMETER	VOLTMETER	CARRIAGE TRAVEL SPEED
11-19-65 ± 3%	11-19-65 ± 3%	12 in/min
8-17-65 Power Supply		
Shunt ± 1%		
DATE INSP.	DATE INSP.	DATE INSP.

RECORDER (AMMETER)	RECORDER (VOLTMETER)	FLOWMETERS	CURVE NO.
1-24-66 ± 3%	1-24-66 ± 2%	BAC	139249
		BAC	139250

INERT GAS

CYLINDER NO.	VENDOR	DATE INSP.	O_2	H_2	N_2	H_2O	CO_2	OTHER
7069T	MATHESON	1-20-66	—	—	6.0%	—	—	—
66955	MATHESON	1-20-66	—	—	5.7%	—	—	—
63148	MATHESON	1-20-66	1.5%	—	—	—	—	—
62979	MATHESON	1-20-66	1.5%	—	—	—	—	—
20667T	MATHESON	1-20-66	—	1.22%	—	—	—	—
12890	MATHESON	1-20-66	—	1.25%	—	—	—	—

REMARKS & OBSERVATION

Introduced gases checked independent with gas chromatograph.

Vacuum gage (Ion gage) on Control Panel certified 1-24-66.

Panels developed smutty appearance following cleaning process.

This material failed the MIL-H-6088 accelerated corrosion tests. Corrosion penetrated the end grain to a depth of 0.015 inch and surface to 0.006 inch. This test is not a requirement of BMS-7-105C.

BOEING NO. ______ PAGE →

Figure 3: PRE-WELD MATERIAL EVALUATION DATA SHEET

HEAT NUMBER	MECHANICAL PROPERTIES					METALLOGRAPHIC ANALYSIS		
	Y.S. (.2% OFFSET) KSI	U.S. KSI	E% (1/2 INCH)	E% (1 INCH)	E% (2 INCH)	GRAIN SIZE	ACCELERATED CORROSION	MICRO-HARDNESS
#AE50132-0	55.3-55.7	67.8-68.2	8.0	9.0-9.5	—	ASTM 5-6	NO PENETRATION	R_A 47
#EE51389-1	L* 57.4-57.8	L 70.3-71.3	L 16.0-26.0	L 15.0-16.5	L 10.5-11.5	ASTM 5-6	PENETRATION TO 0.015" (END) 0.006" (SURFACES)	R_B 81-82.5
	T* 55.7-57.2	T 70.9-71.5	T 16.0-22.0	T 14.0-16.0	T 10.0-11.5			

	CHEMICAL ANALYSIS									
	Cu	Mn	Si	V	Zn	Ti	Fe	Mg	Zr	Al
#AE50132-0	5.8-6.8	.20-.40	0.20	0.05-0.15	0.10	0.10-0.20	0.30	0.02	0.10-0.25	BAL.
#EE51389-1	6.37-6.40	.32	.10-.12	.085-.090	.06-.07	.055-.065	.14-.21	.011-.014	0.13-0.16	BAL.

* L - LONGITUDINAL
T - TRANSVERSE

Figure 4: COMPARISON OF PHASE I & II MATERIAL

WELD SCHEDULE

The criterion for the establishment of a weld schedule was to consistently produce high quality weldments having minimum undercut, good penetration, and a low level of porosity using commercially pure helium shielding gas. The small amount of porosity occurring with the program weld schedule was considered advantageous for the investigation of gas effects on the residual porosity. This residual porosity probably originates from a metallurgical or contamination condition in the filler wire or base metal. It therefore would be of interest to determine if improvements in quality can be achieved with gas additions. A typical weld schedule used in Phase II is shown on the weldment experimental data sheet, Figure 5. The only variations in schedule from Phase I were: (1) a program amperage increase of 5 amp in the initial 2 inches of weld; and (2) a five-fold increase in shielding gas flow. The 5 amp increase allowed the desired weld form to be reached rapidly, yielding more usable inches of weld for evaluation. The initial 2 inches of weld were not included in the evaluation of the weldments.

WELDING PROCEDURE SUMMARY

Several variations in the fabrication procedures used to prepare the weldment panels were made in Phase II to improve measurement control during the process. The following steps summarize the procedure established for Phase II welding.

Step 1 — The chemically cleaned panels were mechanically scraped along the surfaces to be welded to remove contaminants and the oxide layer.

Step 2 — The surface condition of the scraped joints was then analyzed for uniformity by a Boeing-developed contact potential apparatus. The test equipment is shown in Figure 6 and consists of: (1) a sensing element; (2) a mechanical traversing mechanism; and (3) a readout system. The principle of operation is basically the measurement of the potential difference generated by two dissimilar metals due to the difference between their work functions. A gold reference electrode is used in the sensing element. A radioactive source provides an electrical path between the gold element and the part to be tested, eliminating the need for physical contact. Small amounts of surface contaminants such as oils, greases, moisture, and oxides cause a change in the contact potential reading.

The usefulness of this addition measurement became evident when the instrument was initially placed into operation. As variations were detected, careful visual inspection of the scraped surface would show small discontinuities in these suspect areas. As a result of these observations, the welder's technique for scraping the joining surfaces was rapidly improved to a point where rescraping of panels was seldom required. Figure 7 is a contact potential plot of a typical set of panels. The upper set of curves show the surface variation of a matched pair of weldment panels. It is of interest to note that the two curves for the panels A and B, obtained from adjacent areas of the same Plate of material, follow a similar pattern. This was characteristic of all pairs

WELDMENT EXPERIMENTAL DATA SHEET
(INERT GAS WELDMENT STUDY EFFECTS)

GASES UNDER STUDY

TYPE	CONCENTRATION
H_2	500
H_2O	500
N_2	500
O_2	500

PANEL NO. 1402-AB-851-03
DATE 3-8-66
PROGRAM NO. QCDPA 2-5963 Phase II

WELDMENT SCHEDULE

WELD SETTING

CURRENT 240 AMPS
ARC VOLTAGE 13
WIRE FEED 36 IPM
TRAVEL SPEED 12 IPM
ELECTRICAL CHARACTERISTIC DC - SP
Automatic Voltage Controlled

ENVIRONMENTAL CONDITIONS

PLATE TEMPERATURE 70°F
CHAMBER PRESSURE 3 x 10^{-5}
EVACUATION 12:25 - 1:40 MINUTES
3 x 10^{-5} PRESSURE
FINAL CLEANING TIME 12:15
WELD TIME 1:45
CONTACT POTENTIAL 1.22 VOLTS

MATERIAL

	WELD PANEL	FILLER PANEL
ALLOY	2219	2319
CONDITION	T87	0
HEAT NO.	EE 51389-1	Control 5622
VENDOR	Reynolds	Linde
DIMENSION	11" x 36"	.062" Dia.
LOT NO.		218021
WELD JOINT DESIGN		

REMARKS & OBSERVATION

Weld panels chemically cleaned per BAC 5765 Method I, PSD 5-14 solution
1. Handscraped prior to welding. Single pass, horizontal position.
Longitudinal gas flow on root side, inlet at start end.

FIXTURING

	HOLD DOWN BAR	BACKUP BAR
MATERIAL	Mallory 3 copper	Tough Pitch Copper Bus Bar
SPACE	.650"	5/32" R. .312" deep
DRAWING NO.	SK11-024249	SK2-5963-2-II
DESIGN	Weld Side	Rubber Seal; Water Tube

TORCH CONFIGURATION

CUP
TYPE Linde
SIZE 10 (5/8")
ATTITUDE 90° to workpiece

ELECTRODE
TYPE 2% Thoriated EXTENSION 5/16"
SIZE 1/8" Diameter LOCATION
TIP SHAPE 30° included angle with .040" flat
5 minute break-in on copper block

EQUIPMENT

WELDING
1. Wolf Controlled Atmospheric Chamber
2. Wolf Electronic Controls
3. Wolf Welding Torch & Accessories (Linde)
4. Vickers Std. 400 Ampere Power Supply
5. Esterline Recorders
6. Flatbed Lab Type Welding Fixture
7.

ANALYTICAL
1. Bendix T.O.F. Mass Spectrometer
2. Alnor Dewpoint Indicator
3. Honeywell 1508 Visicorder
4. Boeing H_2 Monitor — For
5. Boeing O_2 Monitor — Calibration
6. CEC Mositure Monitor — Purposes
7.

BOEING NO. PAGE

WELDMENT EXPERIMENTAL DATA SHEET
(INERT GAS WELDMENT STUDY EFFECTS)

GAS ANALYSIS DATA

FLOW RATE

TORCH 80 CFH
BACKUP 1.33 CFH
1 CFM
2 CFM
3 CFM
4 CFM
PREFLOW MIN.
POSTFLOW MIN.

M/S BACKGROUND

	M/E	AMPS	CHANNEL
1.	2	.1x10^{-9}	2
2.	18	—	—
3.	28	.38x10^{-9}	4
4.	32	.9x10^{-10}	6

TOTAL PRESSURE 2 x 10^{-8}

M/S CONC. SETTING

	M/E	AMPS	CHANNEL
1.	2	.11x10^{-8}	2
2.	18	—	—
3.	28	.22x10^{-8}	4
4.	32	.14x10^{-8}	6

TOTAL PRESSURE 2 x 10^{-6}

M/S READING DURING TEST — RECORDING CHART NO. — MARK NO. (AMPS)

	M/E	CHANNEL	1	2	3	4
1.	2	2	.11 x 10^{-8}	.10 x 10^{-8}	.09 x 10^{-8}	
2.	4	3	.31 x 10^{-6}	.25 x 10^{-6}	.23 x 10^{-6}	
3.	18	—	—	—	—	
4.	28	4	.25 x 10^{-8}	.21 x 10^{-6}	.20 x 10^{-6}	
5.	32	6	.12 x 10^{-8}	.1 x 10^{-8}	.08 x 10^{-9}	
TOTAL PRESSURE	2 x 10^{-6}		1.9 x 10^{-6}	1.6 x 10^{-6}	1.4 x 10^{-6}	

M/S CALCULATED DATA

	M/E	CHANNEL	AMP/100 PPM
1.	2	2	.207 x 10^{-9}
2.	28	4	.355 x 10^{-9}
3.	32	6	.260 x 10^{-9}
4.			
5.			

FLOW METER CALCULATED DATA

READING	CONCENTRATION
1044FM	
SS-14.0	500 PPM H_2O

REMARKS & OBSERVATION

	Surface Condition	Surface Color
Face	Scaly	Dull with oxide spots
Root	Sandpaper	Shiny

Face Bead Irregularities — Undercut full length

Root Bead Penetration — Normal

Comments - None

BOEING NO. PAGE

Figure 5: TYPICAL EXPERIMENTAL WELDMENT DATA SHEET

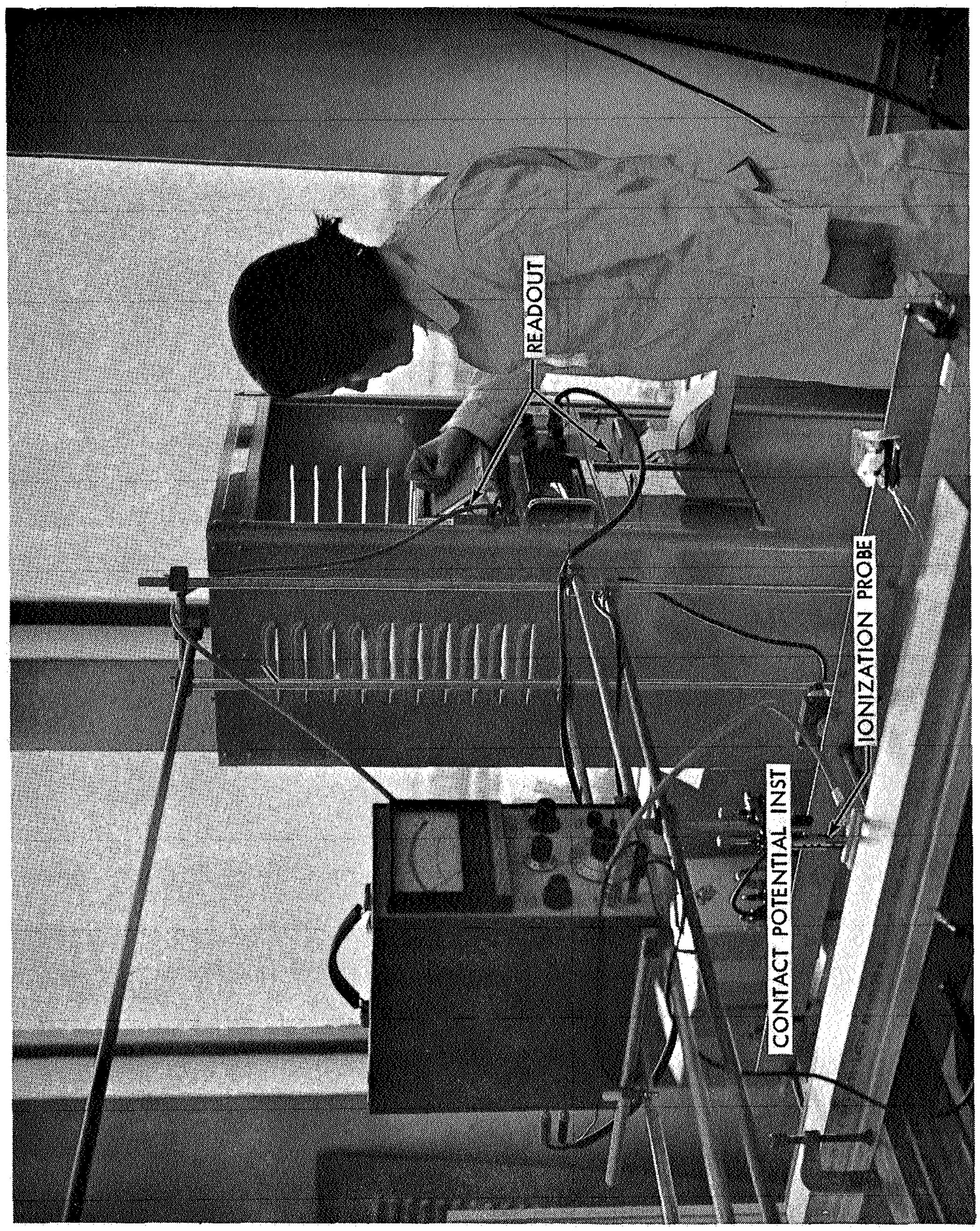

Figure 6: CONTACT POTENTIAL APPARATUS

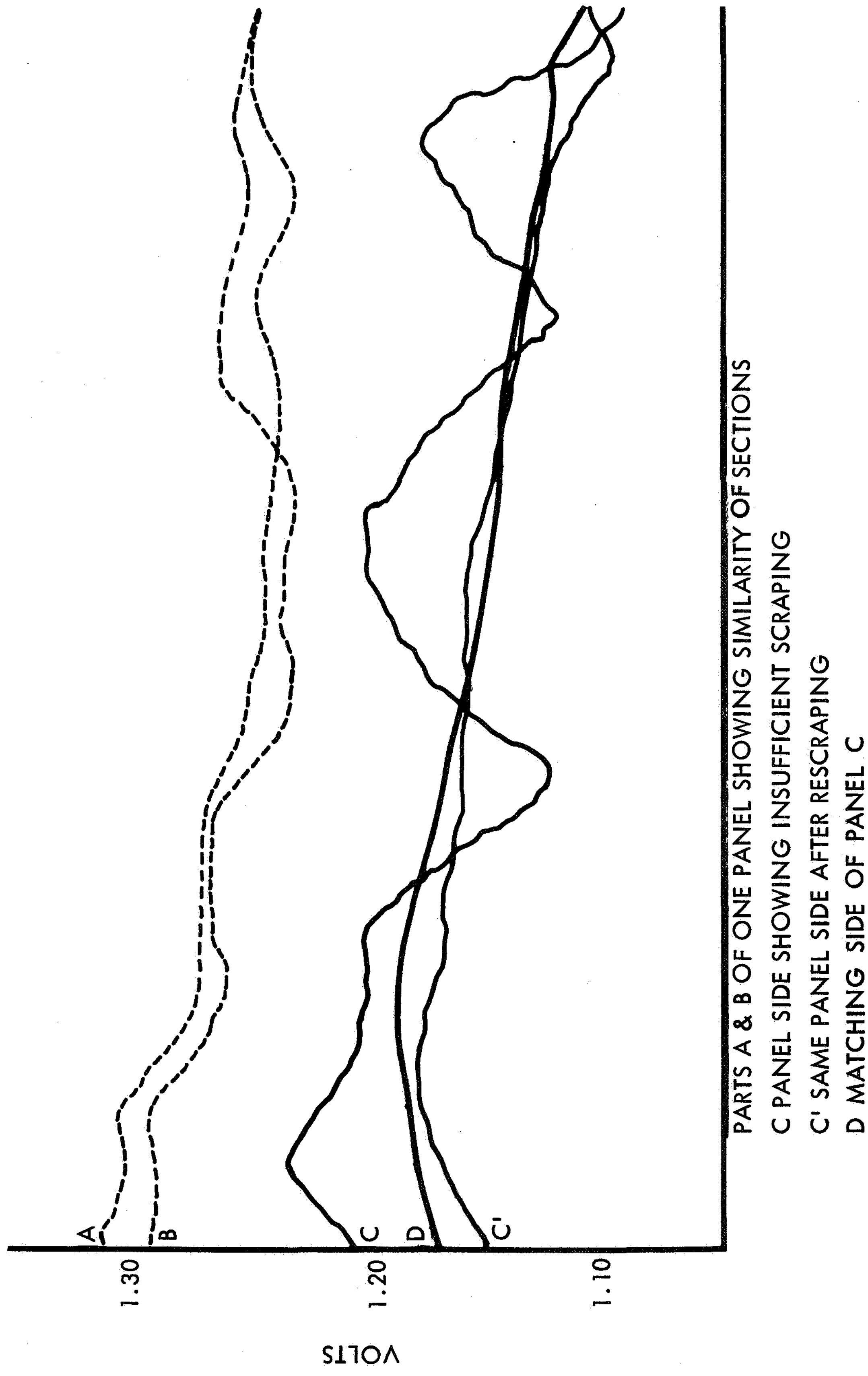

Figure 7: TYPICAL CONTACT POTENTIAL CURVES

of panels sufficiently scraped. Obvious variations were observed when the panel was contaminated, shown by curve C. After rescraping, the measurement along the surface would correspond to the matching panel, shown in curves C' and D.

Step 3 — The panels were placed in the atmosphere control chamber and evacuation was initiated. Clamping of the panels allowed for thermal expansion and contraction during welding. The upper panel was clamped securely in place while the lower panel received less clamping torque, permitting the majority of the movement to take place along the lower panel.

Step 4 — The chamber was evacuated and adjustment of gas contamination was initiated by passing helium gas to atmosphere and introducing required concentrations into the flow. In Phase I, the adjustment was made flowing helium into the chamber. This new step allowed more time for measurement and adjustment of the gas concentrations yeilding better accuracy, as well as speeding up the welding process.

Step 5 — The chamber was back-filled with helium and the shielding gas flow was started. The concentrations of the shielding gas were again measured at the weld cup and final adjustments made.

Step 6 — The weld was made observing the gas analysis, the voltage and amperage reading, and the formation of weld bead.

Step 7 — The panel was unloaded, the fixture cleaned and prepared for the next weld.

WELDMENT EVALUATION PROCEDURES

Following radiographic analysis, the weldment panels were machined to obtain the required specimens for evaluation. The cut pattern for the test specimens is shown in Figure 8 and consists of 2 gravimetric, 2 tensile, 3 fatigue, and 1 metallographic samples. The excess material was identified and stored in the event that additional tests should be required. The test specimen configuration is shown in Figure 9 and evaluation was performed as follows.

GRAVIMETRIC SAMPLES

The gravimetric samples were prepared by machining the majority of the base metal from the weld bead. A sample of base metal was also taken adjacent to the gravimetric sample to obtain a density comparison reference. The density was determined in the manner described in the Phase I report.

FATIGUE AND TENSILE SAMPLES

The fatigue and tensile specimens were machined from the weldment panel at predetermined locations. Many of the panels had some degree of undercut along the top edge of the weld, due to weld bead sag. Because it was the intent of the fatigue and tensile tests to determine the effect of the contaminants on the mechanical properties of the actual weld material, it was determined that the undercut condition should be eliminated. As a result, all test specimens were reduced in gage from 0.25 to 0.20 inch which provided samples of uniform dimensions for test and comparison.

METALLOGRAPHIC ANALYSIS

The purpose of the metallographic analysis was to provide additional porosity information particularly in the areas of microporosity and total percent voids. Also, variations in crystal growth and microstructure were to be reviewed. One specimen was prepared per weldment as described in the Phase I report.

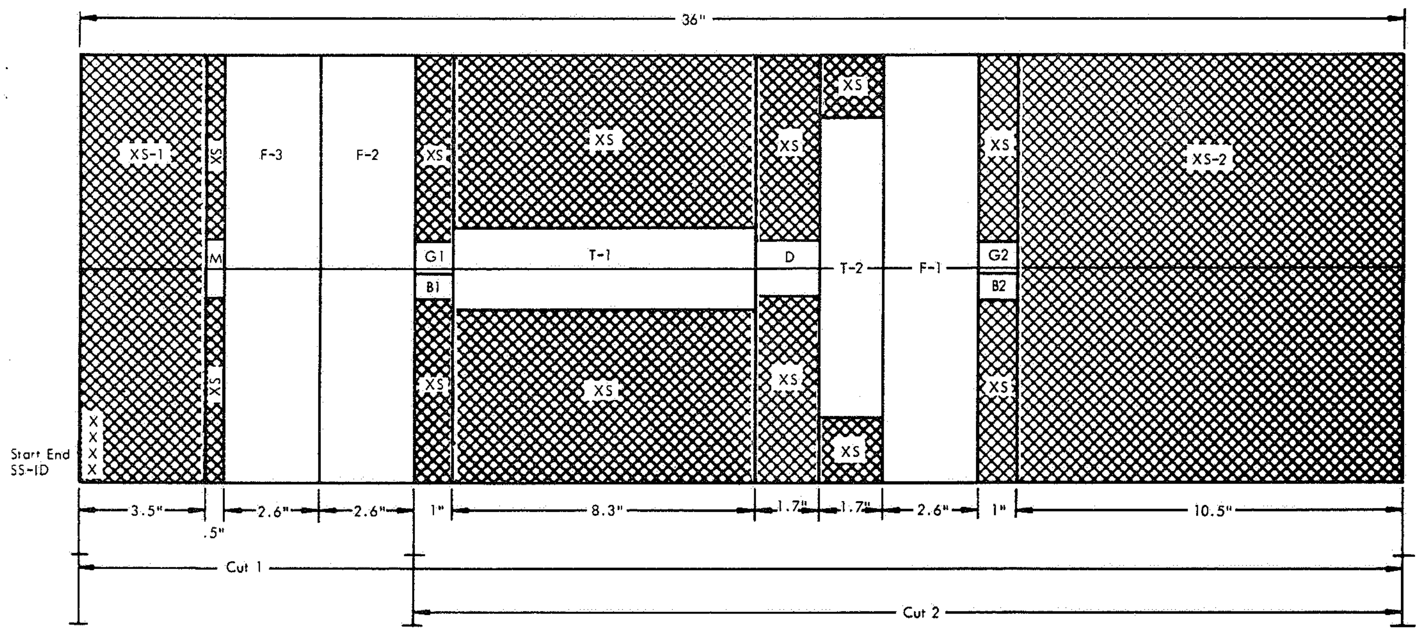

CODE	DESCRIPTION OF CUT
M	.5" x 1" Metallographic Sample (One/Panel)
F	Fatigue Sample (Three/Panel on Cut 1, one/Panel on Cut 2)
G	1" x 1.5" Gravimetric Sample (Two/Panel)
B	Base Metal Gravimetric Sample
T	Tensile Strength Sample (One Horizontal, One Vertical/Panel)
D	1.5" x .75" Display Sample (One/Panel)
[cross-hatch symbol]	Excess Material

Figure 8: SAMPLE CUT PATTERN

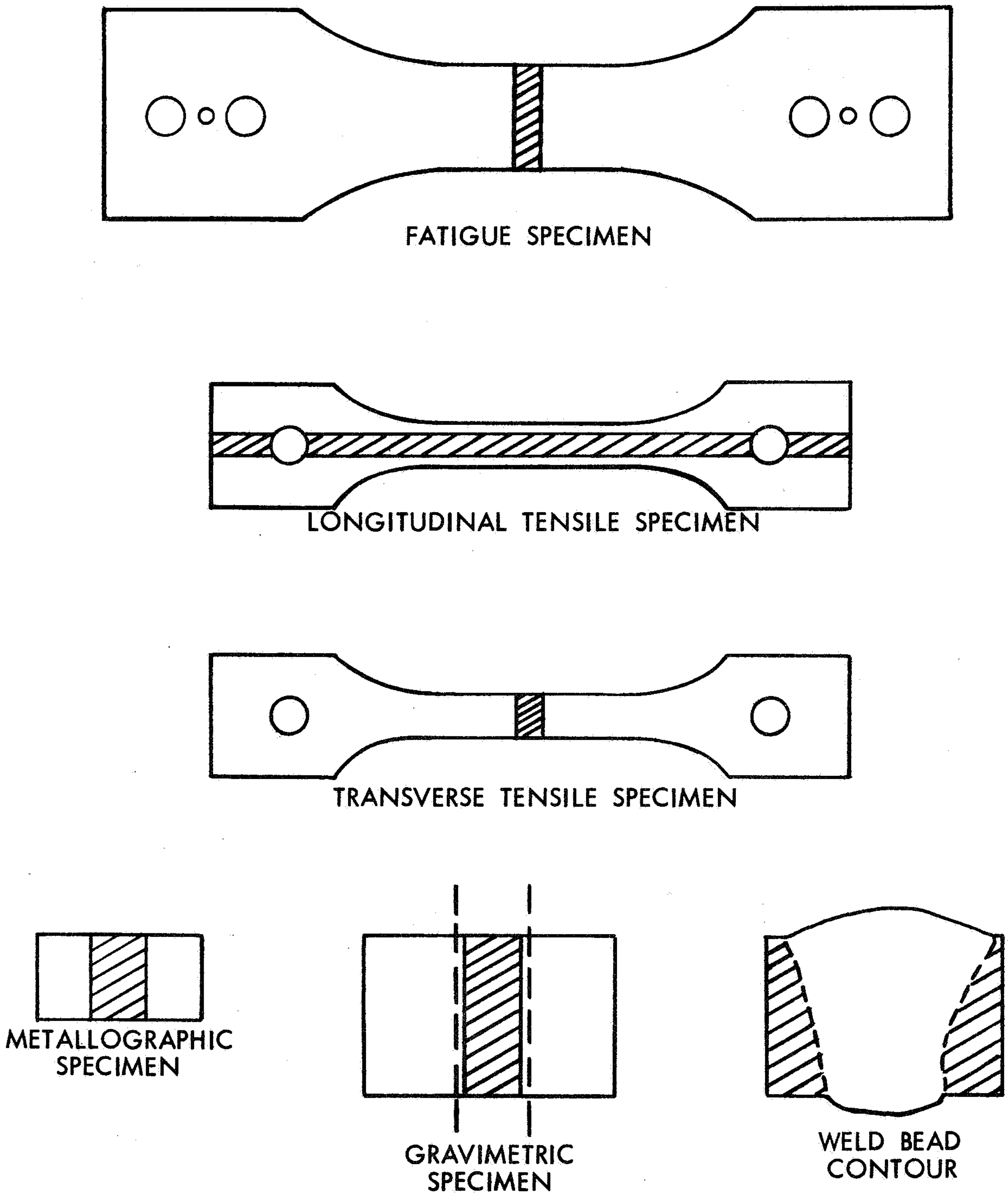

Figure 9: SPECIMEN DIAGRAMS

STATISTICAL PROGRAM

STATISTICAL EVALUATION

The data from Phase II of this program has been analyzed to study the significance of the effects and interactions of the contaminants as they relate to the various measures of weld quality. Regression equations have also been obtained to relate the level of contamination to weld quality. Following is a discussion of the experimental design, the statistical analysis, and the significant results of the analysis.

EXPERIMENTAL DESIGN

The experimental design for Phase II is basically a response surface design to provide the data needed to fit mathematical models for each measure of weld quality. The design consists of selected combinations of the four contaminating gases (oxygen, hydrogen, nitrogen, and water vapor), which provide the conditions for welding the test panels. For purposes of the statistical analysis, the design can be separated into several parts, as shown.

A 2^4 Factorial

All 16 combinations of the four contaminants at two levels (Low Level = 250 ppm; High Level = 750 ppm).

Variation From the Center of the Factorial

Varying each contaminant at three levels (5, 250, and 750 ppm) while holding the other three contaminants constant at 500 ppm.

A 1/2 Replicate of a 2^4 Factorial

Eight of the 16 combinations of the four contaminants at two levels (Low Level = 100 ppm; High Level = 750 ppm).

Replication at the Center of the Factorial

Six repeated welds with all four contaminants at 500 ppm.

Replication With the Base Gas

Ten repeated welds with the base gas. All four contaminants are $\leq$ 5 ppm.

Variation of Individual Contaminants

Varying each contaminant at five levels (100, 250, 500, 750, and 1000 ppm) with the other three contaminants $\leq$ 5 ppm.

A 1/2 Replicate of a 2^4 Factorial

Eight of the 16 combinations of the four contaminants at two levels (Low Level ≤ 5 ppm; High Level = 1000 ppm).

Note: With more than one contaminant at 1000 ppm welding became very erratic; therefore these panels were not all welded.

This data has also been arranged in this order on the data sheets (Figures 10 through 19). The data in Figures 10 through 13 show the radiographic analysis results for all weld panels included in the program. Those weld panels marked with an asterisk (*) were not evaluated for the other weld quality characteristics (density, metallographic porosity, tensile strength, and fatigue life) shown in Figures 14 through 19. A total of 66 weld panels were evaluated for all measures of weld quality. The results from these panels were used for the statistical analysis.

STATISTICAL ANALYSIS

The following measures of weld quality are considered for the statistical analysis.

Radiographic Analysis

Y_1 = Defects per Inch of Weld Bead (porosity sizes up to 0.024 inch)

Y_2 = Defects per Inch of Weld Bead (porosity sizes 0.025 to 0.049 inch)

Y_3 = Defects per Inch of Weld Bead (porosity sizes 0.050 to 0.150 inch)

Y_4 = Total Defects per Inch of Weld Bead (porosity sizes up to 0.150 inch)

Y_5 = Defects per Gram of Weld Bead (porosity sizes up to 0.024 inch)

Y_6 = Defects per Gram of Weld Bead (porosity sizes 0.025 to 0.049 inch)

Y_7 = Defects per Gram of Weld Bead (porosity sizes 0.050 to 0.150 inch)

Y_8 = Total Defects per Gram of Weld Bead (porosity sizes up to 0.150 inch)

Note: Y_5 through Y_8 were obtained by dividing Y_1 through Y_4 by the weight of the weld bead (grams per inch) for each panel to eliminate any effect due to variations in the weld bead between panels.

Density

Y_9 = Weld Bead Density

Y_{10} = Base Metal Density - Weld Bead Density

Note: Y_{10} was obtained as the difference between the density of the base metal and the weld bead to eliminate any effect due to variations between panels.

PANEL NUMBER	LEVELS OF CONTAMINATION EXPERIMENTAL DESIGN - PHASE II				RADIOGRAPHIC ANALYSIS Y = DEFECTS PER INCH OF WELD BEAD												
					TOP			CENTER			BOTTOM			TOTAL			
	O_2	H_2	N_2	H_2O	TO .024"	TO .049"	TO .150"	TO .024"	TO .049"	TO .150"	TO .024"	TO .049"	TO .150"	TO .024"	TO .049"	TO .150"	TOTAL
610-860-04	100	5	5	5	.00	.00	.00	.00	.00	.03	.00	.03	.00	.00	.03	.03	.06
604-840-03	250				.06	.00	.00	.21	.21	.03	.47	.18	.06	.74	.39	.09	1.22
604-848-01	250				.68	.32	.09	.47	.56	.50	.09	.09	.09	1.24	.97	.68	2.89
602-840-01	500				.03	.00	.00	.00	.00	.00	.12	.12	.09	.15	.12	.09	.36
603-840-02	500				.00	.00	.00	.21	.18	.00	.00	.09	.03	.21	.27	.03	.51
* 506-842-05	750				.03	.00	.00	.21	.06	.00	.21	.12	.03	.45	.18	.03	.66
* 605-841-03	750				.00	.00	.00	.12	.09	.00	.35	.09	.09	.47	.18	.09	.74
* 601-839-02	1000				.06	.00	.00	.00	.00	.00	.30	.09	.00	.36	.09	.00	.45
* 607-842-06	1000	5	5	5	.06	.00	.00	.12	.06	.03	.29	.21	.03	.47	.27	.06	.80
509-860-03	5	100	5	5	.00	.00	.00	.00	.00	.00	.12	.06	.06	.12	.06	.06	.24
606-846-03		250			.24	.55	.15	.00	.00	.00	.00	.00	.00	.24	.55	.15	.94
503-840-04		500			2.00	.06	.00	4.00	.29	.03	6.00	2.00	.29	12.00	2.35	.32	14.67
507-847-01		500			4.00	.06	.00	4.00	.24	.03	5.00	2.00	.18	13.00	2.30	.21	15.51
* 502-837-03		750			15.00	.03	.00	4.00	.18	.00	9.00	.70	.39	28.00	.91	.39	29.30
* 504-842-02		750			5.00	.09	.00	8.00	.62	.50	4.00	1.00	.75	17.00	1.71	1.25	19.96
* 501-837-01		1000			22.00	.03	.00	4.00	.27	.03	10.00	1.73	.58	36.00	2.03	.61	38.64
* 508-847-04		1000			18.00	3.00	1.21	8.00	.44	.00	19.00	.24	.00	45.00	3.68	1.21	49.89
505-842-04	5	2500	5	5	100.00	1.00	.06	50.00	.80	.53	150.00	2.00	.85	300.00	3.80	1.44	305.24
710-860-06	5	5	100	5	.29	.06	.00	.00	.00	.00	.00	.00	.00	.29	.06	.00	.35
703-841-04			250		.03	.00	.00	.09	.12	.03	.47	.38	.06	.59	.50	.09	1.18
704-841-05			250		.00	.00	.00	.24	.09	.00	.65	.06	.12	.89	.15	.12	1.16
707-847-03			500		.00	.03	.00	.00	.00	.00	.26	.15	.03	.26	.18	.03	.47
709-847-06			500		.30	.24	.00	.06	.00	.00	.00	.03	.00	.36	.27	.00	.63
* 701-836-01			750		.00	.00	.00	.25	.16	.06	2.00	.38	.28	2.25	.54	.34	3.13
* 705-842-03			750		.56	.68	.26	.12	.18	.03	.00	.00	.00	.68	.86	.29	1.83
* 702-841-02			1000		.00	.00	.00	.00	.03	.00	.24	.09	.03	.24	.12	.03	.39
* 708-847-05			1000		.53	.32	.03	.06	.00	.00	.03	.03	.00	.62	.35	.03	1.00
* 706-846-02	5	5	5000	5	.03	.00	.00	.06	.00	.00	.15	.06	.03	.24	.06	.03	.33

Figure 10: RADIOGRAPHIC POROSITY DATA

PANEL NUMBER	LEVELS OF CONTAMINATION EXPERIMENTAL DESIGN - PHASE II				RADIOGRAPHIC ANALYSIS Y = NO. OF DEFECTS PER INCHES OF WELD BEAD												
					TOP			CENTER			BOTTOM			TOTAL			
	O_2	H_2	N_2	H_2O	TO .024"	TO .049"	TO .150"	TO .024"	TO .049"	TO .150"	TO .024"	TO .049"	TO .150"	TO .024"	TO .049"	TO .150"	TOTAL
807-855-06	5	5	5	100	.26	.35	.12	.06	.12	.06	.00	.03	.00	.32	.50	.18	1.00
809-860-05				100	.00	.12	.06	.00	.09	.03	.03	.00	.00	.03	.21	.09	.33
802-838-02				250	.45	.27	.12	.09	.09	.00	.00	.00	.00	.54	.36	.12	1.02
806-852-01				250	.00	.06	.00	.00	.00	.00	.00	.03	.00	.00	.09	.00	.09
803-838-03				500	1.52	.88	.09	.21	.06	.06	.00	.00	.00	1.73	.94	.15	2.82
805-851-05				500	.94	.18	.09	.12	.00	.00	.15	.00	.00	1.21	.18	.09	1.48
* 804-851-04				750	.24	.12	.03	.24	.06	.00	.62	.03	.00	1.10	.21	.03	1.34
* 808-858-06				750	2.00	.12	.09	.24	.00	.03	1.47	.00	.00	3.71	.12	.12	3.95
* 801-838-01	5	5	5	1000	3.00	.32	.06	.26	.00	.00	.12	.00	.00	3.38	.32	.06	3.76
* 1103-850-01	1000	1000	5	5	39.00	.74	.44	19.00	.26	.06	10.00	.00	.00	68.00	1.00	.50	69.50
* 1101-848-04	1000	5	1000	5	.00	.03	.00	.00	.00	.00	.00	.00	.00	.00	.03	.00	.03
* 1401-849-02	1000	5	1000	5	.15	.12	.06	.09	.06	.00	.03	.00	.00	.27	.18	.06	.51
* 1301-849-01	5	1000	1000	5	49.00	1.15	.09	49.00	.29	.00	1.00	.00	.00	99.00	1.44	.09	100.53
* 1001-848-02	5	1000	1000	5	23.00	.29	.06	10.00	.15	.03	11.00	.00	.00	44.00	.44	.09	44.53
* 1004-853-01	5	1000	1000	1000	140.00	3.00	.26	30.00	.06	.00	30.00	.09	.00	200.00	3.15	.26	203.41

Figure 11: RADIOGRAPHIC POROSITY DATA

PANEL NUMBER	LEVELS OF CONTAMINATION EXPERIMENTAL DESIGN - PHASE II				RADIOGRAPHIC ANALYSIS Y = DEFECTS PER INCH OF WELD BEAD												
					TOP			CENTER			BOTTOM			TOTAL			
	O_2	H_2	N_2	H_2O	TO .024"	TO .049"	TO .150"	TO .024"	TO .049"	TO .150"	TO .024"	TO .049"	TO .150"	TO .024"	TO .049"	TO .150"	TOTAL
1205-854-03	250	250	250	250	4.00	.29	.06	3.00	.09	.00	5.00	.06	.03	12.00	0.44	0.09	12.53
1208-857-04	750	250	250	250	.50	.47	.09	.24	.21	.00	.03	.03	.00	0.77	0.71	0.09	1.57
1105-853-03	250	750	250	250	3.00	.21	.00	2.00	.09	.00	2.00	.00	.00	7.00	0.30	0.00	7.30
1404-853-06	750	750	250	250	.09	.09	.03	.00	.06	.06	.06	.03	.00	0.15	0.18	0.09	0.42
1104-852-03	250	250	750	250	4.00	.15	.03	2.00	.06	.00	3.00	.06	.03	9.00	0.27	0.06	9.33
1009-857-02	750	250	750	250	.03	.21	.09	.00	.00	.00	.00	.03	.35	0.03	0.24	0.44	0.71
1405-854-05	250	750	750	250	14.00	.24	.03	4.00	.09	.06	2.00	.00	.00	20.00	0.33	0.09	20.42
1203-852-04	750	750	750	250	.26	.24	.06	.09	.12	.09	.03	.00	.00	0.38	0.36	0.15	0.89
1006-854-06	250	250	250	750	5.00	.00	.00	2.00	.06	.00	3.00	.18	.06	10.00	0.24	0.06	10.30
1005-854-01	750	250	250	750	3.00	1.00	.53	3.00	.12	.09	8.00	2.1	.06	14.00	1.33	0.68	16.01
1209-858-04	250	750	250	750	22.00	.70	.06	5.00	.29	.06	11.00	.09	.00	38.00	1.08	0.12	39.20
1010-858-02	750	750	250	750	15.00	.59	.03	4.00	.09	.00	1.00	.03	.00	90.00	0.71	0.03	20.74
1003-852-02	250	250	750	750	5.00	.32	.12	5.00	.09	.03	10.00	.18	.03	20.00	0.59	0.18	20.77
1310-859-05	750	250	750	750	1.00	.12	.12	2.00	.06	.00	3.00	.00	.00	6.00	0.18	0.12	6.30
1204-853-04	250	750	750	750	4.00	.18	.00	13.00	.12	.03	12.00	.15	.00	29.00	0.45	0.03	29.48
1202-851-01	750	750	750	750	70.00	7.00	.29	20.00	.18	.03	1.00	.06	.00	91.00	7.24	0.32	98.56
1106-854-02	5	500	500	500	10.00	.21	.06	5.00	.09	.00	25.00	.12	.06	40.00	0.42	0.12	40.54
1207-856-03	250	500	500	500	4.00	.24	.06	1.00	.12	.03	1.00	.00	.00	6.00	0.36	0.09	6.45
1206-855-03	750	500	500	500	18.00	.32	.00	7.00	.18	.03	35.00	.06	.03	60.00	0.56	0.06	60.62
1409-857-06	500	5	500	500	2.00	.44	.06	1.00	.09	.00	1.00	.09	.03	4.00	0.62	0.09	4.71
1110-858-03	500	250	500	500	1.00	.06	.00	3.00	.12	.00	2.00	.00	.03	6.00	0.18	0.03	6.21
1107-855-02	500	750	500	500	30.00	.50	.09	10.00	.29	.00	10.00	.09	.00	50.00	0.88	0.09	50.97
* 1302-851-02	500	1000	500	500	40.00	1.38	.15	7.00	.06	.03	2.00	.00	.00	49.00	1.44	0.18	50.62
1403-852-06	500	500	5	500	.35	.12	.00	.15	.03	.00	.09	.00	.00	0.59	0.15	0.00	0.74
1309-858-05	500	500	250	500	7.00	.12	.03	3.00	.00	.00	5.00	.00	.00	15.00	0.12	0.03	15.15
1406-855-05	500	500	750	500	80.00	1.00	.06	17.00	.18	.06	3.00	.09	.00	100.00	1.27	0.12	101.39
1201-848-05	500	500	500	5	.49	.14	.00	.34	.29	.06	.06	.06	.00	0.89	0.49	0.06	1.44
1109-857-03	500	500	500	250	6.00	.32	.03	1.00	.12	.03	2.00	.06	.00	9.00	0.50	0.06	9.56
1306-855-04	500	500	500	750	20.00	.26	.12	10.00	.06	.00	20.00	.00	.03	50.00	0.32	0.15	50.47

* DROPPED FROM TEST PLAN FOLLOWING RADIOGRAPHIC STUDY

Figure 12: ALUMINUM INERT GAS WELDMENT EFFECTS STUDY - PHASE II (RADIOGRAPHIC POROSITY DATA)

PANEL NUMBER	LEVELS OF CONTAMINATION EXPERIMENTAL DESIGN - PHASE II				RADIOGRAPHIC ANALYSIS Y = DEFECTS PER INCH OF WELD BEAD												
					TOP			CENTER			BOTTOM			TOTAL			
	O_2	H_2	N_2	H_2O	TO .024"	TO .049"	TO .150"	TO .024"	TO .049"	TO .150"	TO .024"	TO .049"	TO .150"	TO .024"	TO .049"	TO .150"	TOTAL
1307-856-04	100	100	100	100	.06	.09	.09	.03	.03	.00	.00	.00	.00	.06	.12	.09	.27
1111-859-03	750	100	100	750	.06	.03	.00	.12	.12	.00	2.00	.35	.06	2.18	.50	.06	2.74
1407-857-01	100	750	100	750	7.00	.47	.18	2.00	.12	.00	5.00	.03	.00	14.00	.62	.18	14.80
1410-859-01	750	750	100	100	1.00	.06	.00	1.00	.18	.00	1.00	.12	.03	3.00	.36	.03	3.39
1007-856-01	750	100	750	100	.09	.12	.00	.00	.00	.00	.00	.00	.00	.09	.12	.00	.21
1411-860-01	100	750	750	100	1.00	.15	.03	1.00	.09	.03	2.00	.06	.00	4.00	.30	.06	4.36
1108-856-02	100	100	750	100	.09	.09	.03	.03	.00	.00	.00	.00	.00	.12	.09	.03	.24
1011-859-02	500	500	500	500	1.00	.06	.00	3.00	.06	.00	25.00	.74	.00	29.00	.86	.00	29.86
1210-859-04					9.00	.12	.03	13.00	.18	.00	8.00	.03	.00	30.00	.33	.03	30.36
1304-853-05					10.00	.24	.00	10.00	.06	.00	20.00	.06	.00	40.00	.36	.00	40.36
1305-854-04					9.00	.26	.03	6.00	.09	.00	15.00	.03	.03	30.00	.38	.06	30.44
1308-857-05					9.00	.41	.32	5.00	.18	.00	7.00	.03	.00	21.00	.62	.32	21.94
1402-851-03	500	500	500	500	4.00	.35	.12	2.00	.00	.00	2.00	.00	.00	8.00	.35	.12	8.47
				Average	7.000	0.240	0.083	6.500	0.095	0.000	12.833	0.148	0.005	26.333	0.483	0.088	26.905
901-837-02	5	5	5	5	.00	.06	.09	.15	.00	.00	.57	.26	.12	.72	.32	.21	1.25
* 902-839-01					.00	.00	.00	.12	.06	.00	.41	.26	.15	.53	.32	.15	1.00
* 903-841-01					.00	.03	.00	.09	.03	.00	.21	.18	.06	.30	.24	.06	.60
904-842-01					.00	.00	.00	.18	.24	.06	.26	.26	.06	.44	.50	.12	1.06
906-846-01					.21	.30	.03	.06	.15	.00	.00	.00	.03	.27	.45	.06	.78
907-847-02					.00	.00	.00	.00	.00	.00	.03	.00	.00	.03	.00	.00	.03
* 908-848-03					.09	.03	.12	.09	.06	.00	.00	.00	.00	.18	.09	.12	.39
* 910-855-01					.00	.00	.3	.00	.00	.00	.03	.00	.00	.03	.00	.03	.06
* 905-843-01					.00	.00	.0	.09	.15	.03	.06	.21	.12	.15	.36	.15	.66
* 909-853-02	5	5	5	5	.15	.09	.15	.15	.15	.03	.00	.03	.00	.30	.07	.18	.75
				Average	.045	.051	.042	.093	.084	.012	.157	.120	.054	.295	.255	.108	.658

* DROPPED FROM TEST PLAN FOLLOWING RADIOGRAPHIC STUDY

Figure 13 : ALUMINUM INERT GAS WELDMENT EFFECTS STUDY - PHASE II (RADIOGRAPHIC POROSITY DATA)

PANEL NUMBER	LEVELS OF CONTAMINATION EXPERIMENTAL DESIGN - PHASE II				gm/INCH OF WELD BEAD	C_X = CC/gm OF WELD BEAD				RADIOGRAPHIC ANALYSIS Y = DEFECTS PER GRAM OF WELD BEAD				WELD BEAD DENSITY	BASE METAL MINUS WELD BEAD DENSITY	METALLO-GRAPHIC POROSITY VOL. FRAC. %
	O_2	H_2	N_2	H_2O		O_2	H_2	N_2	H_2O	TO .024"	TO .049"	TO .150"	TOTAL			
1205-854-03	250	250	250	250	3.61818	0.1568	0.1568	0.1568	0.1568	3.316	0.122	0.025	3.463	2.82742	0.01160	0.5
1208-857-04	750	250	250	250	3.61332	0.4710	0.1570	0.1570	0.1570	0.213	0.196	0.025	0.434	2.83605	0.00289	0.5
1105-853-03	250	750	250	250	3.83781	0.1478	0.4434	0.1478	0.1478	1.823	0.078	0.000	1.901	2.82778	0.01143	0.5
1404-853-06	750	750	250	250	4.08150	0.4169	0.4169	0.1390	0.1390	0.037	0.044	0.022	0.103	2.83235	0.00756	0.5
1104-852-03	250	250	750	250	3.94334	0.1438	0.1438	0.4314	0.1438	2.282	0.068	0.015	2.365	2.82610	0.01226	1.0
1009-857-02	750	250	750	250	3.59867	0.4728	0.1576	0.4728	0.1576	0.008	0.067	0.122	0.197	2.83416	0.00143	0.0
1405-854-05	250	750	750	250	4.01432	0.1413	0.4239	0.4239	0.1413	4.982	0.082	0.022	5.086	2.82176	0.01628	3.0
1203-852-04	750	750	750	250	3.72171	0.4572	0.4572	0.4572	0.1524	0.102	0.097	0.040	0.239	2.83362	0.00716	0.5
1006-854-06	250	250	250	750	3.72054	0.1524	0.1524	0.1524	0.4572	2.688	0.064	0.016	2.768	2.81588	0.02069	2.0
1005-854-01	750	250	250	750	3.96989	0.4287	0.1429	0.1429	0.4287	3.526	0.335	0.171	4.032	2.82416	0.01309	1.0
1209-858-04	250	750	250	750	3.92799	0.1444	0.4332	0.1444	0.4332	9.674	0.275	0.030	9.979	2.78872	0.05043	2.0
1010-858-02	750	750	250	750	3.93643	0.4323	0.4323	0.1441	0.4323	5.081	0.180	0.008	5.269	2.79879	0.03657	1.0
1003-852-02	250	250	750	750	3.97986	0.1425	0.1425	0.4275	0.4275	5.025	0.148	0.045	5.218	2.81696	0.01687	1.0
1310-859-05	750	250	750	750	3.92150	0.4338	0.1446	0.4338	0.4338	1.530	0.046	0.031	1.607	2.82844	0.01094	0.5
1204-853-04	250	750	750	750	3.88008	0.1462	0.4386	0.4386	0.4386	7.474	0.116	0.008	7.598	2.82148	0.01789	1.0
1202-851-01	750	750	750	750	3.72609	0.4567	0.4567	0.4567	0.4567	24.422	1.943	0.086	26.451	2.80388	0.03562	2.0
1106-854-02	5	500	500	500	3.99448	0.0028	0.2840	0.2840	0.2840	10.014	0.105	0.030	10.149	2.80253	0.03735	10.0
1207-856-03	250	500	500	500	3.98000	0.1425	0.2850	0.2850	0.2850	1.508	0.090	0.023	1.621	2.82862	0.01089	1.0
1206-855-03	750	500	500	500	3.88303	0.4382	0.2922	0.2922	0.2922	15.451	0.144	0.015	15.610	2.82306	0.01381	1.0
1409-857-06	500	5	500	500	4.12169	0.2752	0.0028	0.2752	0.2752	0.970	0.150	0.022	1.142	2.83505	0.00492	0.5
1110-858-03	500	250	500	500	3.84591	0.2950	0.1475	0.2950	0.2950	1.560	0.047	0.008	1.615	2.82144	0.01711	1.0
1107-855-02	500	750	500	500	3.78277	0.2999	0.4498	0.2999	0.2999	13.218	0.233	0.024	13.475	2.80432	0.03477	2.0
1403-852-06	500	500	5	500	3.86536	0.2935	0.2935	0.0029	0.2935	0.153	0.039	0.000	0.192	2.82700	0.01372	1.0
1309-858-05	500	500	250	500	3.79723	0.2988	0.2988	0.1494	0.2988	3.950	0.032	0.008	3.990	2.81812	0.02186	1.0
1406-855-05	500	500	750	500	3.70419	0.3063	0.3063	0.4594	0.3063	26.996	0.343	0.032	27.371	2.79564	0.04379	1.0

Figure 14: ALUMINUM INERT GAS WELDMENT EFFECTS STUDY POROSITY ANALYSIS DATA

PANEL NUMBER	LEVELS OF CONTAMINATION EXPERIMENTAL DESIGN - PHASE II				gm/INCH OF WELD BEAD	C_X = CC/gm OF WELD BEAD				RADIOGRAPHIC ANALYSIS Y = DEFECTS PER GRAM OF WELD BEAD				WELD BEAD DENSITY	BASE METAL MINUS WELD BEAD DENSITY	METALLO-GRAPHIC POROSITY VOL. FRAC. %
	O_2	H_2	N_2	H_2O		O_2	H_2	N_2	H_2O	TO .024"	TO .049"	TO .150"	TOTAL			
1201-848-05	500	500	500	5	4.08737	0.2776	0.2776	0.2776	0.0028	0.218	0.120	0.015	0.353	2.83301	0.00702	0.5
1109-857-03	500	500	500	250	3.99737	0.2838	0.2838	0.2838	0.1419	2.251	0.125	0.015	2.391	2.83039	0.00918	0.5
1306-855-04	500	500	500	750	3.70805	0.3060	0.3060	0.3060	0.4589	13.484	0.086	0.040	13.610	2.82302	0.01678	2.0
1307-856-04	100	100	100	100	3.64110	0.0623	0.0623	0.0623	0.0623	0.016	0.033	0.025	0.074	2.84115	0.00212	0.0
1111-859-03	750	100	100	750	4.02866	0.4224	0.0563	0.0563	0.4224	0.541	0.124	0.015	0.680	2.82870	0.01129	0.5
1407-857-01	100	750	100	750	3.62907	0.0625	0.4689	0.0625	0.4689	3.858	0.171	0.050	4.079	2.80516	0.03454	1.0
1410-859-01	750	750	100	100	3.79648	0.4482	0.4482	0.0598	0.0598	0.790	0.095	0.008	0.843	2.82220	0.01733	1.0
1007-856-01	750	100	750	100	4.11768	0.4133	0.0551	0.4133	0.0551	0.022	0.029	0.000	0.051	2.83637	0.00030	0.5
1411-860-01	100	750	750	100	3.69292	0.0614	0.4608	0.4608	0.0614	1.083	0.081	0.016	1.180	2.83060	0.01058	0.5
1108-856-02	100	100	750	100	3.81441	0.0595	0.0595	0.4461	0.0595	0.031	0.024	0.008	0.063	2.84180	0.00273	0.5
1011-859-02	500	500	500	500	3.73538	0.3037	0.3037	0.3037	0.3037	7.764	0.230	0.000	7.994	2.80402	0.03258	2.0
1210-859-04					4.20118	0.2700	0.2700	0.2700	0.2700	7.141	0.078	0.007	7.226	2.81019	0.02896	1.0
1304-853-05					4.28002	0.2651	0.2651	0.2651	0.2651	9.346	0.084	0.000	9.430	2.82275	0.01552	1.0
1305-854-04					4.02303	0.2820	0.2820	0.2820	0.2820	7.457	0.094	0.015	7.566	2.82041	0.01931	2.0
1308-857-05					4.05065	0.2801	0.2801	0.2801	0.2801	5.184	0.153	0.079	5.416	2.82330	0.01569	1.0
1402-851-03	500	500	500	500	3.78724	0.2996	0.2996	0.2996	0.2996	2.112	0.092	0.032	2.236	2.81921	0.02036	1.0
AVERAGE					4.012917	0.28342	0.28342	0.28342	0.28342	39.004	0.1218	0.0221	6.6446	2.816647	0.022070	1.333
901-837-02	5	5	5	5	3.45353	0.0033	0.0033	0.0033	0.0033	0.208	0.093	0.061	0.362	2.84298	- 0.00613	0.5
904-842-01					3.33459	0.0034	0.0034	0.0034	0.0034	0.132	0.150	0.036	0.318	2.84326	- 0.00584	0.0
906-846-01					3.47562	0.0033	0.0033	0.0033	0.0033	0.078	0.129	0.017	0.224	2.84401	- 0.00510	0.0
907-847-02	5	5	5	5	3.98376	0.0028	0.0028	0.0028	0.0028	0.008	0.000	0.000	0.008	2.84405	- 0.00629	0.0
AVERAGE					3.561875	0.00320	0.00320	0.00320	0.00320	0.1065	0.0930	0.0285	0.2280	2.843575	- 0.005840	0.125

Figure 15: ALUMINUM INERT GAS WELDMENT EFFECTS STUDY POROSITY ANALYSIS DATA

PANEL NUMBER	LEVELS OF CONTAMINATION EXPERIMENTAL DESIGN - PHASE II				gm/INCH OF WELD BEAD	C_X = CC/gm OF WELD BEAD				RADIOGRAPHIC ANALYSIS Y = DEFECTS PER GRAM OF WELD BEAD				WELD BEAD DENSITY	BASE METAL MINUS WELD BEAD DENSITY	METALLO-GRAPHIC POROSITY VOL. FRAC. %
	O_2	H_2	N_2	H_2O		O_2	H_2	N_2	H_2O	TO .024"	TO .049"	TO .150"	TOTAL			
610-860-04	100	5	5	5	4.31412	0.0526	0.0026	0.0026	0.0026	0.000	0.007	0.007	0.014	2.84452	-0.00240	0.0
604-840-03	250				3.52222	0.1610	0.0032	0.0032	0.0032	0.210	0.111	0.026	0.347	2.84892	-0.00670	0.0
609-848-01	250				3.48373	0.1628	0.0032	0.0032	0.0032	0.356	0.278	0.195	0.829	2.85011	-0.00705	0.0
602-840-01	500				3.68270	0.3081	0.0031	0.0031	0.0031	0.041	0.032	0.024	0.097	2.85233	-0.00939	0.5
603-840-02	500	5	5	5	3.41291	0.3324	0.0033	0.0033	0.0033	0.062	0.079	0.009	0.150	2.84884	-0.00499	0.0
509-860-03	5	100	5	5	3.24229	0.0035	0.0700	0.0035	0.0035	0.037	0.018	0.018	0.073	2.84308	-0.00534	0.5
606-846-03		250			3.14390	0.0036	0.1804	0.0036	0.0036	0.076	0.175	0.048	0.299	2.84819	-0.00551	0.0
503-840-04		500			3.80270	0.0030	0.2983	0.0030	0.0030	3.156	0.618	0.084	3.858	2.82397	0.01229	1.0
507-847-01		500			3.62153	0.0031	0.3133	0.0031	0.0031	3.590	0.635	0.058	4.283	2.82192	0.01548	1.0
505-842-04	5	2500	5	5	3.75902	0.0030	1.5090	0.0030	0.0030	79.808	1.011	0.383	81.202	2.75590	0.08122	10.0
710-860-06	5	5	100	5	3.46638	0.0033	0.0033	0.0654	0.0033	0.084	0.017	0.000	0.101	2.84212	-0.00683	0.0
703-841-04			250		3.43318	0.0033	0.0033	0.1652	0.0033	0.172	0.146	0.026	0.344	2.84173	-0.00600	0.0
704-841-05			250		3.87906	0.0029	0.0029	0.1462	0.0029	0.229	0.039	0.031	0.299	2.84230	-0.00705	0.0
707-847-03			500		3.46367	0.0033	0.0033	0.3275	0.0033	0.075	0.052	0.009	0.136	2.84166	-0.00530	0.0
709-847-06	5	5	500	5	3.25209	0.0035	0.0035	0.3488	0.0035	0.111	0.083	0.000	0.194	2.84243	-0.00723	0.0
807-855-06	5	5	5	100	3.62840	0.0031	0.0031	0.0031	0.0625	0.088	0.138	0.050	0.276	2.84066	-0.00554	0.5
809-860-05				100	3.46181	0.0033	0.0033	0.0033	0.0655	0.009	0.061	0.026	0.096	2.83953	-0.00400	0.5
802-838-02				250	3.47009	0.0033	0.0033	0.0033	0.1634	0.156	0.104	0.035	0.295	2.83486	0.00018	0.5
806-852-01				250	3.29820	0.0034	0.0034	0.0034	0.1720	0.000	0.027	0.000	0.027	2.83555	-0.00041	0.5
803-838-03				500	3.50069	0.0032	0.0032	0.0032	0.3241	0.494	0.268	0.043	0.805	2.83241	0.00307	0.5
805-851-05	5	5	5	500	3.15097	0.0036	0.0036	0.0036	0.3600	0.384	0.057	0.028	0.469	2.82646	0.00947	1.0

Figure 16: ALUMINUM INERT GAS WELDMENT EFFECTS STUDY POROSITY ANALYSIS DATA

PANEL NO.	EXPERIMENTAL LEVEL OF CONTAMINATION IN PARTS PER MILLION (PPM)				FATIGUE DATA – TRANSVERSE WELD					TENSILE DATA – LONGITUDINAL WELD						TENSILE DATA – TRANSVERSE WELD					
					SPEC. NO.	NO. OF CYCLES TO FAILURE				SPEC. NO.	ULTIMATE STRENGTH PSI	YIELD STRENGTH PSI	ELONGATION % LENGTH IN			SPEC. NO.	ULTIMATE STRENGTH PSI	YIELD STRENGTH PSI	ELONGATION % LENGTH IN		
	O_2	H_2	N_2	H_2O		F1	F2	F3					.50	1.0	2.0				.50	1.0	2.0
1205-854-03	250	250	250	250	34	180,000	254,000	169,000	198,000	34T1	43,400	21,900	22	17	14	34T2	39,000	24,900	16	8	4.0
1208-857-04	750	250	250	250	63	337,000	630,000	61,000	235,000	63T1	43,800	21,900	24	20	16	63T2	40,200	24,800	16	8	4.0
1105-853-03	250	750	250	250	45	270,000	227,000	469,000	306,000	45T1	43,600	21,600	26	20	16	45T2	38,500	23,800	14	7	3.5
1404-853-06	750	750	250	250	38	318,000	245,000	245,000	267,000	38T1	42,500	20,400	26	20	17	38T2	36,500	23,600	12	6	3.0
1104-852-03	250	250	750	250	39	181,000	200,000	640,000	285,000	39T1	44,300	22,600	22	16	15	39T2	35,400	23,300	12	6	3.0
1009-857-02	750	250	750	250	59	437,000	158,000	600,000	346,000	59T1	45,500	24,200	24	19	14	59T2	40,300	25,200	14	7	3.5
1405-854-05	250	750	750	250	69	642,000	225,000	421,000	393,000	69T1	43,100	21,200	24	21	16	69T2	35,300	23,900	10	5	2.5
1203-852-04	750	750	750	250	32	108,000	454,000	930,000	357,000	32T1	45,000	23,700	22	18	16	32T2	38,200	24,900	18	9	4.5
1006-854-06	250	250	250	750	72	298,000	170,000	174,000	207,000	72T1	45,000	22,600	20	15	13	72T2	38,400	23,800	14	7	3.5
1005-854-01	750	250	250	750	73	90,000	38,000	319,000	103,000	73T1	43,000	21,200	22	17	15	73T2	34,300	24,300	10	5	2.5
1209-858-04	250	750	250	750	54	73,000	137,000	49,000	78,800	54T1	37,400	21,500	12	9	6	54T2	32,000	22,700	10	5	2.5
1010-858-02	750	750	250	750	50	64,000	614,000	262,000	218,000	50T1	42,700	21,200	20	16	13	50T2	34,200	22,900	10	5	2.5
1003-852-02	250	250	750	750	40	948,000	258,000	293,000	415,000	40T1	43,800	21,700	27	22	17	40T2	39,500	24,700	18	9	4.5
1310-859-05	750	250	750	750	57	228,000	269,000	415,000	294,000	57T1	42,400	20,400	20	14	12	57T2	38,800	23,300	18	9	4.5
1204-853-04	500	500	500	500	37	140,000	53,000	171,000	108,000	37T1	42,000	20,600	24	18	15	37T2	33,000	23,100	10	5	2.5
1202-851-01	750	750	750	750	60	57,000	92,000	73,000	72,600	60T1	40,800	20,800	22	16	12	60T2	34,300	24,100	10	5	2.5
1106-854-02	5	500	500	500	41	29,000	139,000	113,000	76,900	41T1	42,500	22,700	18	13	11	41T2	34,000	25,300	10	5	2.5
1207-856-03	250	500	500	500	62	45,000	66,000	277,000	93,700	62T1	43,200	21,200	28	20	15	62T2	36,400	23,700	12	6	3.0
1206-855-03	750	500	500	500	43	118,000	272,000	382,000	231,000	43T1	45,400	24,100	24	18	15	43T2	38,200	25,200	14	7	3.5
1409-857-06	500	5	500	500	68	165,000	345,000	431,000	291,000	68T1	44,100	21,500	26	20	17	68T2	38,700	24,200	14	7	3.5
1110-858-03	500	250	500	500	44	273,000	169,000	135,000	184,000	44T1	43,500	21,100	24	18	15	44T2	37,300	24,800	12	6	3.0
1107-855-02	500	750	500	500	74	73,000	191,000	69,000	98,700	74T1	44,700	23,000	24	18	15	74T2	31,800	24,200	8	4	2.0
1403-852-06	500	500	5	500	35	385,000	448,000	358,000	395,000	35T1	43,900	22,100	24	18	15	35T2	38,300	23,700	14	7	3.5
1309-858-05	500	500	250	500	51	125,000	508,000	99,000	185,000	51T1	44,300	22,200	24	19	16	51T2	33,900	23,600	10	5	2.5

* GRIP FAILURE

** 5 SPECIMENS TESTED AT DIFFERENT STRESSES TO ESTABLISH S/N CURVE

*** NO FAILURE

Figure 17: FATIGUE AND TENSILE DATA WELDED 2219-T87 ALUMINUM ALLOY SHEET INERT GAS WELDMENT EFFECTS STUDY

PANEL NO.	EXPERIMENTAL LEVEL OF CONTAMINATION IN PARTS PER MILLION (PPM)				FATIGUE DATA – TRANSVERSE WELD					TENSILE DATA – LONGITUDINAL WELD						TENSILE DATA – TRANSVERSE WELD					
	O_2	H_2	N_2	H_2O	SPEC. NO.	NO. OF CYCLES TO FAILURE F1	F2	F3		SPEC. NO.	ULTIMATE STRENGTH PSI	YIELD STRENGTH PSI	ELONGATION % LENGTH IN .50	1.0	2.0	SPEC. NO.	ULTIMATE STRENGTH PSI	YIELD STRENGTH PSI	ELONGATION % LENGTH IN .50	1.0	2.0
1406-855-05	500	500	750	500	66	165,000	12,000*	145,000	155,000	66T1	43,800	22,200	21	17	15	66T2	35,600	24,100	10	5	2.5
1201-848-05	500	500	500	5	58	102,000	338,000	226,000	198,000	58T1	43,300	20,800	24	20	16	58T2	39,000	23,600	16	8	4.0
1109-857-03	500	500	500	250	70	91,000	319,000	83,000	134,000	70T1	43,300	21,700	20	18	15	70T2	37,900	24,900	12	6	3.0
1306-855-04	500	500	500	750	75	182,000	110,000	218,000	163,000	75T1	45,100	23,000	22	18	15	75T2	36,100	24,600	10	5	2.5
1307-856-04	100	100	100	100	76	129,000	174,000	252,000	178,000	76T1	44,300	21,500	30	25	20	76T2	39,200	24,500	20	10	5.0
1111-859-03	750	100	100	750	31	229,000	475,000	361,000	340,000	31T1	43,500	21,600	28	21	18	31T2	38,500	23,500	16	8	4.0
1407-857-01	100	750	100	750	64	115,000	98,000	107,000	106,000	64T1	43,100	23,300	20	15	12	64T2	32,400	24,000	8	4	2.0
1410-859-01	750	750	100	100	33	249,000	82,000	86,000	121,000	33T1	43,700	21,800	24	19	17	33T2	35,900	23,900	12	6	3.0
1007-856-01	750	100	750	100	65	178,000	245,000	157,000	190,000	65T1	43,700	22,400	26	21	16	65T2	39,700	23,800	18	9	4.5
1411-860-01	100	750	750	100	52	231,000	207,000	131,000	184,000	52T1	43,700	21,700	22	18	15	52T2	39,100	26,000	16	8	4.0
1108-856-02	100	100	750	100	67	568,000	287,000	690,000	483,000	67T1	44,400	22,400	30	23	19	67T2	39,000	24,300	14	7	3.5
1011-854-02	500	500	500	500	36	204,000	74,000	121,000	122,000	36T1	42,700	21,900	18	16	13	36T2	32,500	23,100	10	5	2.5
1210-857-04	500	500	500	500	53	46,000	223,000	696,000	193,000	53T1	43,200	21,200	18	16	14	53T2	32,500	24,100	10	5	2.5
1304-823-05	500	500	500	500	55	53,000	98,000	222,000	105,000	55T1	43,100	21,500	20	17	15	55T2	36,100	25,100	12	6	3.0
1303-854-04	500	500	500	500	71	183,000	322,000	277,000	254,000	71T1	43,400	21,700	22	19	16	71T2	37,500	24,300	12	6	3.0
1308-857-05	500	500	500	500	61	173,000	214,000	290,000	221,000	61T1	42,900	21,200	18	15	14	61T2	35,200	24,000	12	6	3.0
1402-851-03	500	500	500	500	46	242,000	246,000	170,000	216,000	46T1	44,100	22,300	24	19	15	46T2	33,400	24,900	10	5	2.5
AVERAGE									176,000		43,233	21,633	20.0	17.0	14.5		34,533	24,250	11.0	5.5	2.75
901-837-02	5	5	5	5	2	104,000	1,278,000	1,438,000*	576,000	2T1	43,600	21,500	34	22	20	2T2	38,900	25,000	14	7	3.5
904-842-01	5	5	5	5	15	190,000	195,000	113,000	161,000	15T1	45,000	23,800	24	19	15	15T2	41,000	26,400	16	8	4.0
906-846-01	5	5	5	5	17	155,000	1,133,000*	1,203,000	596,000	17T1	45,600	23,800	22	19	16	17T2	40,800	26,200	14	7	3.5
907-847-02	5	5	5	5	11	597,000	473,000	2,001,000***	827,000	11T1	43,600	21,000	35	25	20	11T2	39,600	25,300	18	9	4.5
AVERAGE									462,000		44,450	22,525	28.8	21.2	17.8		40,075	25,725	15.5	7.8	3.88
610-860-04	100	5	5	5	42	271,000	1,110,000	1,289,000	729,000	42T1	43,700	21,200	31	23	18	42T2	39,800	23,900	16	8	4.0

* GRIP FAILURE

** 5 SPECIMENS TESTED AT DIFFERENT STRESSES TO ESTABLISH S/N CURVE

*** NO FAILURE

Figure 18: FATIGUE AND TENSILE DATA WELDED 2219-T87 ALUMINUM ALLOY SHEET INERT GAS WELDMENT EFFECTS STUDY

PANEL NO.	Experimental Level of Contamination in Parts per Million (PPM): O_2	H_2	N_2	H_2O	Fatigue Data – Transverse Data: SPEC. NO.	No. of Cycles to Failure: F1	F2	F3		Tensile Data – Longitudinal Weld: SPEC. NO.	ULTIMATE STRENGTH PSI	YIELD STRENGTH PSI	Elongation % in Length: .50	1.0	2.0	Tensile Data – Transverse Weld: SPEC. NO.	ULTIMATE STRENGTH	YIELD STRENGTH PSI	Elongation % in Length: .50	1.0	2.0
604-840-03	250	5	5	5	21	401,000*			401,000	21T1	43,400	21,000	30	23	18	21T2	39,700	23,100	18	9	4.5
609-848-01	250	5	5	5	4	65,000	572,000	1,324,000	366,000	4T1	44,000	21,700	25	20	15	4T2	39,900	24,500	16	8	4.0
602-840-01	500	5	5	5	23	648,000			648,000	23T1	44,000	21,800	31	24	20	23T2	39,100	24,900	14	7	3.5
603-840-02	500	5	5	5	25	2,582,000***	462,000	222,000	642,000	25T1	45,000	22,900	30	24	19	25T2	39,400	25,500	14	7	3.5
509-860-03	5	100	5	5	24	798,000	506,000	414,000	551,000	24T1	43,400	21,000	32	23	20	24T2	39,100	24,100	18	9	4.5
606-846-03	5	250	5	5	5	341,000	465,000	376,000	391,000	5T1	44,400	22,800	22	20	16	5T2	40,300	25,100	14	7	3.5
503-840-04	5	500	5	5	12	126,000			126,000	12T1	43,000	20,800	22	18	16	12T2	38,000	23,800	14	7	3.5
507-847-01	5	500	5	5	10	208,000	124,000	127,000	148,000	10T1	43,700	22,100	26	21	17	10T2	39,100	25,100	16	8	4.0
505-842-02	5	2,500	5	5	13	8,000			8,000	13T1	37,400	20,900	14	11	8	13T2	27,200	23,800	8	4	2.0
710-860-06	5	5	100	5	27	564,000	237,000	2,000,000***	644,000	27T1	43,600	21,800	32	25	19	27T2	38,000	20,700	18	9	4.5
703-841-04	5	5	250	5	20	163,000			163,000	20T1	43,400	21,200	28	20	16	20T2	39,400	24,800	20	10	5.0
704-841-05	5	5	250	5	29	234,000	161,000	188,000	192,000	29T1	44,000	22,000	30	23	17	29T2	39,500	25,000	18	9	4.5
707-847-03	5	5	500	5	1	598,000	2,000,000***	2,100,000***	1,359,000	1T1	42,500	20,500	32	23	18	1T2	39,100	23,800	18	9	4.5
709-847-06	5	5	500	5	7	403,000			403,000	7T1	44,000	21,600	28	22	17	7T2	38,800	24,000	18	9	4.5
807-855-06	5	5	5	100	19	1,016,000*			1,016,000	19T1	43,700	21,400	30	22	17	19T2	38,000	23,900	18	9	4.5
809-860-05	5	5	5	100	28	733,000*	954,000	210,000	528,000	28T1	44,100	25,700	32	23	17	28T2	38,600	25,700	18	9	4.5
802-838-02	5	5	5	250	30	474,000	313,000	471,000	412,000	30T1	43,400	21,300	28	21	18	30T2	38,200	23,100	18	9	4.5
806-852-01	5	5	5	250	22	711,000			711,000	22T1	44,900	22,700	30	23	20	22T2	39,300	23,700	16	8	4.0
803-838-03	5	5	5	500	26	237,000	61,000	679,000	214,000	26T1	44,100	22,600	30	21	16	26T2	38,300	25,000	16	8	4.0
805-851-05	5	5	5	500	18	409,000			409,000	18T1	42,400	20,700	30	21	17	18T2	38,500	23,500	16	8	4.0

* GRIP FAILURE

** 5 SPECIMENS TESTED AT DIFFERENT STRESSES TO ESTABLISH S/N CURVE

*** NO FAILURE

Figure 19: FATIGUE AND TENSILE DATA WELDED 2219-T87 ALUMINUM ALLOY SHEET INERT GAS WELDMENT EFFECTS STUDY

Metallographic Analysis

Y_{11} = Volume Percent Porosity

Tensile Test

Y_{12} = Longitudinal — Ultimate Strength (psi)

Y_{13} = Longitudinal — Yield Strength (psi)

Y_{14} = Longitudinal — Elongation (percent in 2.0 inch length)

Y_{15} = Transverse — Ultimate Strength (psi)

Y_{16} = Transverse — Yield Strength (psi)

Y_{17} = Transverse — Elongation (percent in 2.0 inch length)

Fatigue Test

Y_{18} = Transverse — Cycles to Failure

FACTORIAL ANALYSIS

The results of the complete 2^4 factorial part of the experiment, where each contaminant was considered at two levels (250 and 750 ppm) were analyzed first. The purpose of this analysis was to estimate the effects and interactions of the contaminants and determine their significance. The results of this analysis are shown in Figure 20. The main effect of each contaminant is the average change in weld quality (Y_i) resulting from increasing that contaminant from 250 to 750 ppm. For example, the average effect of increasing hydrogen from 250 to 750 ppm is to decrease the longitudinal ultimate strength by 1762.5 psi.

The interaction effect provides a means of determining whether the effects of the contaminants are independent or whether the effect of increasing a contaminant depends on the levels of the other contaminants. For example, if there is an interaction between two (or more) contaminants this means that the effect of increasing one of those contaminants changes as the levels of the other contaminants change.

All effects and interactions have been tested for significance. Significant effects are indicated by a single asterisk and highly significant effects by a double asterisk. An effect is considered significant if there is less than a 5 percent chance (α = 0.05) that a difference this large could occur due to the random variation between weld panels and highly significant if there is less than a 1 percent chance (α = 0.01).

If an interaction is significant, the contaminants are not independent. When studying significant effects, the highest order interactions should be studied first and then all lower-order interactions or main effects contained within the higher-order interaction will also be explained.

EFFECT	RADIOGRAPHIC ANALYSIS								DENSITY		METALLOGRAPHIC POROSITY Vf (%)	TENSILE STRENGTH						FATIGUE
	Y = DEFECTS PER INCH OF WELD BEAD				Y = DEFECTS PER GRAM OF WELD BEAD				WELD BEAD DENSITY	BASE METAL MINUS WELD BEAD DENSITY		LONGITUDINAL			TRANSVERSE			TRANSVERSE
	TO .024"	TO .049"	TO .150"	TOTAL	TO .024"	TO .049"	TO .150"	TOTAL				ULTIMATE PSI	YIELD PSI	ELONGATION 2.0 INCHES %	ULTIMATE PSI	YIELD PSI	ELONGATION 2.0 INCHES %	CYCLES TO FAILURE
MAIN EFFECTS																		
O_2	-1.584	0.966**	C.161*	-0.516	-0.293	0.244**	0.C43*	-0.006	0.C05669	-0.005274	-0.625	387.5	12.5	0.38	712.5	362.5	0.12	- 12,275
H_2	16.716*	0.832**	-0.111	17.436*	4.376*	0.221**	-0.C29	4.568*	-C.010099*	0.011646*	0.500	-1762.5**	- 687.5	-0.62	-2987.5**	-662.5	-0.75**	- 35,325
N_2	9.186	0.584**	C.C29	9.799	2.433	0.159**	0.009	2.601	0.004406	-C.004476	0.125	687.5	362.5	0.88	212.5	212.5	0.25	82.225*
H_2O	22.334**	1.124**	0.066	23.524**	5.832**	0.294**	0.015	6.142**	-0.C17616**	0.C16436**	0.500	-1762.5**	- 937.5	-2.62**	-2362.5**	-687.5	-0.38*	-111,325*
2-FACTOR INTERACTIONS																		
$O_2 \times H_2$	5.966	0.676**	-0.074	6.569	1.715	0.184**	-0.019	1.880	-0.003444	0.002994	0.000	837.5*	287.5	0.88	387.5	137.5	0.25	19,475
$O_2 \times N_2$	6.436	0.689**	0.006	7.131	1.868	0.190**	0.004	2.062	-0.002219	0.003236	-0.125	- 262.5	737.5	-2.62**	1387.5*	262.5	0.50**	- 20,575
$O_2 \times H_2O$	10.084	0.869**	0.029	10.981	2.718	0.231**	0.006	2.955	-0.002611	0.002859	C.250	- 212.5	- 712.5	-0.12	-1037.5	-287.5	-0.38*	- 18,025
$H_2 \times N_2$	9.621	0.944**	0.059	10.624	2.658	0.256**	0.015	2.929	0.003869	-0.002784	C.500	487.5	37.5	0.88	- 312.5	537.5	-0.12	- 67,025
$H_2 + H_2O$	15.284*	0.954**	-0.024	16.214*	4.095*	0.249**	-0.003	4.350*	-0.008044*	0.008084	-0.125	-1062.5*	237.5	-2.12**	-1387.5*	-162.5	-0.50**	-100,075*
$N_2 \times H_2O$	6.814	0.691**	-0.089	7.416	1.937	0.191**	-0.023	2.105	0.006396	-0.005389	-C.50C	- 462.5	-1112.5	1.38	1462.5*	162.5	0.50**	- 11,525
3- FACTOR INTERACTIONS																		
$O_2 \times H_2 \times N_2$	10.371	1.139**	0.081	11.591	2.744	0.302**	0.020	3.066	-0.002876	0.003349	C.000	- 612.5	312.5	-0.12	- 387.5	237.5	0.12	- 22,325
$O_2 \times H_2 \times H_2O$	7.534	0.759**	-0.016	8.276	2.038	0.207**	-0.002	2.242	-0.003379	0.001356	0.375	1037.5*	362.5	0.88	1687.5*	387.5	0.00	62,725
$O_2 \times N_2 \times H_2O$	9.064	0.726**	-0.081	9.709	2.434	0.197**	-0.022	2.609	-0.003899	0.005079	0.750*	-1212.5**	- 587.5	-1.62*	- 762.5	-537.4	-0.25	- 27,325
$H_2 \times N_2 \times H_2O$	5.379	0.731**	0.101	6.211	1.542	0.196**	0.027	1.765	0.004254	-0.004096	-0.125	637.5	62.5	0.88	- 812.5	-112.5	-0.62**	- 61,775
4-FACTOR INTERACTIONS																		
$O_2 \times H_2 \times N_2 \times H_2O$	14.129*	1.026**	0.184*	15.339*	3.725*	0.271**	0.047*	4.043*	-0.004841	0.004131	0.375	-1162.5**	- 212.5	-0.62	- 687.5	437.5	-0.38*	- 17,075
MEAN OF FACTORIAL	17.333	0.916	C.159	18.408	4.511	0.241	0.042	4.794	2.821097	0.017044	1.06	43,019	21,719	14.19	36,744	23,956	3.31	242,712
MEAN AT CENTER (ALL AT 500 ppm)	26.330	0.483	C.088	26.900	6.501	0.122	0.022	6.645	2.816647	0.022070	1.33	43,223	21,633	14.50	34,533	24,250	2.75	185,167
MEAN AT BASE GAS (ALL AT 5 ppm)	0.365	0.318	0.098	0.780	0.106	0.093	0.028	0.228	2.843575	-0.005840	0.125	44,450	22,525	17.75	40,075	25,725	3.88	540,000
STANDARD DEVIATION	10.82	0.213	0.122	10.76	2.530	0.060	0.030	2.518	0.006172	.007099	0.516	756	1174	1.31	1264	746	0.31	59,000
DEGREES OF FREEDOM	5	5	5	5	5	5	5	5	5	5	5	16	16	16	16	16	16	5

* SIGNIFICANT = .05
** HIGHLY SIGNIFICANT = .01

Figure 20: 2^4 FACTORIAL ANALYSIS
LOW LEVEL (-1) = 250 ppm, HIGH LEVEL (+1) = 750 ppm

Figure 20 also shows three averages for each measure of weld quality; the mean of the factorial, the mean at the center of the factorial (500 ppm), and the mean with the base gas ($\leq$ 5 ppm). The mean with the base gas can be compared with the mean at the center of the factorial to show the effect of welding with all contaminants at 500 ppm. The mean of the factorial can be compared with the mean at the center to determine whether the relationship between the contaminants and weld quality is linear or curved. If the relationship is linear these two means will be approximately equal.

The standard deviation and its associated degrees of freedom are also tabulated in Figure 20 for each measure of weld quality. For all porosity, density, and fatigue data, the standard deviation is based on the repeated welds at the center of the factorial. For these measures of weld quality the variability increases as the value of Y_i increases; therefore, the repeated welds with the base gas were not included. For the tensile data, the variability did not change as the strength increased; therefore, all repeated welds were used to estimate the standard deviation. The standard deviation shown was used to test the significance of the effects and interactions.

REGRESSION ANALYSIS

The data was next analyzed to obtain regression equations relating the levels of contamination to each measure of weld quality. A stepwise regression procedure programmed for the 1107 computer was used to obtain regression equations for each measure of weld quality. The program computes a sequence of multiple regression equations in a stepwise manner. At each step, the variable that makes the greatest reduction in the error sum of squares (the variation between actual and estimated values) is added. The stepwise procedures continues to add terms until no further improvement can be made. Because the factorial analysis indicated that many of the interactions are significant and that some of the relationships may be nonlinear, the following model was used for the stepwise regression program.

$$
\begin{aligned}
Y_i = {} & b_o + b_1 X_1 + \dots + b_4 X_4 + b_{12} X_1 X_2 + \dots + b_{34} X_3 X_4 \\
& + b_{123} X_1 X_2 X_3 + \dots b_{234} X_2 X_3 X_4 + b_{1234} X_1 X_2 X_3 X_4 \\
& + b_{11} X_1^2 + \dots + b_{44} X_4^2
\end{aligned}
$$

where

Y_i = Weld quality

X_1 = Oxygen

X_2 = Hydrogen

X_3 = Nitrogen

X_4 = Water vapor

This model includes a constant (b_0) plus all terms from the factorial analysis plus all squared terms. For each measure of weld quality only those terms that provide a significant contribution will be included in the final equation. The regression equations obtained will be the best equations for estimating Y_i when considering the above model; i.e., the equations obtained will provide the minimum variation between the actual results obtained in the experiment and those predicted by the equation.

Two separate regression analyses have been performed using the above model. These analyses consider the levels of contamination as parts per million (ppm) and cubic centimeters per gram of weld bead (cc/gm). These two analyses are described as follows.

Regression Analysis (ppm) — In this analysis the levels of contamination, X_i, are the ppm in the shield gas envelope. For purposes of the statistical analysis the levels of contamination have been coded as:

$$X_1 = \frac{\text{Oxygen (ppm)} - 500}{250}$$

$$X_2 = \frac{\text{Hydrogen (ppm)} - 500}{250}$$

$$X_3 = \frac{\text{Nitrogen (ppm)} - 500}{250}$$

$$X_4 = \frac{\text{Water Vapor (ppm)} - 500}{250}$$

The coding results in the following values for X_i.

CONTAMINATION LEVELS

ppm	X_i
5	-1.98
100	-1.6
250	-1.0
500	0.0
750	1.0
1000	2.0

The results of the stepwise regression analysis relating weld quality (Y_i) to the contamination levels (X_i) are shown in Figure 21. This figure shows the regression coefficients (b's) for each term included in the model for a particular Y_i. A blank space means that the term was not included because it would not improve the regression equation.

REGRESSION COEFFICIENTS		RADIOGRAPHIC ANALYSIS								DENSITY		METALLOGRAPHIC POROSITY Vf (%)	TENSILE STRENGTH						FATIGUE
		Y = DEFECTS PER INCH OF WELD BEAD				Y = DEFECTS PER GRAM OF WELD BEAD				WELD BEAD DENSITY	BASE METAL MINUS WELD BEAD DENSITY		LONGITUDINAL			TRANSVERSE			TRANSVERSE
		TO 024"	TO .049"	TO .150"	TOTAL	TO .024"	TO .049"	TO .150"	TOTAL				ULTIMATE PSI	YIELD PSI	ELONGATION 2.0 INCHES %	ULTIMATE PSI	YIELD PSI	ELONGATION 2.0 INCHES %	CYCLES TO FAILURE
CONSTANT	b_o	0.346	0.289	0.1135	0.973	0.497	0.073	0.0364	0.184	2.843729	-0.006718	- 0.159	43,893.2	22,256.3	17.90	39,568.6	24,710.8	4.38	565,733.0
$C_1 = O_2$	b_1	37.028	- 1.339		36.379		- 0.387		9.475	0.023798		- 9.109		- 4,986.0	3.70		- 4,039.8	- 3.19	
$C_2 = H_2$	b_2		5.666	0.0906		- 1.668	1.524	-0.0089	2.501	-0.055221	0.055085	4.677		- 1,934.6	- 6.11		- 565.6	- 1.42	-1,447,506.0
$C_3 = N_2$	b_3			-0.2846								6.895		- 5,233.0	- 7.50		- 3,084.9		- 861,089.2
$C_4 = H_2O$	b_4							-0.1061		-0.046169	0.048942	9.143		3,457.7		-13,643.7		- 2.94	- 349,033.8
C_1C_2	b_{12}	- 45.368	- 10.323	-2.2262	- 54.671		- 2.793	-0.3104	- 18.924		-0.025901	- 19.765		- 9,161.1	12.83		- 10,707.6		1,170,000.0
C_1C_3	b_{13}	109.280			102.727	31.963		0.3111	26.879	-0.097848		- 7.989		5,160.0	-22.94	5,921.0			2,156,142.0
C_1C_4	b_{14}	128.105	4.077		124.948	37.043	0.984		31.674			- 7.833							
C_2C_3	b_{23}	- 291.900	- 3.507		- 293.235	- 79.352	- 0.980		- 79.976	0.147796	-0.095920						14,846.1		
C_2C_4	b_{24}	- 242.374	12.445		- 242.568	- 65.956			- 66.061	0.106230			- 6,999.5	18,728.7	-25.52	-28,375.1	7,196.1	- 5.54	1,690,687.0
C_3C_4	b_{34}	- 242.877			- 244.525	- 62.695	3.208		- 64.670	0.104080		34.327		18,607.6			29,192.8	3.14	
$C_1C_2C_3$	b_{123}		- 30.511	2.8556			- 8.163						35,506.6	45,862.4	17.82	18,903.0		17.18	3,732,061.0
$C_1C_2C_4$	b_{124}		- 43.020				- 11.474			-0.313889									
$C_1C_3C_4$	b_{134}		- 75.607	1.9983			- 19.866	0.5549				- 84.204		-47,520.0	-24.17		- 53,937.7		
$C_2C_3C_4$	b_{234}	3700.963	- 84.707		3696.638	1008.744	- 22.547		961.052	-1.558196	0.821496	- 47.919		-58,868.1	49.04	-21,024.5	- 94,782.0	-18.50	-4,612,720.0
$C_1C_2C_3C_4$	b_{1234}	-3454.515	589.403		-3234.374	-1018.781	158.077		-778.182	2.795562	-1.109247	236.884	-77,208.0				171,591.3		
C_1^2	b_{11}	- 113.150	6.273	0.8192	- 107.030	- 15.404	1.734		- 27.136		0.001664	30.386		12,983.9			13,925.1	4.90	
C_2^2	b_{22}	118.927	- 2.122	0.4688	120.835	32.502	- 0.578	0.1428	30.607			1.074	- 2,593.8	653.1		- 4,785.2			685,284.1
C_3^2	b_{33}											- 16.539		7,493.9	19.33				3,022,714.0
C_4^2	b_{44}										-0.047731	- 17.809		-12,919.6	- 3.82	30,143.0	- 7,383.8	6.52	
COEFFICIENT OF DETERMINATION R^2		.934	.889	.669	.936	.934	.892	.651	.938	.889	.894	.696	.485	.286	.665	.762	.234	.687	.511
COEFFICIENT OF CORRELATION R		.966	.943	818	.968	.966	.944	.807	.968	.943	.946	.834	.697	.535	.816	.873	.488	.829	.715
STANDARD ERROR OF THE EST. S_{y_i}		11.51	.380	.128	11.55	3.035	.101	.035	3.061	.0061	.0058	1.08	1.028	.985	1.662	1.420	.895	.493	185,298
DEGREES OF FREEDOM DF		54	52	58	54	55	52	59	53	55	57	50	61	50	54	58	53	56	55

CODE FOR CONTAMINATION LEVELS (C_i) WHERE $C_i = R_i/W$ = CC OF GAS (i)/gm OF WELD BEAD
C_1 = CC OF O_2/gm OF WELD BEAD; C_3 = CC OF N_2/gm OF WELD BEAD; R_i = CC OF GAS (i)/INCH OF WELD
C_2 = CC OF H_2/gm OF WELD BEAD; C_4 = CC OF H_2O/gm OF WELD BEAD; W = GRAMS/INCH OF WELD

Figure 21: REGRESSION ANALYSIS (CC/gm)

The following information is also included in Figure 21: (1) the coefficient of determination (R^2) which is a measure of the portion of the variation of Y_i, which can be explained by the fitted equation; (2) the coefficient of multiple correlation (R) which is a number between 0.0 and 1.0, which indicates the degree of combined relationship of the independent variables (X_i's) to the dependent variable (Y_i's); (3) the standard error of the estimate (Sy_i) which is a measure of the variation of the actual test results of Y_i from the estimated values over the various levels of the X_i's; and (4) the degrees of freedom (DF) associated with the estimate of Sy_i. This is the number of test results (66) minus the number of terms (b's) in the regression equation.

Regression Analysis (cc/gm) — In this analysis the contamination level is in terms of the cubic centimeters of contaminant available per gram of weld bead formed (C_i). The value X_i is replaced by C_i for each contaminant in the regression model previously described.

C_1 = cc of O_2/gm of weld bead

C_2 = cc of H_2/gm of weld bead

C_3 = cc of N_2/gm of weld bead

C_4 = cc of H_2O/gm of weld bead

where

$$C_i = \frac{R_i}{W} = \text{cc of Contaminant (i)/gram of weld bead}$$

R_i = cc of Contaminant (i)/inch of weld bead

W = Grams/inch of weld bead

This results in the following values for R_i

CONTAMINATION LEVEL

ppm	R_i = cc/in.
5	0.01134
100	0.2269
250	0.5672
500	1.1345
750	1.7017
1000	2.2690

The appropriate value of R_i is divided by the value of W (gram/inch of weld bead) for each weld panel. The resulting values of C_i are shown in Figures 14 through 16.

The results of the stepwise regression analysis relating weld quality (Y_i) to the contamination levels (C_i's) are shown in Figure 22. Figure 22 contains the same information as previously described in Figure 21.

STATISTICAL CONCLUSIONS

The significant effects and interactions from the factorial analysis may be further studied by the use of an equation that contains all terms in the significant effect. This equation can then be used to calculate the average values for selected combinations of the contaminants. For example, to study the interaction between H_2 and H_2O for fatigue life, an equation including all combinations of H_2 and H_2O can be written as follows:

$$Y = \text{Mean of Factorial} + \frac{1}{2}\left[\text{Effect x } H_2 + \text{Effect x } H_2O + \text{Effect x } H_2 \text{ x } H_2O\right]$$

$$= 242{,}712 + \frac{1}{2}\left[-\ 35{,}325 \text{ x } H_2 - 111{,}325 \text{ x } H_2O - 100{,}075 \text{ x } H_2 \text{ x } H_2O\right]$$

The above numerical values are circled in Figure 20.

Then the average fatigue life at the combinations of the contaminants at their low (-1) and high (+1) levels may be calculated by using (-1) and (+1) in the equation to represent the levels of contamination as illustrated:

Fatigue Life		H_2 -1	H_2 +1
H_2O	-1	265,988.5	330,738.5
	+1	254,738.5	119,338.5

This shows that increasing H_2 at the low level of H_2O increases fatigue life by 65,000 cycles and increasing H_2O at the low level of H_2 decreases fatigue life by 11,000 cycles. However, if both H_2 and H_2O are increased at the same time, the fatigue life decreases by 147,000 cycles.

Tables of treatment means for all significant effects have not been calculated. However, they can easily be obtained using the above technique for any significant interaction of interest.

The actual test results from the complete experimental design have been plotted for selected measures of weld quality and will be discussed in their respective sections. These plots contain much more data than the 2^4 factorial portion of the design and are included for study of significant effects. The results of the factorial analysis (Figure 20) may be used as a guide to show which effects and interactions are significant and should be studied.

The results of the regression analysis shown in Figures 21 and 22 indicate a high degree of correlation between the levels of contamination and the radiographic results, with the exception of the large (0.050 to 0.150 inch) defects. Comparing

REGRESSION COEFFICIENTS		RADIOGRAPHIC ANALYSIS								DENSITY		METALLOGRAPHIC POROSITY Vf (%)	TENSILE STRENGTH						FATIGUE
		Y = DEFECTS PER INCH OF WELD BEAD				Y = DEFECTS PER GRAM OF WELD BEAD							LONGITUDINAL			TRANSVERSE			TRANSVERSE
		TO .024"	TO .049"	TO .150"	TOTAL	TO .024"	TO .049"	TO .150"	TOTAL	WELD BEAD DENSITY	BASE METAL MINUS WELD BEAD DENSITY		ULTIMATE PSI	YIELD PSI	ELONGATION 2.0 INCHES %	ULTIMATE PSI	YIELD PSI	ELONGATION 2.0 INCHES %	CYCLES TO FAILURE
CONSTANT	b_0	27.581	0.629	0.0948	28.474	7.137	0.163	0.0237	7.002	2.818654	0.019943	1.230	43,511.9	21,930.2	14.29	35,661.3	24,053.9	2.911	155,001.3
$X_1 = O_2$	b_1	- 3.897	0.381		- 3.977	-1.016	0.103	0.0080	-0.991	0.003317	-0.002452	- .350	202.5			374.1		.150	
$X_2 = H_2$	b_2	17.255	0.379		18.032	4.590	0.101		4.824	-0.008300	0.008408		- 516.4		- 0.75	- 1,653.9		- .444	- 36,003.2
$X_3 = N_2$	b_3	14.166	0.316		14.738	3.757	0.085		3.958							458.5	213.2	.149	50,195.2
$X_4 = H_2O$	b_4	15.533	0.495	0.0488	16.444	4.148	0.130	0.0108	4.776	-0.008671	0.008944	.145	- 629.7	- 442.6	- 0.98	- 903.9	- 203.9	- .164	- 16,301.9
X_1X_2	b_{12}	- 3.606	0.439	-0.0252	- 3.754	-0.945	0.119	-0.0070	-0.932			- .040			0.38			.825	22,350.3
X_1X_3	b_{13}		0.445				0.123	0.0073				- .243		105.1	- 0.77	175.8		.671	- 29,597.9
X_1X_4	b_{14}		0.413				0.112	0.0036		0.001364		- .196		- 294.7					
X_2X_3	b_{23}	8.876	0.443		9.613	2.400	0.120		2.678						0.21				
X_2X_4	b_{24}	11.400	0.382		11.991	3.034	0.103		3.060	-0.002597	0.002826		- 251.1		- 0.46	- 652.1	- 126.2	- .191	
X_3X_4	b_{34}	11.880	0.448		12.510	3.158	0.121		3.240		0.000895	.382		- 269.9					
$X_1X_2X_3$	b_{123}		0.448				0.121					.206		195.3					
$X_1X_2X_4$	b_{124}		0.443				0.120				0.000726	.272					70.3		- 24,832.8
$X_1X_3X_4$	b_{134}		0.305	-0.0137			0.084			0.000991				- 126.0	- 0.19				
$X_2X_3X_4$	b_{234}	7.433	0.386		8.009	2.005	0.104		2.181	-0.001419	0.000830	- .079	- 71.7	- 136.8			- 153.5		- 17,585.0
$X_1X_2X_3X_4$	b_{1234}		0.280				0.075					.085		48.0					- 11,819.5
X_1^2	b_{11}		0.116				0.032					.801		221.0			122.7	.888	
X_2^2	b_{22}	2.783	-0.059	0.0132	2.749	0.740	-0.016	0.0034	0.710				- 59.5			- 145.9			16,447.2
X_3^2	b_{33}											- .333		89.9	0.40	277.0			57,576.4
X_4^2	b_{44}	- 2.594	0.110	0.0214	- 2.265	-0.617	0.030	0.0060				- .383	- 207.9	- 305.1		491.0		.168	
COEFFICIENT OF DETERMINATION R^2		.927	.879	.650	.930	.928	.881	.650	0.929	.878	.885	.695	.502	.249	.670	.770	.161	.684	.515
COEFFICIENT OF CORRELATION R		963	.938	.806	.964	.963	.939	.806	.964	.936	.941	.834	.709	.499	.818	.877	.402	.827	.717
STANDARD ERROR OF THE EST. S_{Y_i}		12.090	.418	.129	12.064	3.210	.111	.035	3.206	.0063	.0060	1.064	1.037	.972	1.607	1.422	.890	.495	184,545
DEGREES OF FREEDOM DF		54	47	60	54	54	47	58	55	58	58	52	58	54	57	56	59	56	55

CODE FOR CONTAMINATION LEVEL (X_i)

$X_1 = \frac{O_2\ (ppm) - 500}{250}$ $X_3 = \frac{N_2\ (ppm) - 500}{250}$

$X_2 = \frac{H_2\ (ppm) - 500}{250}$ $X_4 = \frac{H_2O\ (ppm) - 500}{250}$

Figure 22: REGRESSION ANALYSIS (ppm)

the analysis of defects per inch with defects per gram shows essentially no difference in the results. This would indicate that the variation in the size of the weld bead was too small to have any effect on the level of porosity observed. Considering the level contamination as cc/gm rather than ppm results in a slightly better equation as noted by the improvement in R^2 and Sy_i for the radiographic results.

The equations for the density data also show a high correlation. A slight improvement in the equation is obtained for both ppm and cc/gm when the density of the base metal is considered. Also, the equations for cc/gm are better than those for ppm.

The equations for metallographic porosity, tensile strength, and fatigue life do not show good correlation and their usefulness is questionable. Also, considering the levels of contamination as cc/gm rather than ppm did not improve the results.

The regression equations obtained in Figures 21 and 22 have not been evaluated for their ability to estimate weld quality over the complete range covered by the experiment. The usefulness of these equations to predict weld quality has as yet not been established.

WELD SPECIMEN EVALUATION AND RESULTS

RADIOGRAPHIC ANALYSIS

The radiographic analysis is one of the most significant tests conducted in this study in that the size, distribution, and frequency of porosity were determined for each level of contamination. The composite radiographic data, Figures 10, 11, 12, and 13 show: (1) the location of porosity (top, center, and bottom of the weld); (2) the number of pores within a specific size (top, center, and bottom of the weld); and (3) the total number of pores per inch of weldment.

There are many ways to evaluate the data, such as variation of size and distribution with addition of contaminants. In Phase II, the total defects were statistically evaluated and related to individual gases and combinations of gases. Figure 23 is a plot of the individual gas effects. Both hydrogen and water vapor increased porosity. Hydrogen causes the greatest increase in porosity, becoming significant above 250 ppm. The level of porosity remained at the base gas condition with the addition of oxygen and nitrogen.

The frequency of residual porosity, which occurred with base gas, was not reduced by either nitrogen or oxygen.

Figure 24 shows the two factor reactions with other contaminants remaining at 250 ppm. Starting with the upper curve, the following observations are made:

1) Oxygen, nitrogen, and oxygen-hydrogen combination reduced the number of defects;
2) Oxygen and water vapor addition only slightly increased the number of defects;
3) Nitrogen and water vapor, and nitrogen and hydrogen increased porosity;
4) Hydrogen and water vapor, as expected, caused the greatest increase in porosity.

Figure 25 shows the effect of individual gas additions, with other contaminants at the 250 ppm level. At this level of contamination, all gas additions decreased porosity.

Figure 26 shows the effect of addition of individual gases with all other contaminants held at 500 ppm. At this level of contamination the graphs show:

1) The number of defects is increased with addition of N_2, H_2O, and H_2;
2) The number of defects is decreased with additions of oxygen below 250 ppm and increased with addition of oxygen above 250 ppm;
3) Increasing any of the individual contaminants above 250 ppm increases porosity, with oxygen and nitrogen additions resulting in the highest porosity levels.

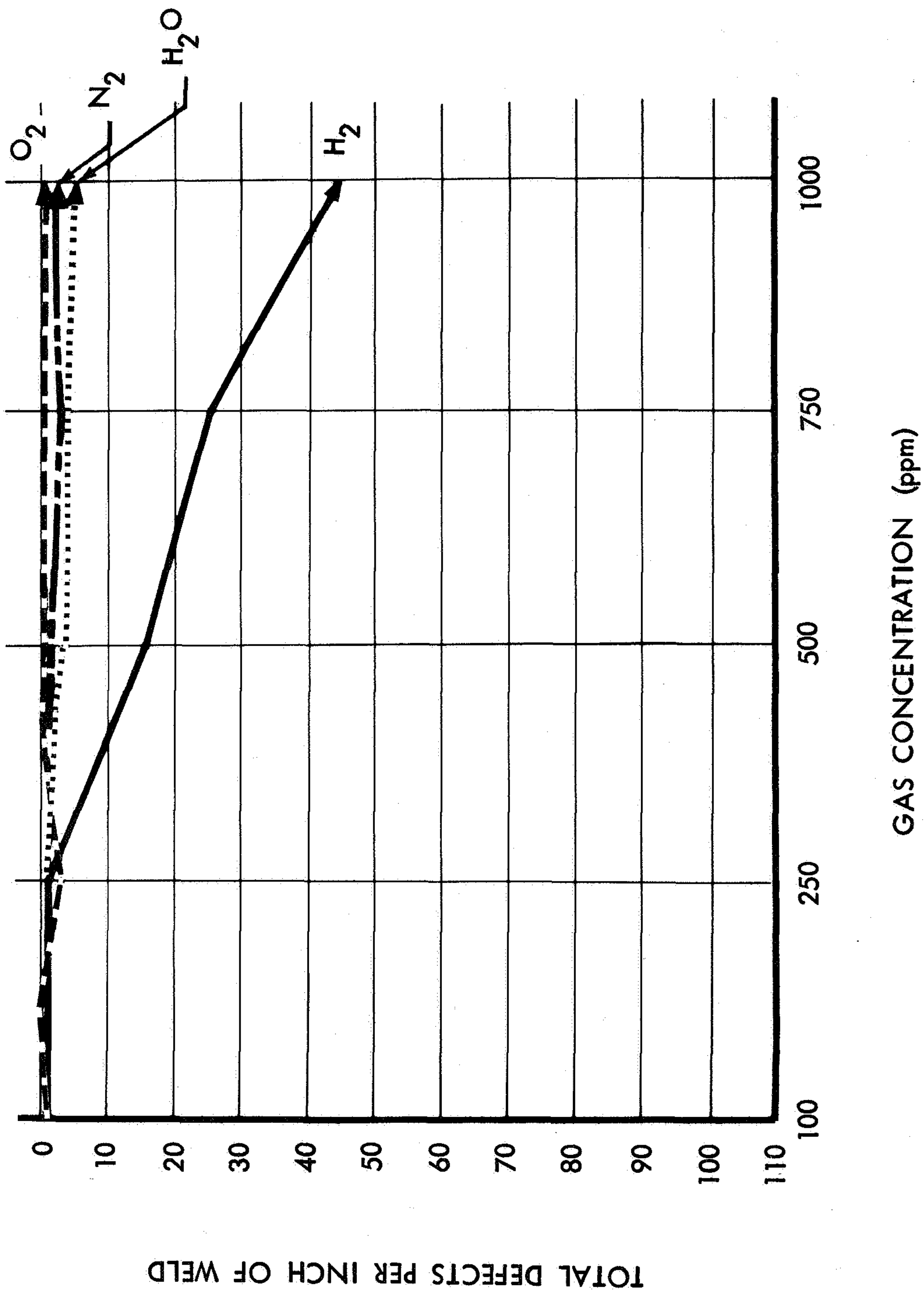

Figure 23 : EFFECT OF INDIVIDUAL GASES CAUSING WELD BEAD DEFECTS (ALL OTHER GASES AT 5 PPM)

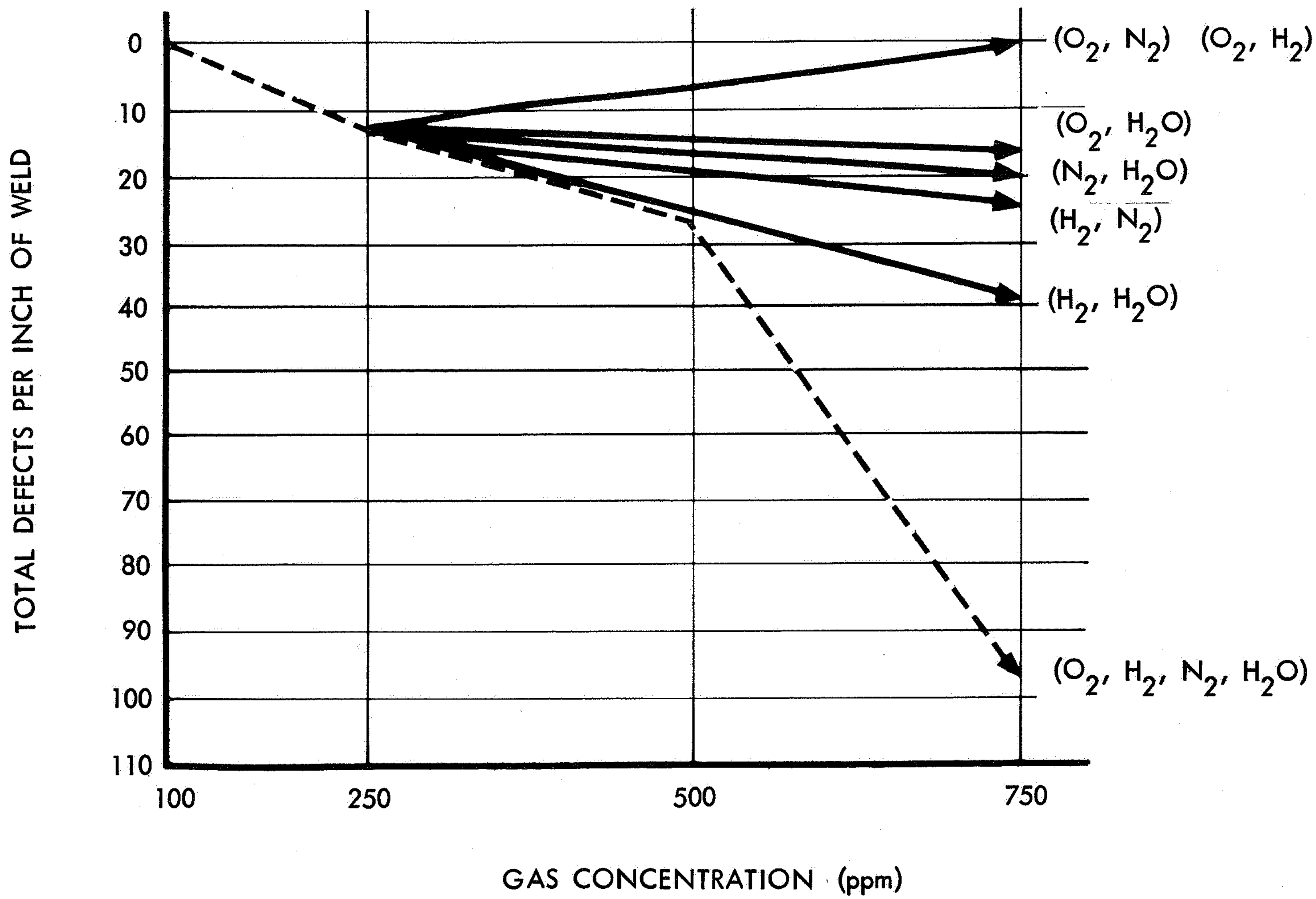

Figure 24 : EFFECT OF COMBINATION OF GASES CAUSING WELD BEAD DEFECTS (ALL OTHER GASES AT 250 PPM)

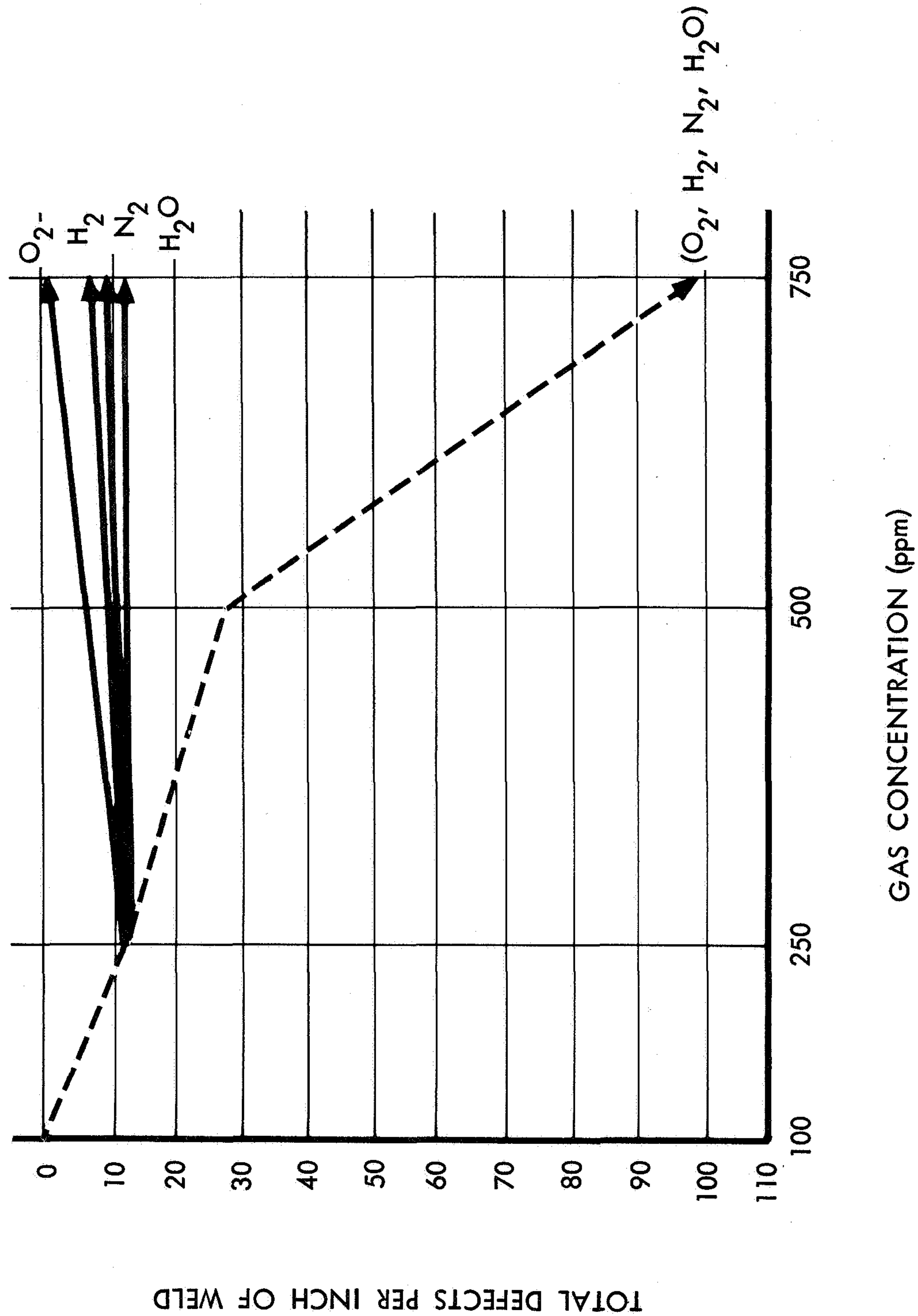

Figure 25: EFFECT OF INDIVIDUAL GASES CAUSING WELD BEAD DEFECTS (ALL OTHER GASES AT 250 PPM)

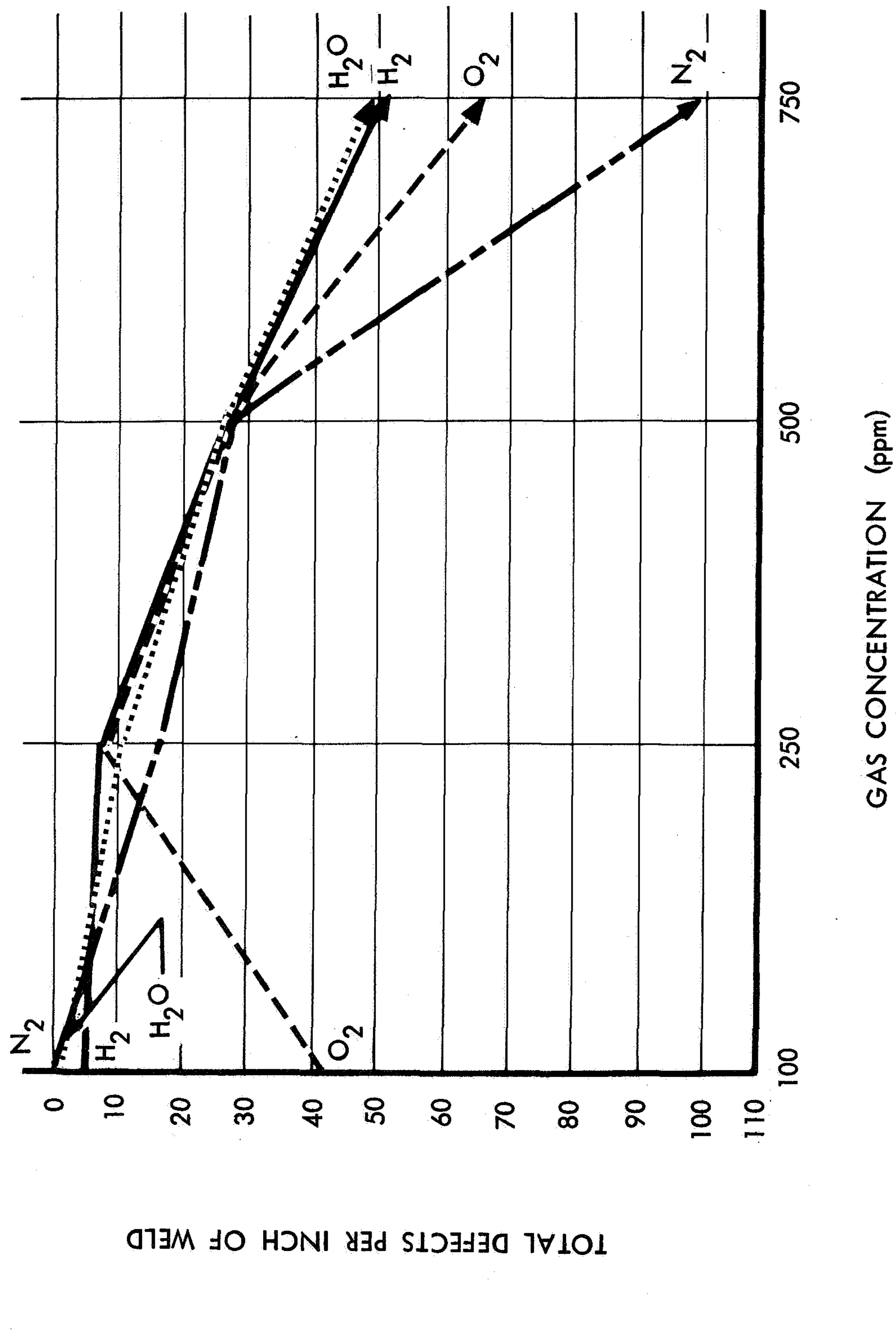

Figure 26: EFFECT OF INDIVIDUAL GASES CAUSING WELD BEAD DEFECTS (ALL OTHER GASES AT 500 PPM)

Figure 27 shows the three factor relationships. Again, those combinations that include oxygen predominantly show fewer defects per inch. Those combinations including hydrogen and water vapor at the high levels show more defects per inch.

Figure 28 shows the two-factor effects with all other contaminants held at 100 ppm. Increases in the number of defects per inch are generally noted with the exception of the nitrogen-oxygen combination.

GRAVIMETRIC POROSITY ANALYSIS

Ten plates of 2219-T87 material from one heat lot were used in the Phase II study. Density was found to change, Figure 29, from plate to plate, which required a base metal sample to be checked for each of the weldments.

The accumulated density and metallographic data is tabulated in Figures 14, 15, and 16. Figure 30 is a graphic plot of density data as related to total cubic centimeters of contamination. The type of gases added are identified by their molecular formula. Some of the gas additive effect on density of the weld bead are easily observed. It is of interest to note that the density of the weld bead was often higher than that of the base metal.

The statistical analysis of the density data is graphically illustrated in Figures 31 through 36. The gas contamination effects shown in this graph follow closely the trends established by the radiographic porosity analysis, except that density increases caused by oxide formation caused some differences.

METALLOGRAPHIC EVALUATION

The metallographic specimens were cross sectioned and examined in the polished and etched conditions.

The porosity was measured as a volume fraction of the total weld portion in the polished condition. Some specimens showed relief from polishing effects simulating cracks.

In general, the porosity was localized along each side of the weld bead. For this reason, the grid used for volume fraction analysis was placed to cover a portion of the central area as well as the porous area. The results of this technique are reproducible within +1 percent for volume fractions up to approximately 10 percent. Above 10 percent the accuracy decreases. The values are given in Figures 14, 15, and 16.

In general, the eteched microstructure remained the same. The central area of the welds exhibit an acicular etch pattern. At higher magnifications the structure is dendritic. The heat affected zone (HAZ) remained about the same width on each sample, range of 0.130 to 0.150 inch. The eutectic melting within the HAZ appears normal with no evidence of porosity. Radiographically, this zone may show

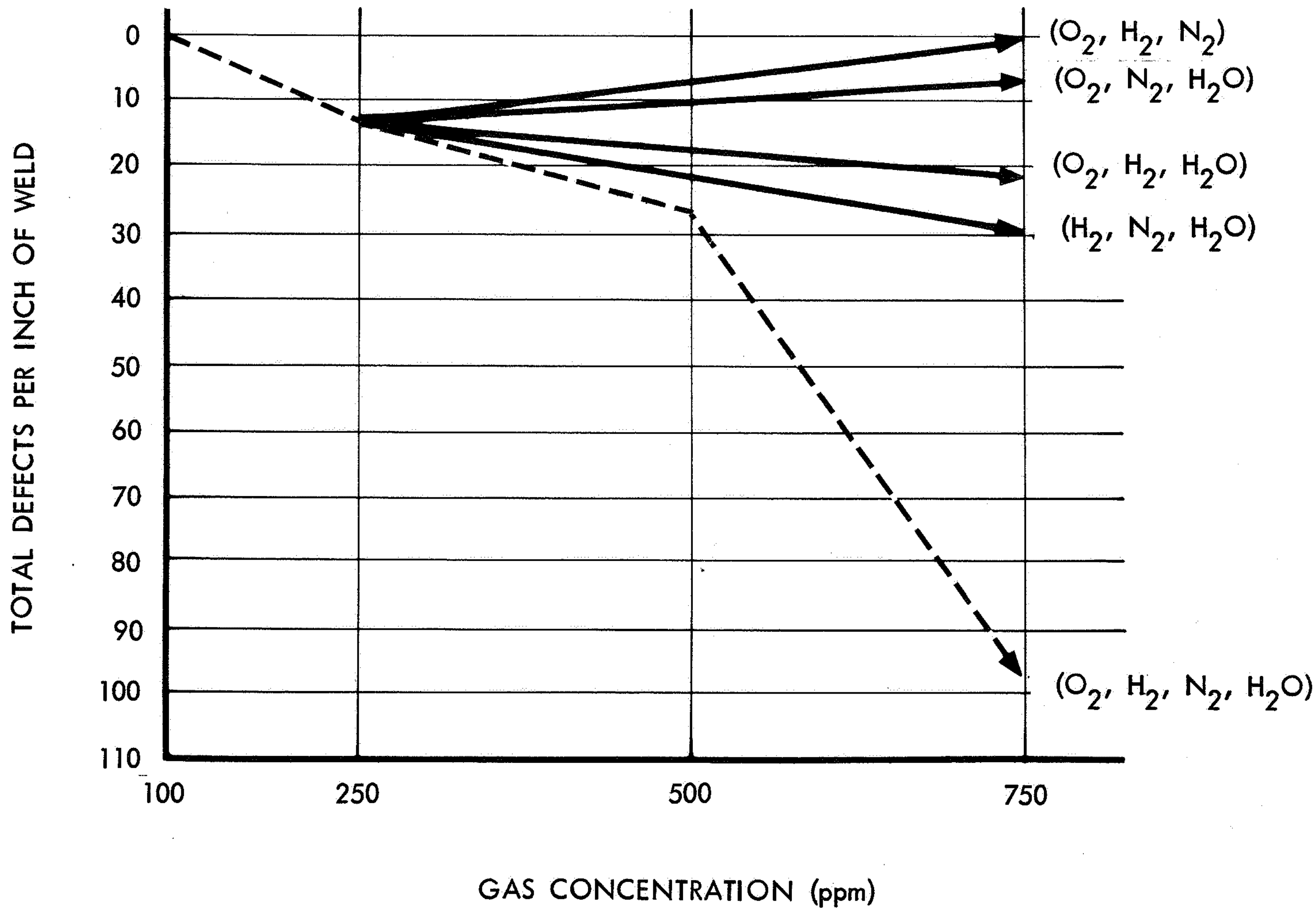

Figure 27: EFFECT OF COMBINATION OF GASES CAUSING WELD BEAD DEFECTS (ALL OTHER GASES AT 250 PPM)

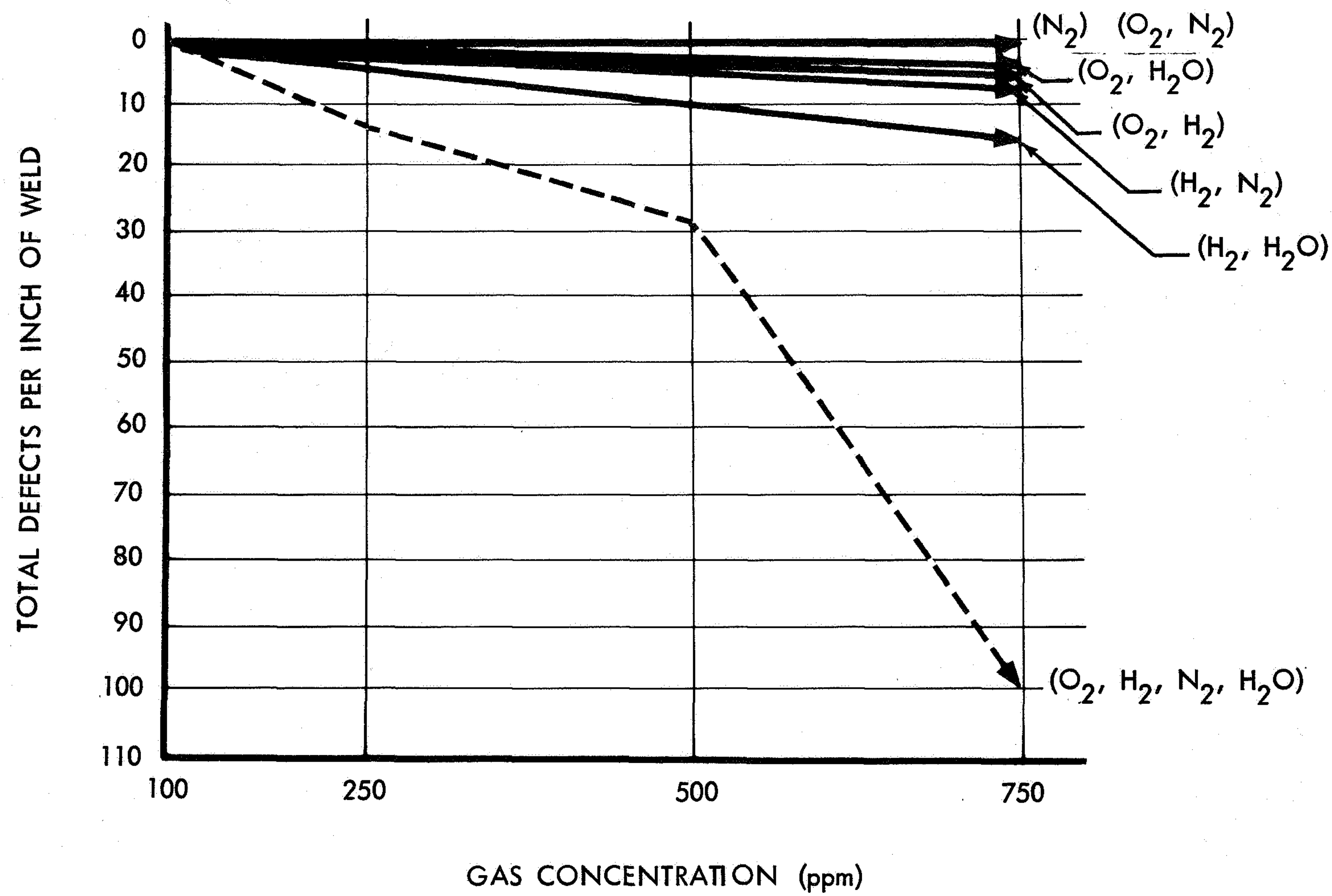

Figure 28: EFFECT OF COMBINATION OF GASES CAUSING WELD BEAD DEFECTS (COMPARISON WITH ALL GASES AT 100 PPM)

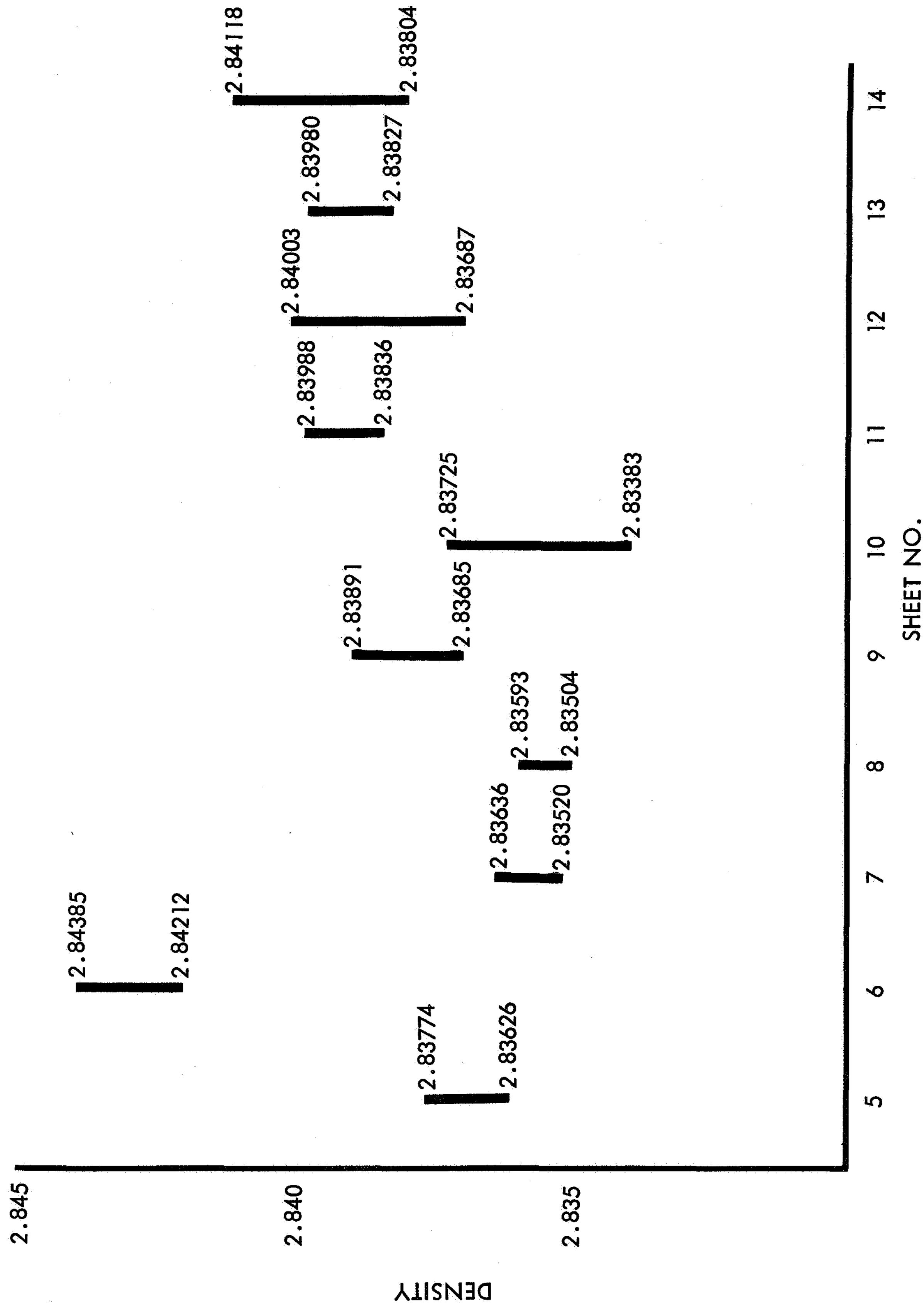

Figure 29: DENSITY VARIATIONS IN BASE METAL

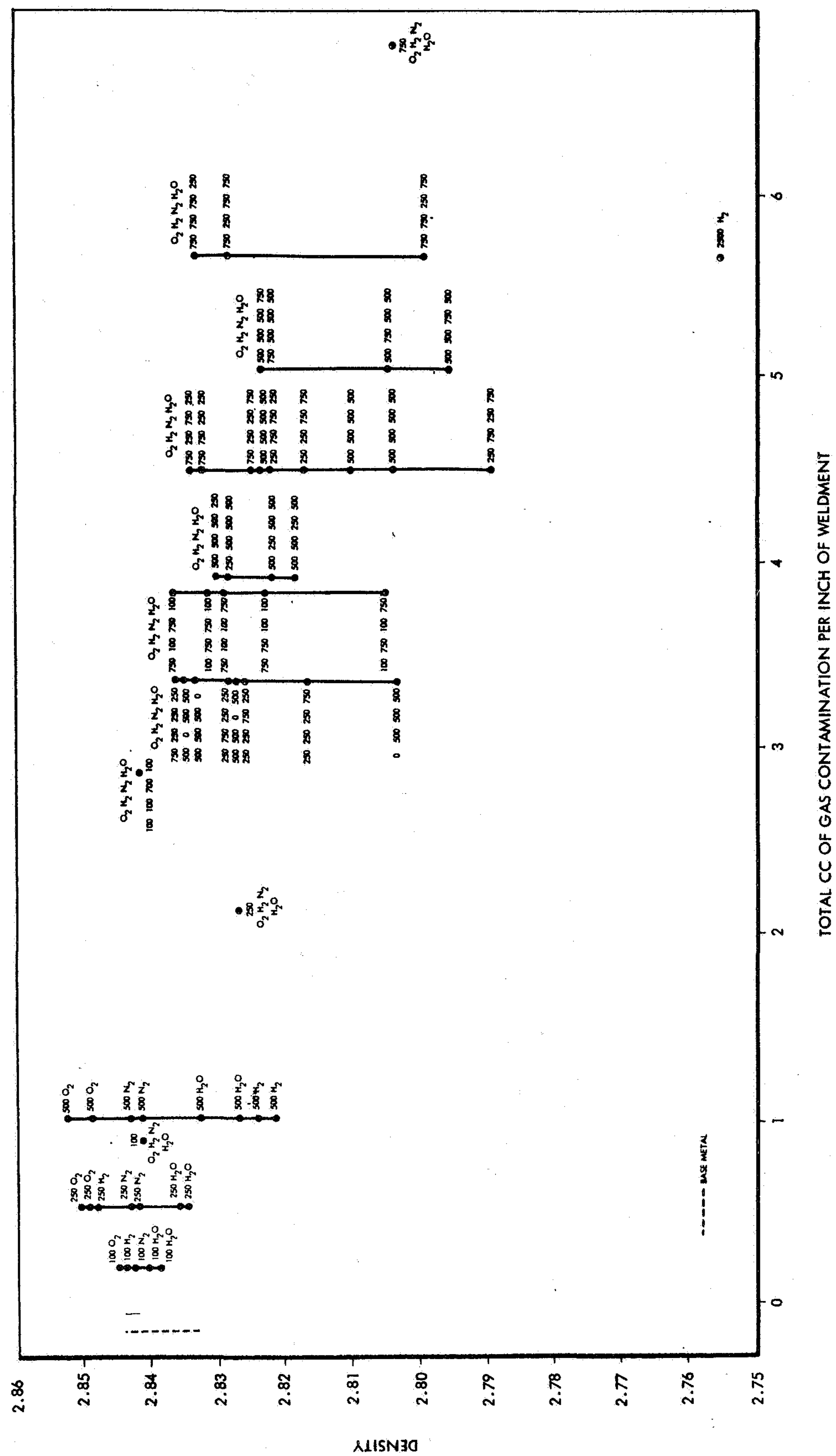

Figure 30: DENSITY TRENDS

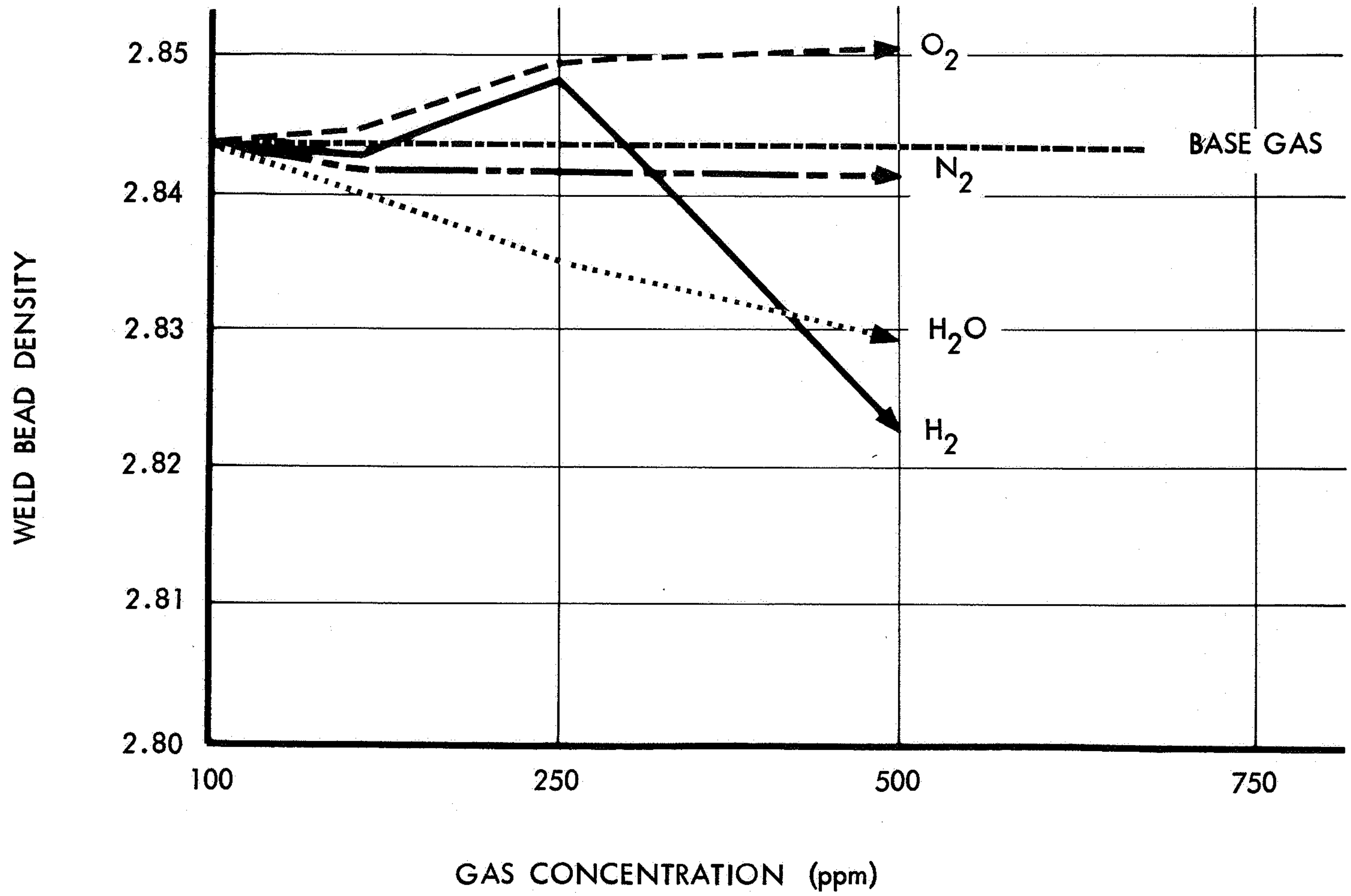

Figure 31: EFFECT OF INDIVIDUAL GASES ON WELD BEAD DENSITY (ALL OTHER GASES AT 5 PPM)

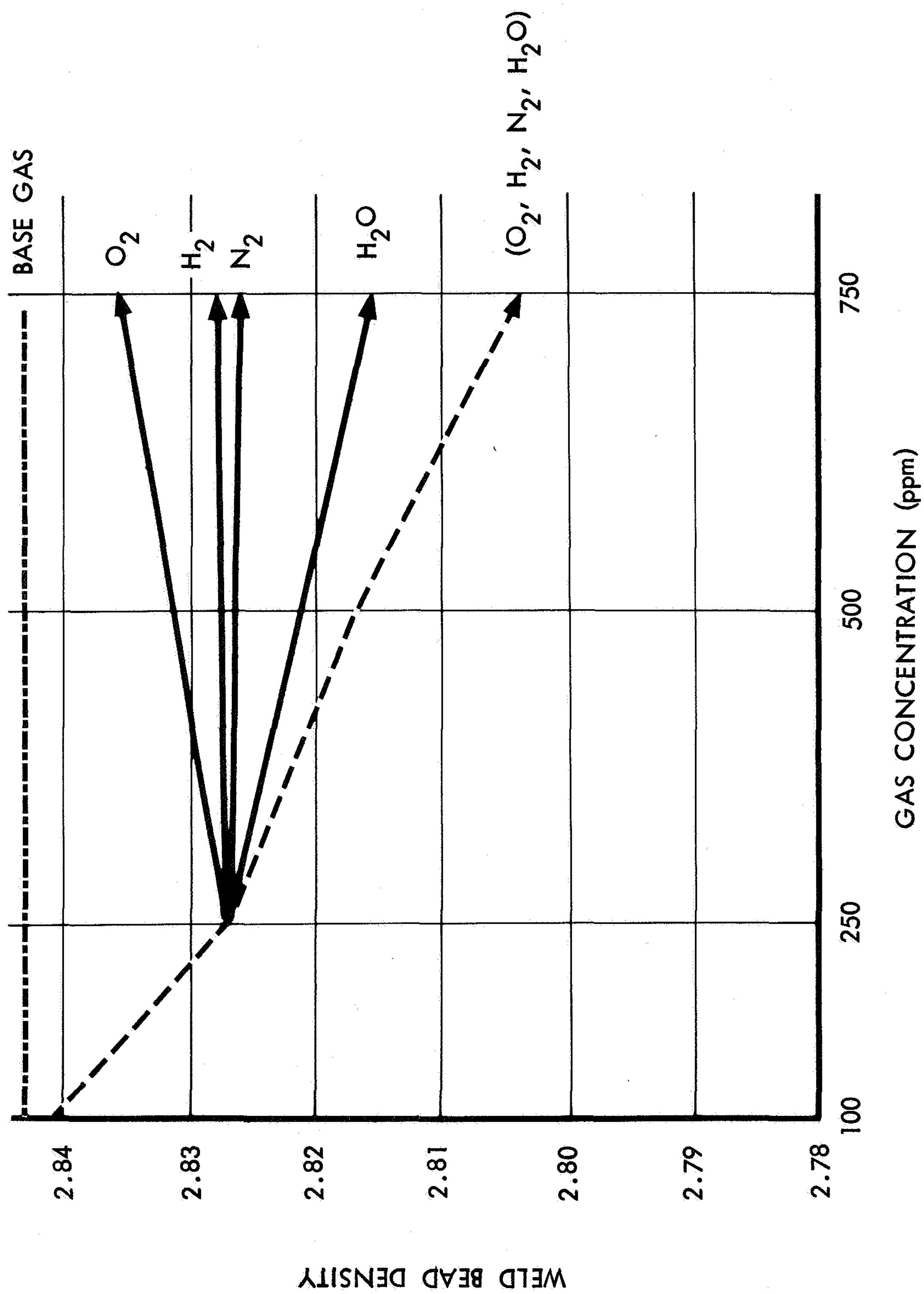

Figure 32 : EFFECT OF INDIVIDUAL GASES ON WELD BEAD DENSITY (ALL OTHER GASES AT 250 PPM)

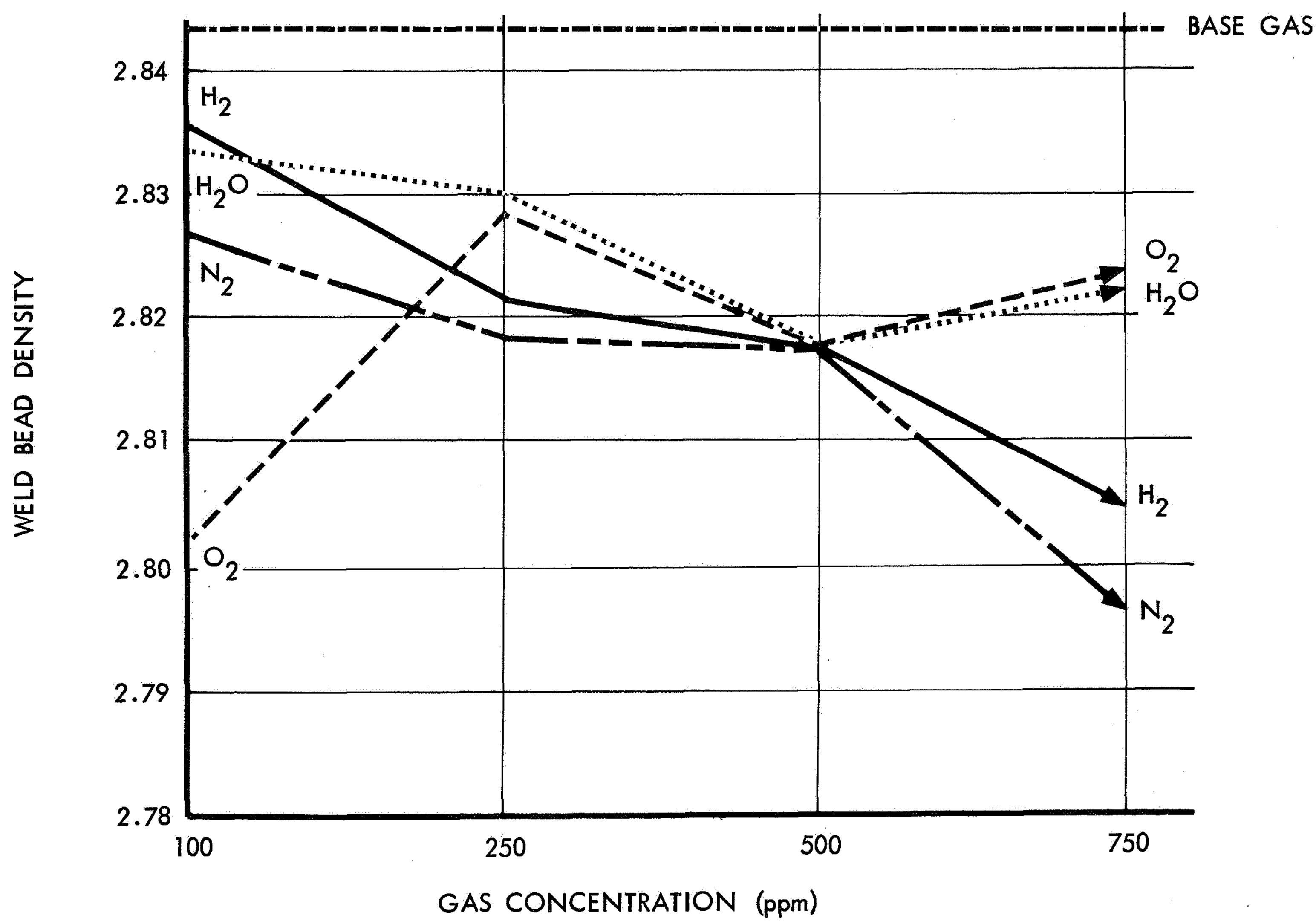

Figure 33: EFFECT OF INDIVIDUAL GASES ON WELD BEAD DENSITY (ALL OTHER GASES AT 500 PPM)

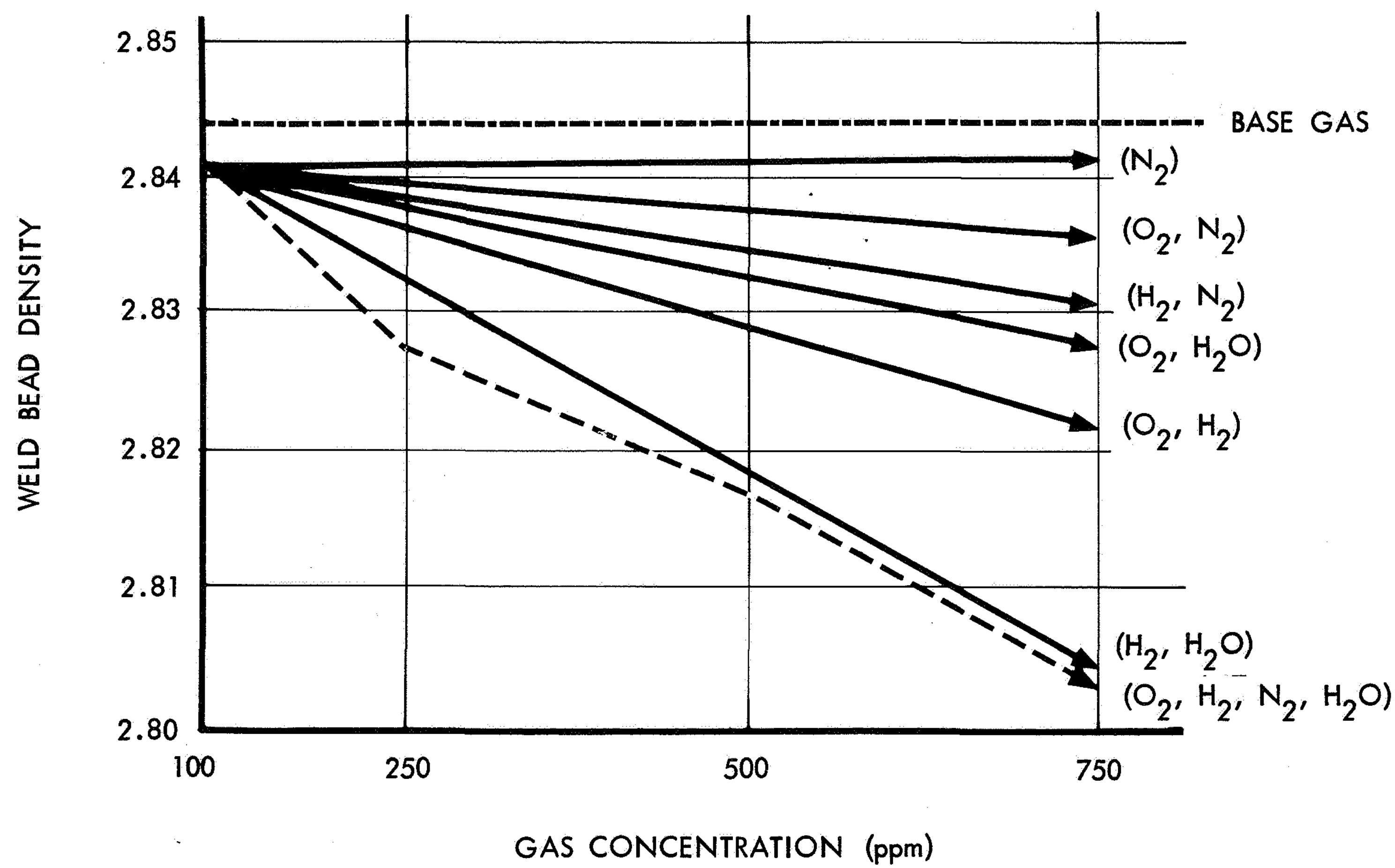

Figure 34: EFFECT OF COMBINATIONS OF GASES ON WELD BEAD DENSITY (COMPARISON WITH ALL GASES AT 100 PPM)

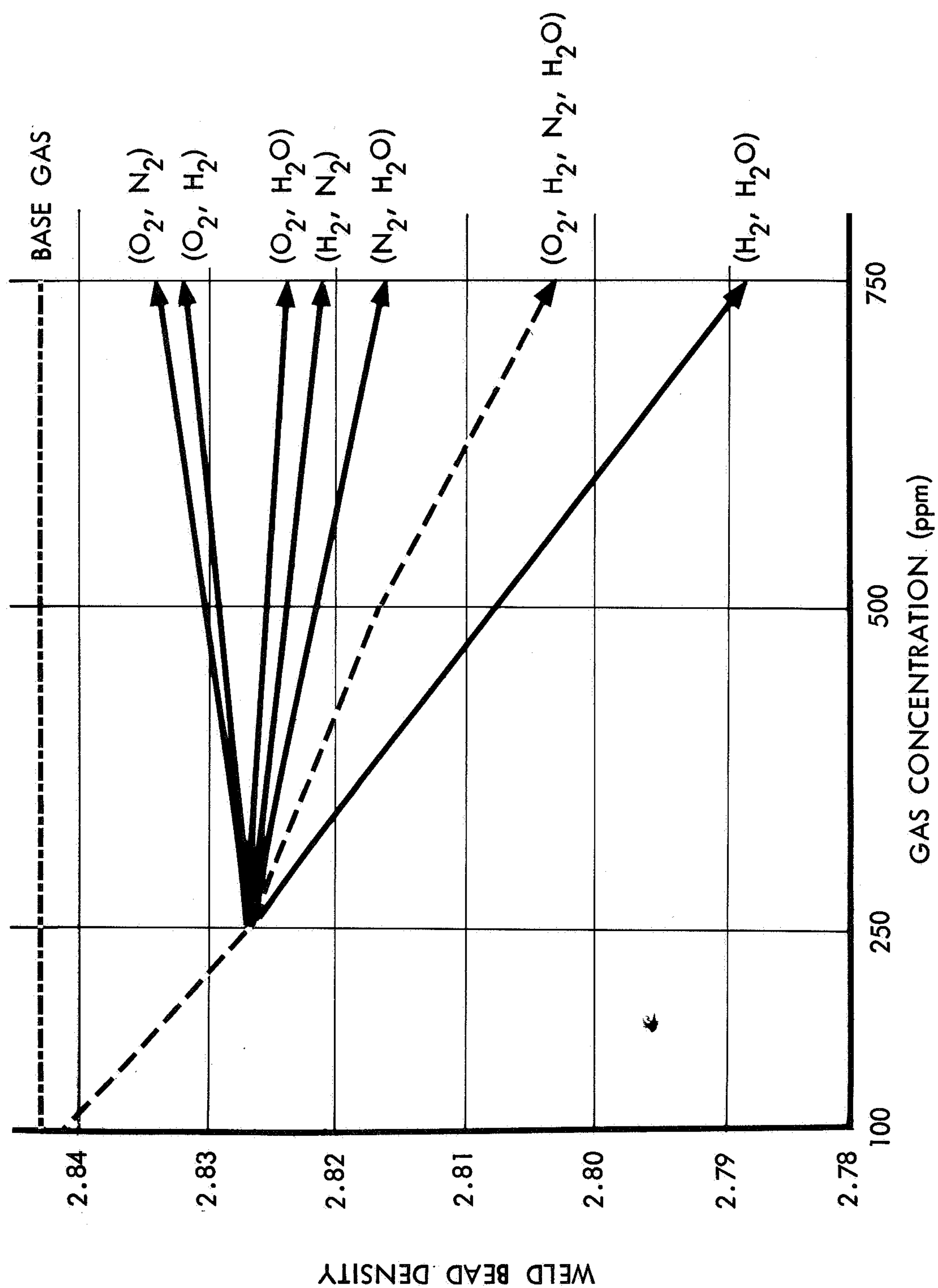

Figure 35: EFFECT OF COMBINATIONS OF GASES ON WELD BEAD DENSITY (ALL OTHER GASES AT 250 PPM)

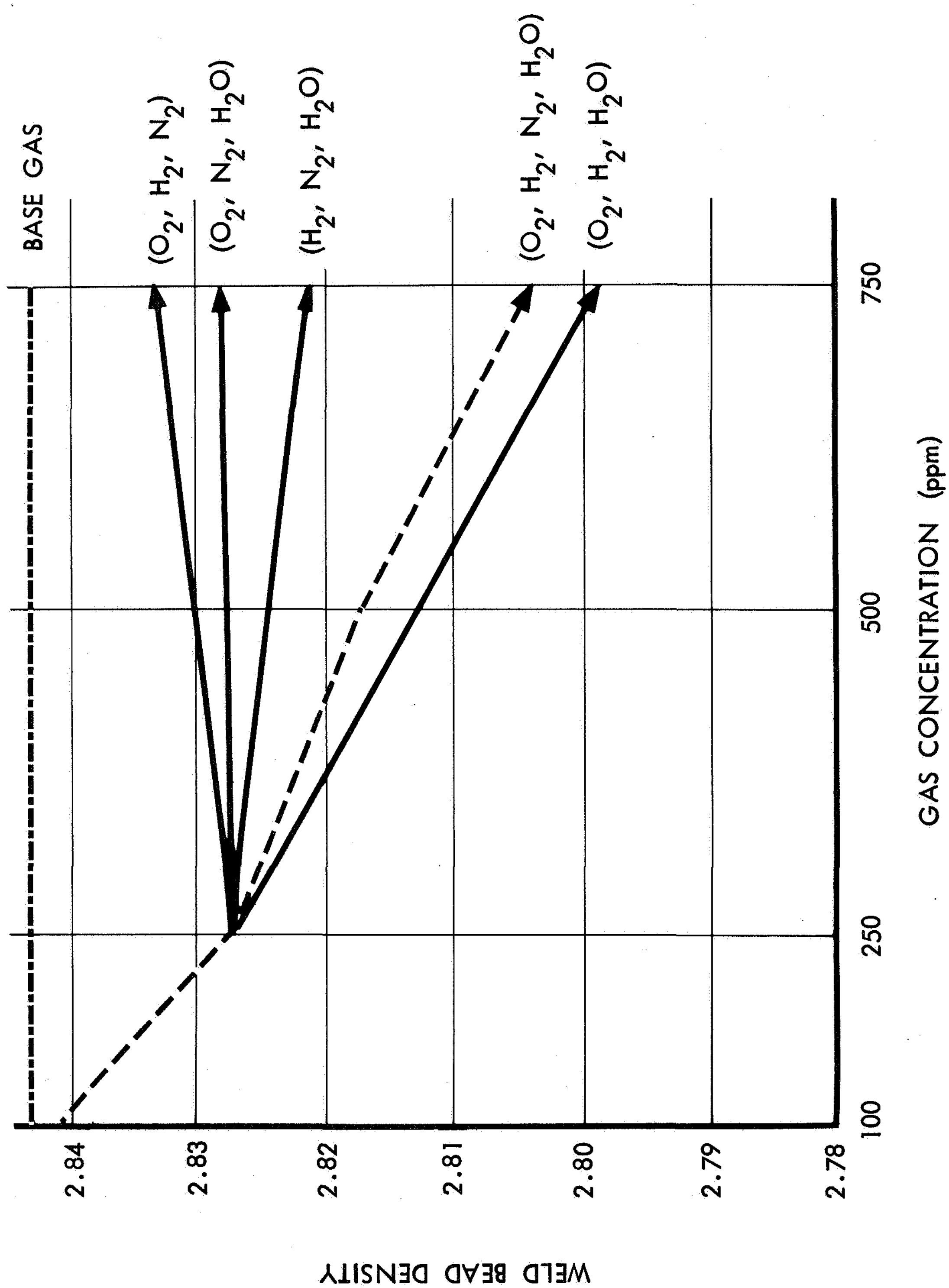

Figure 36 : EFFECT OF COMBINATIONS OF GASES ON WELD BEAD DENSITY (ALL OTHER GASES AT 250 PPM)

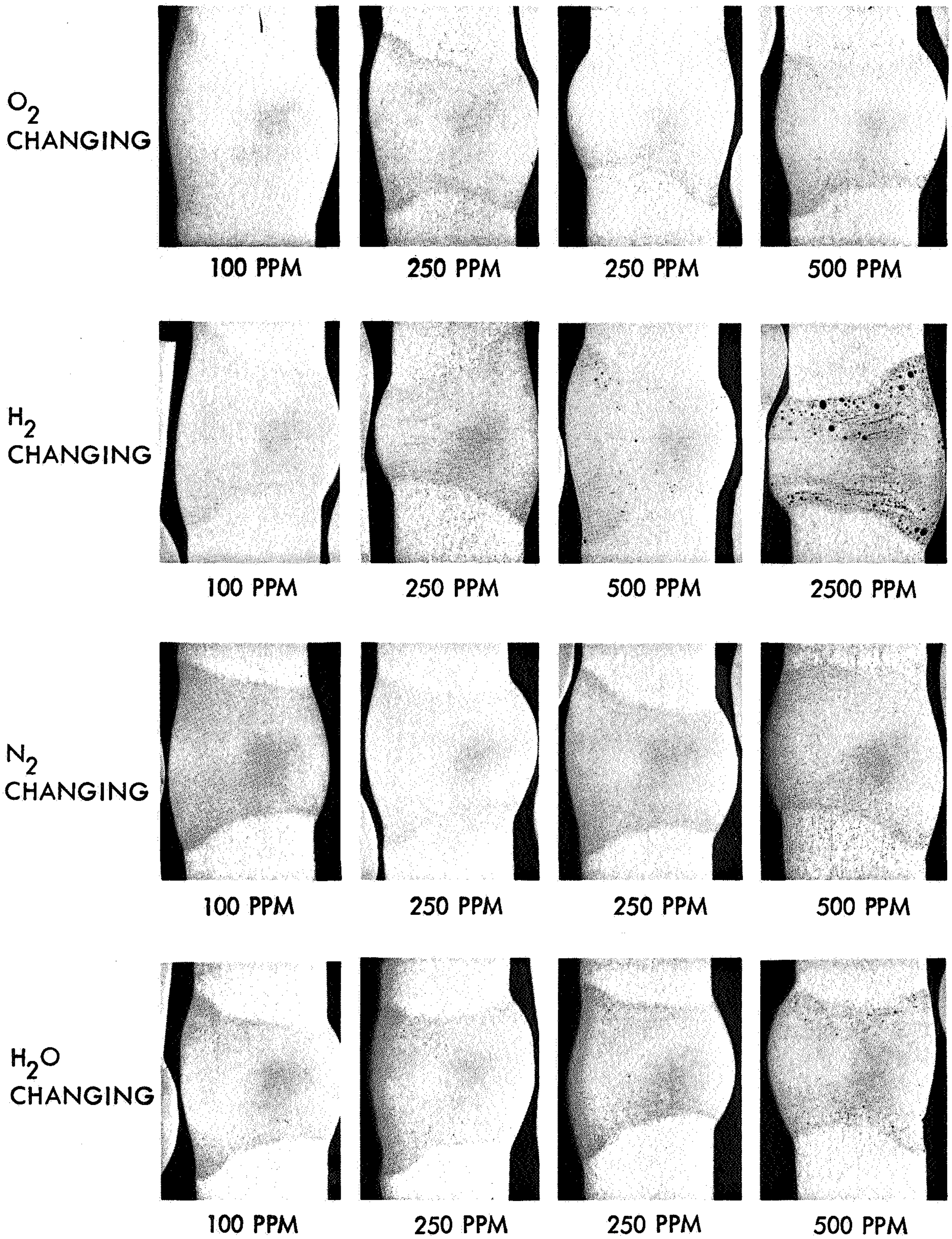

Figure 37: SINGLE GASES IN POLISHED CONDITION

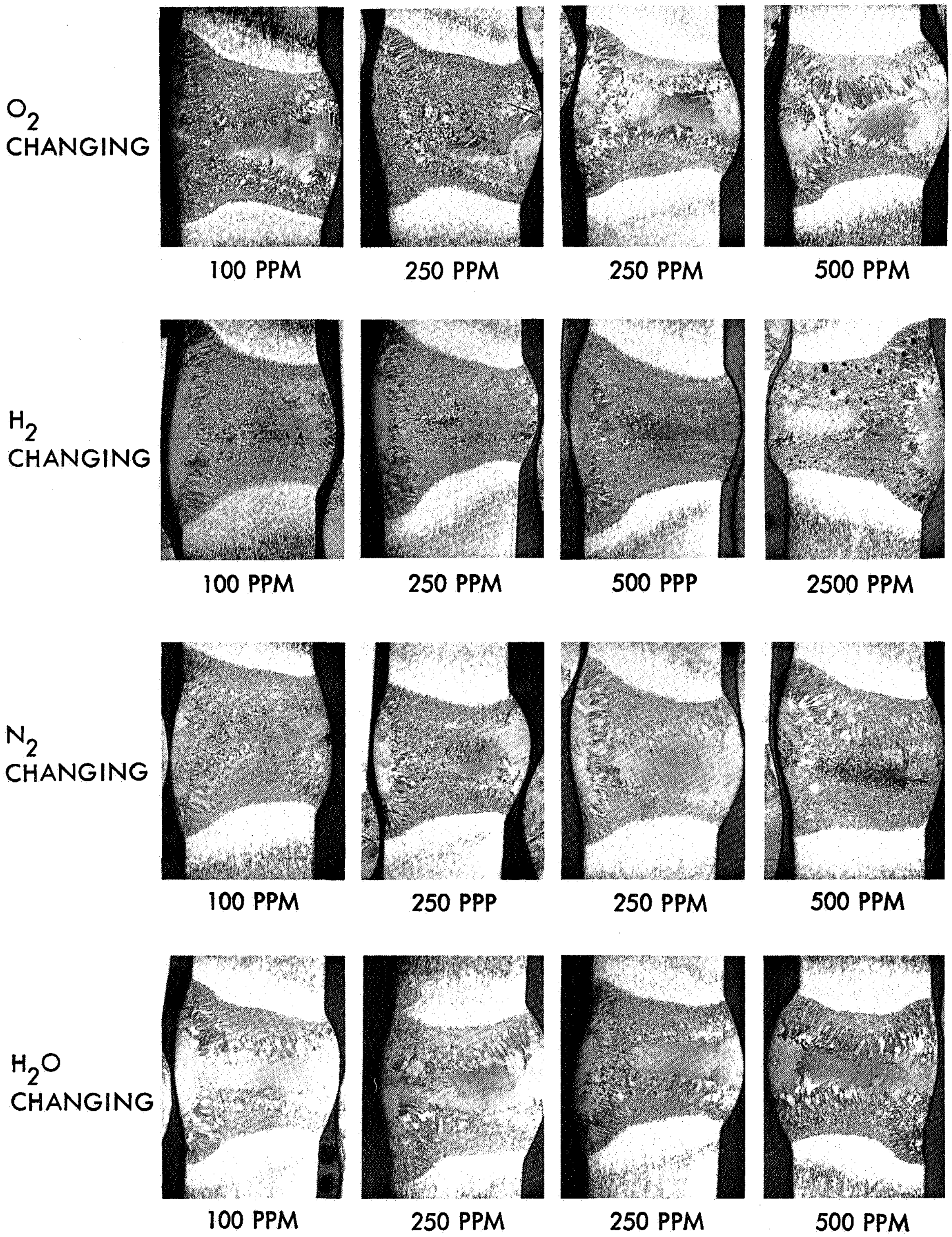

Figure 38: SINGLE GASES IN ETCHED CONDITION

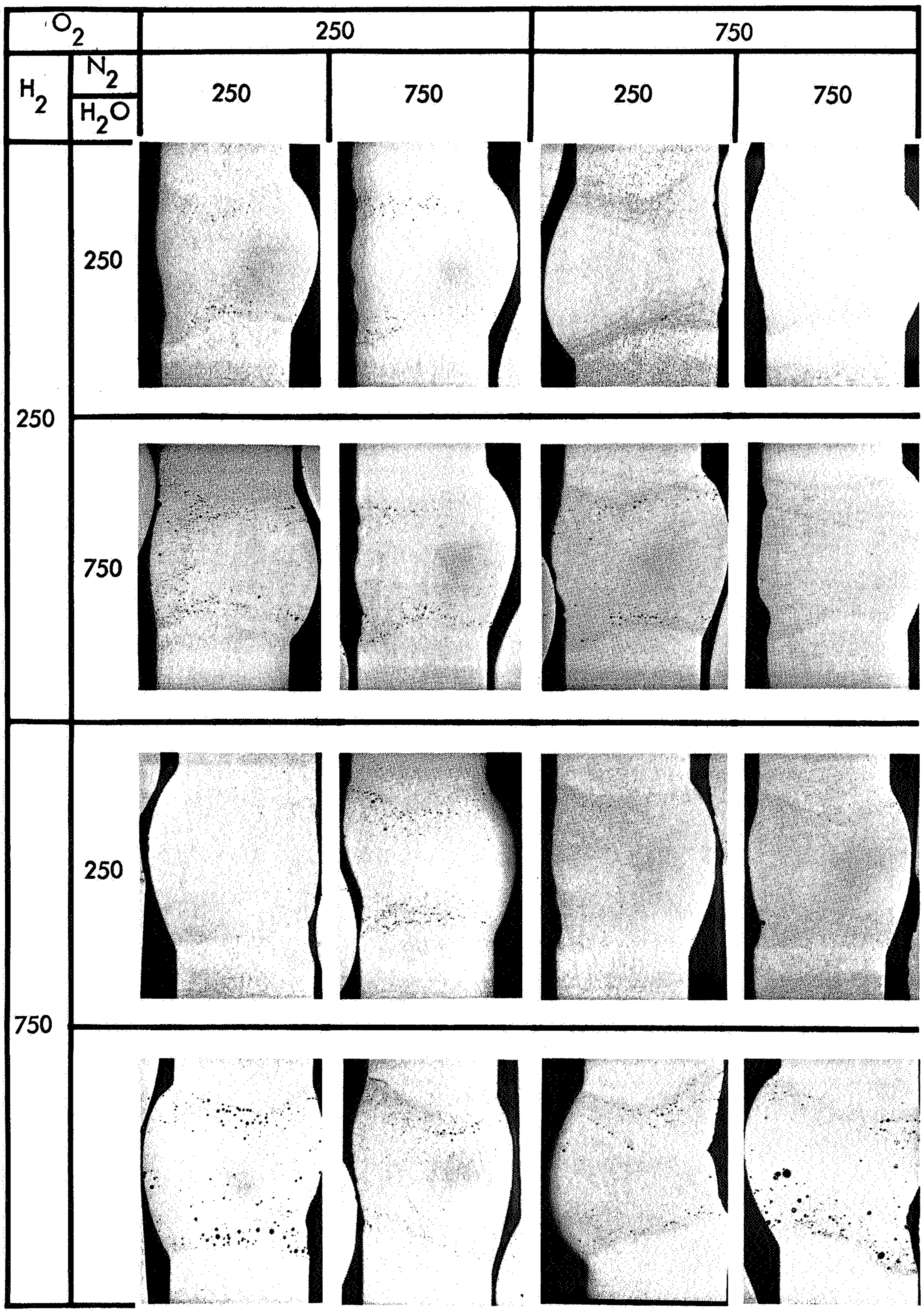

Figure 39: FACTORIAL IN POLISHED CONDITION

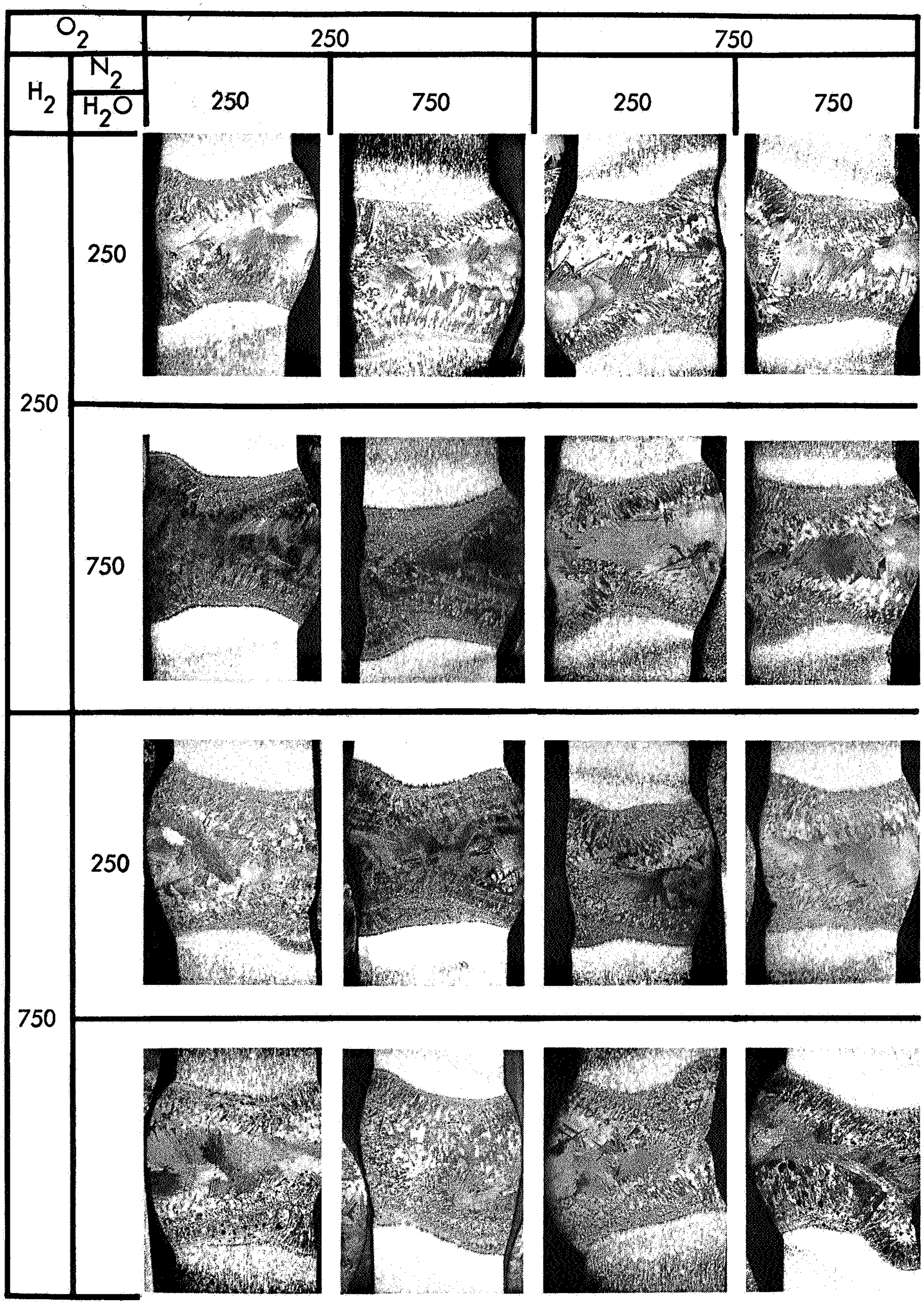

Figure 40: FACTORIAL IN ETCHED CONDITION

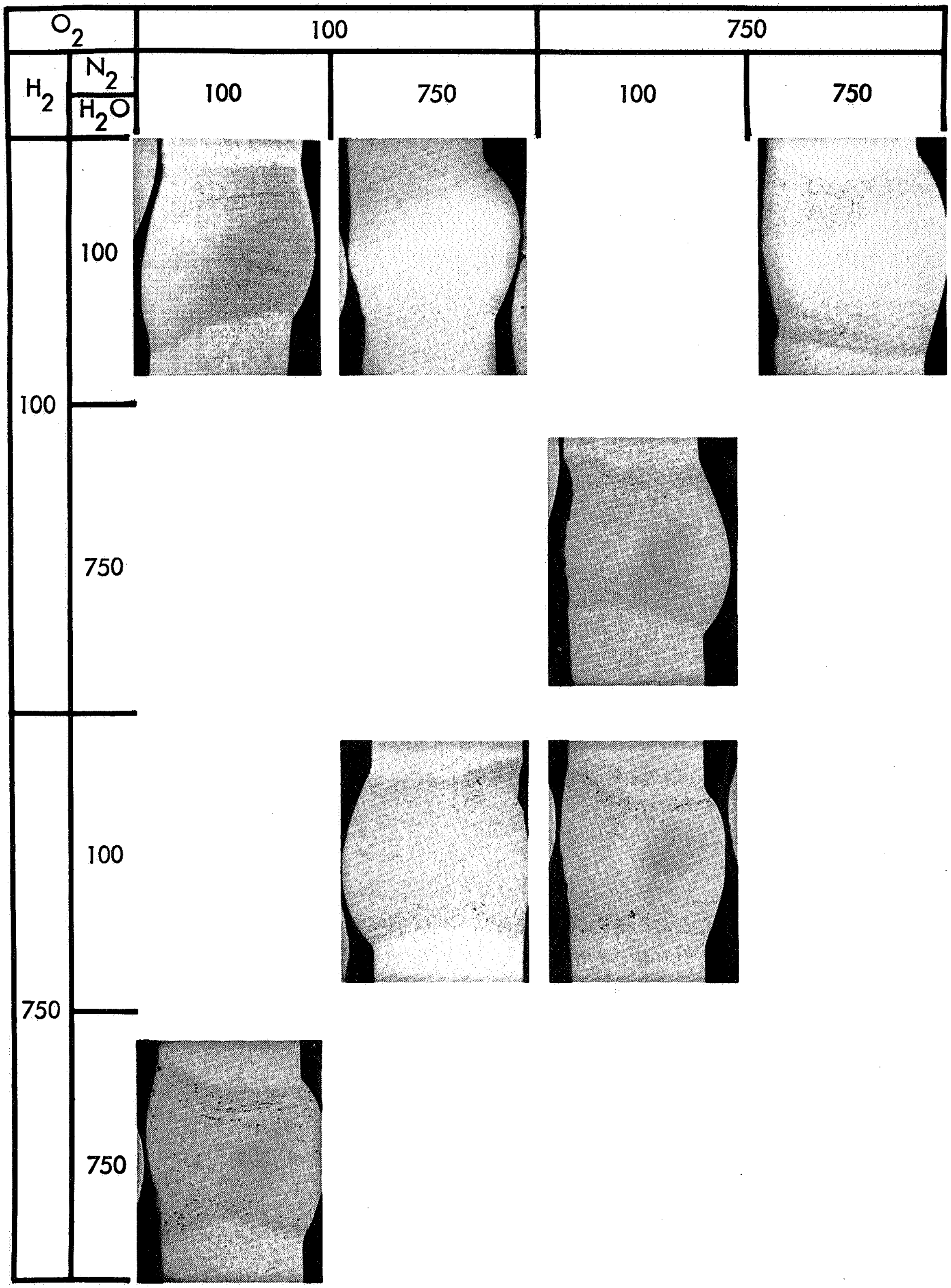

Figure 41: PARTIAL FACTORIAL IN POLISHED CONDITION

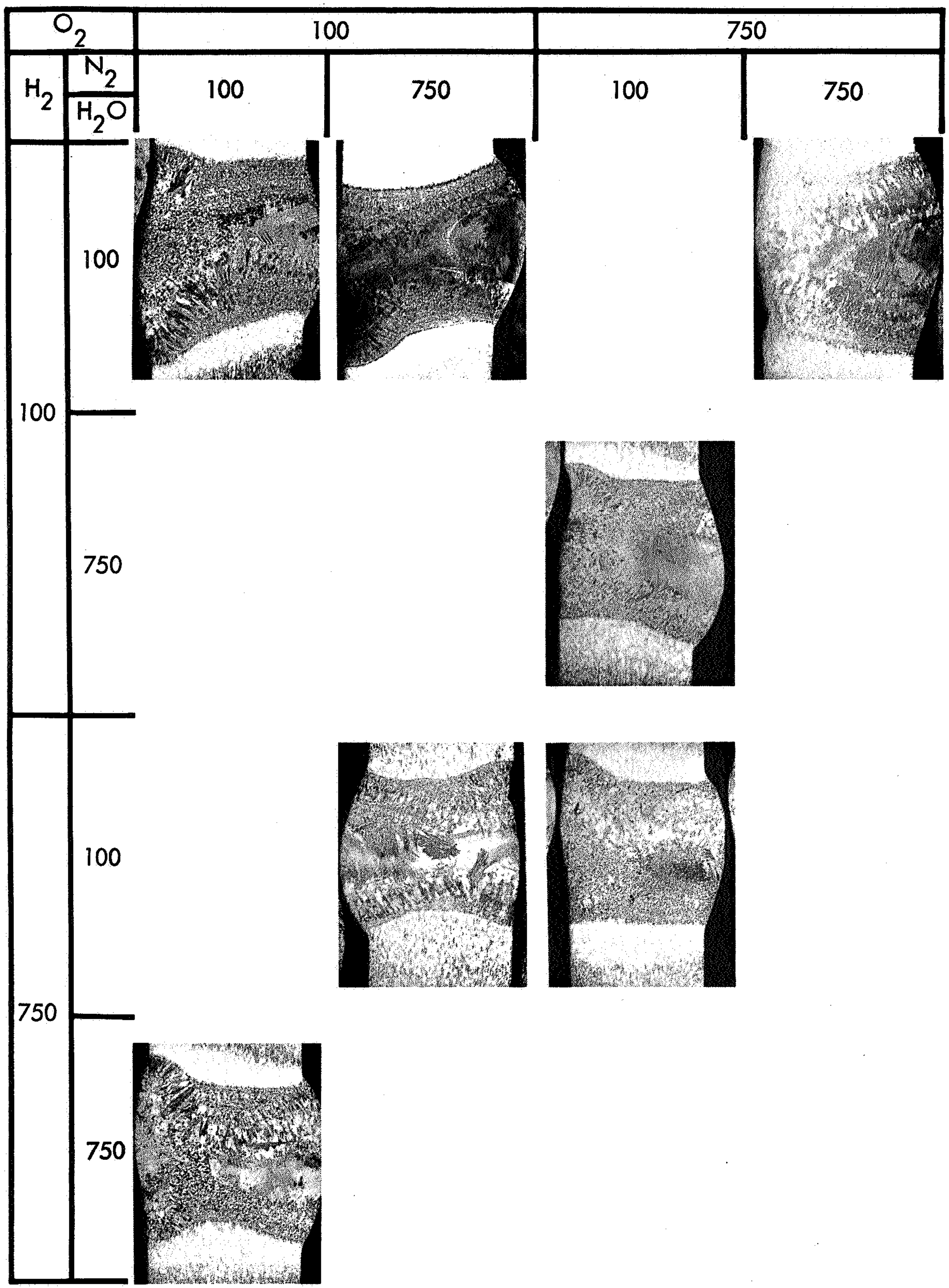

Figure 42: PARTIAL FACTORIAL IN ETCHED CONDITION

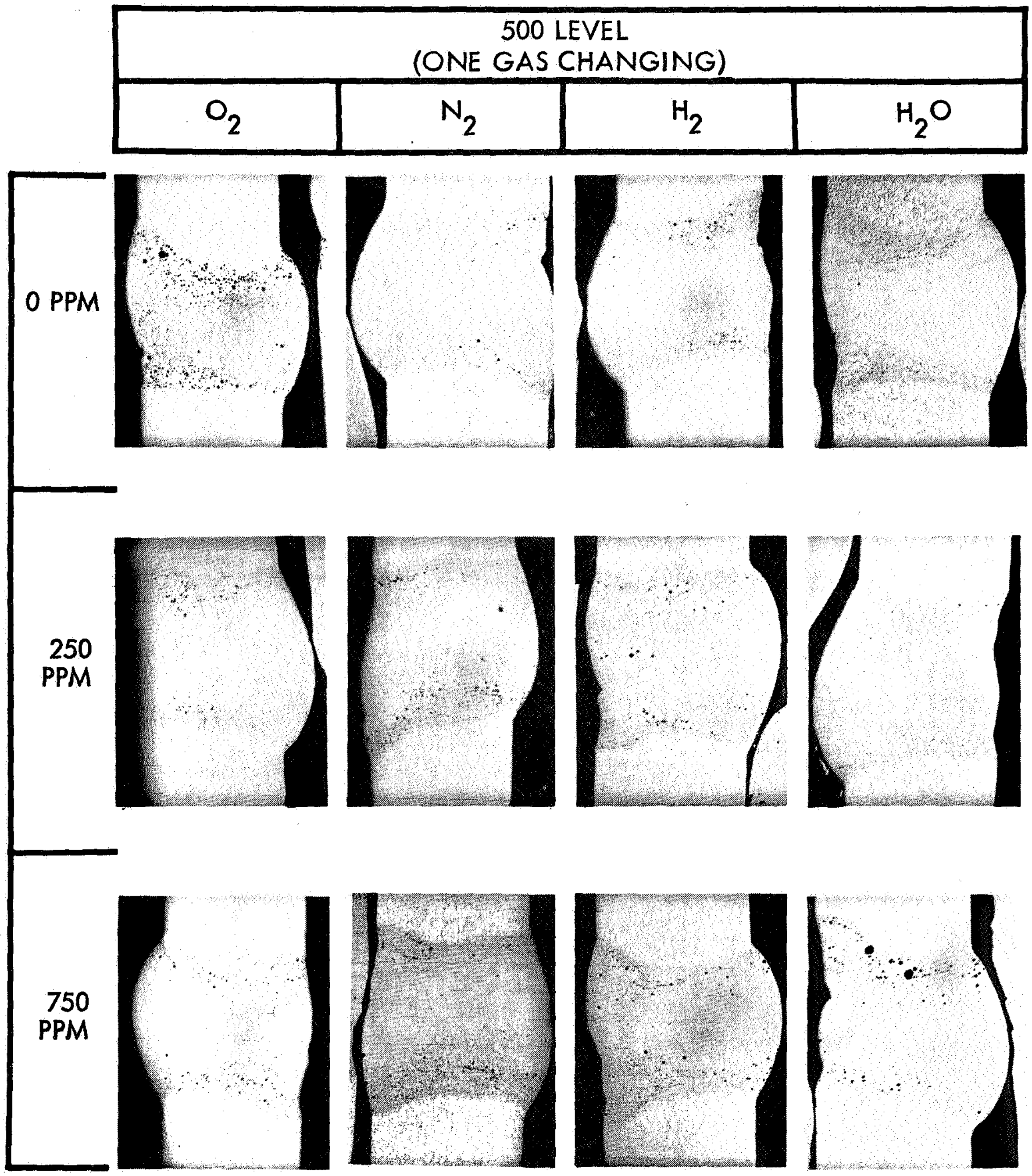

Figure 43: 500 LEVEL IN POLISHED CONDITION

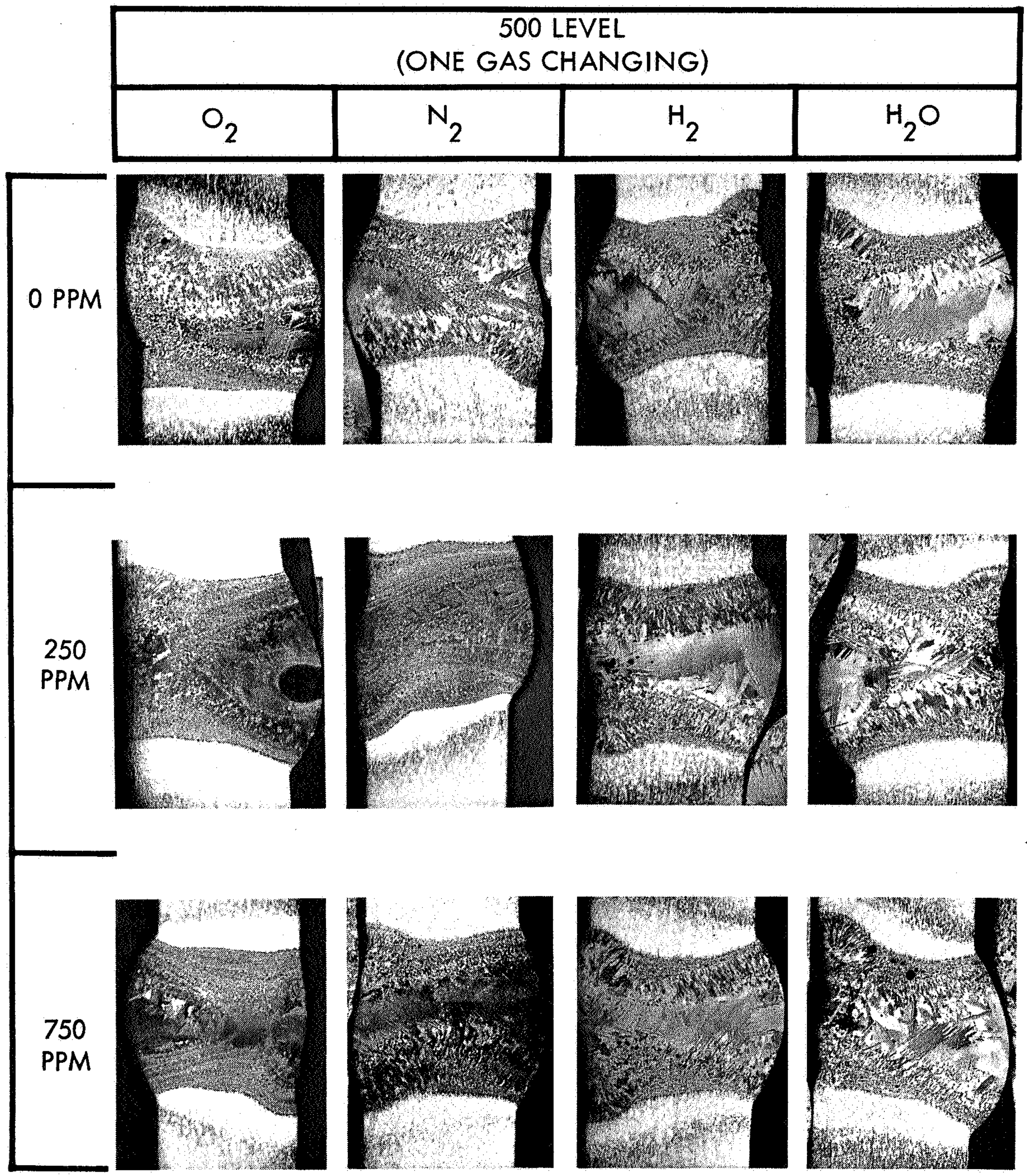

Figure 44: 500 LEVEL IN ETCHED CONDITION

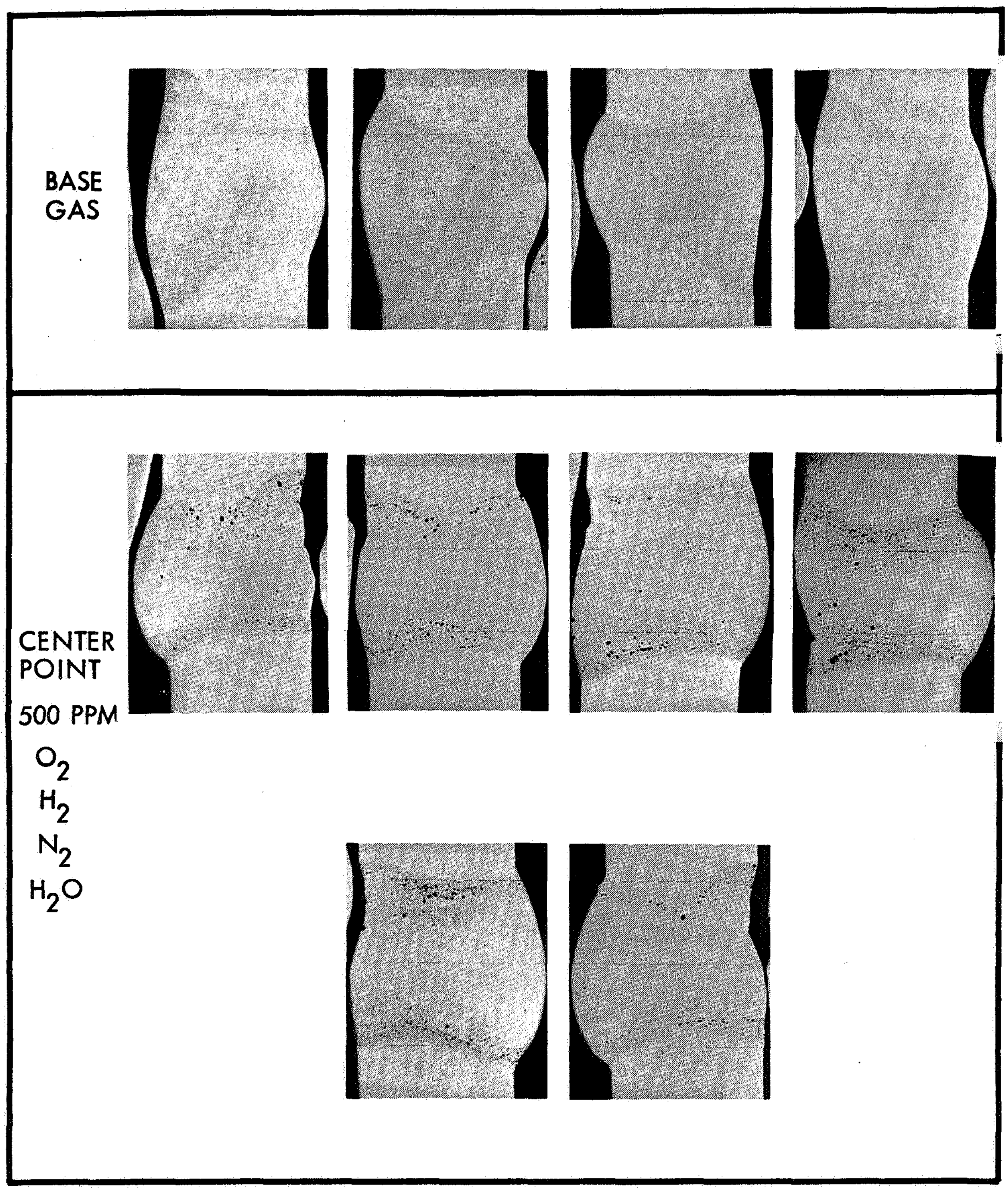

Figure 45: STANDARDS & MID-POINT OF FACTORIAL IN POLISHED CONDITION

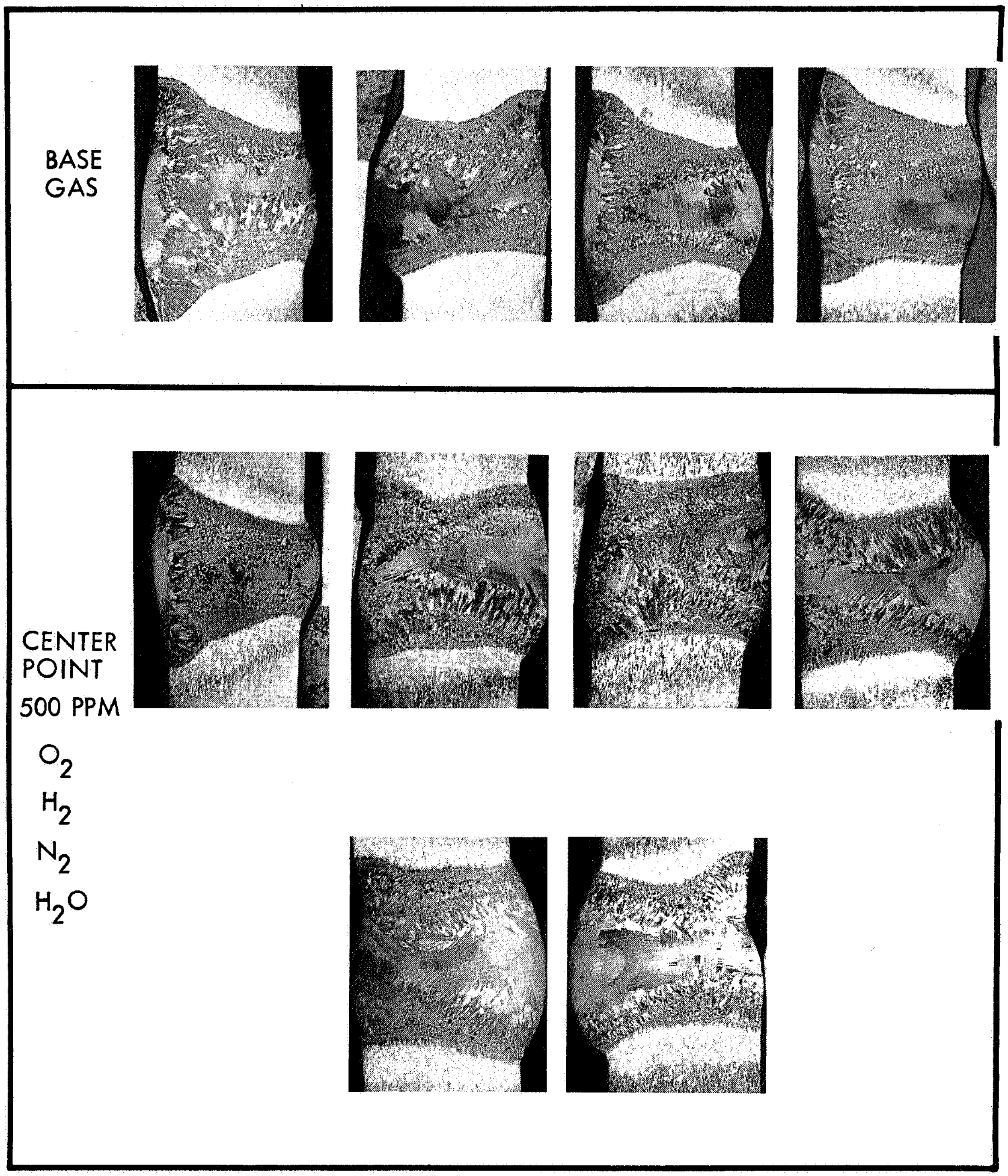

Figure 46: STANDARDS & MID-POINT OF FACTORIAL IN ETCHED CONDITION

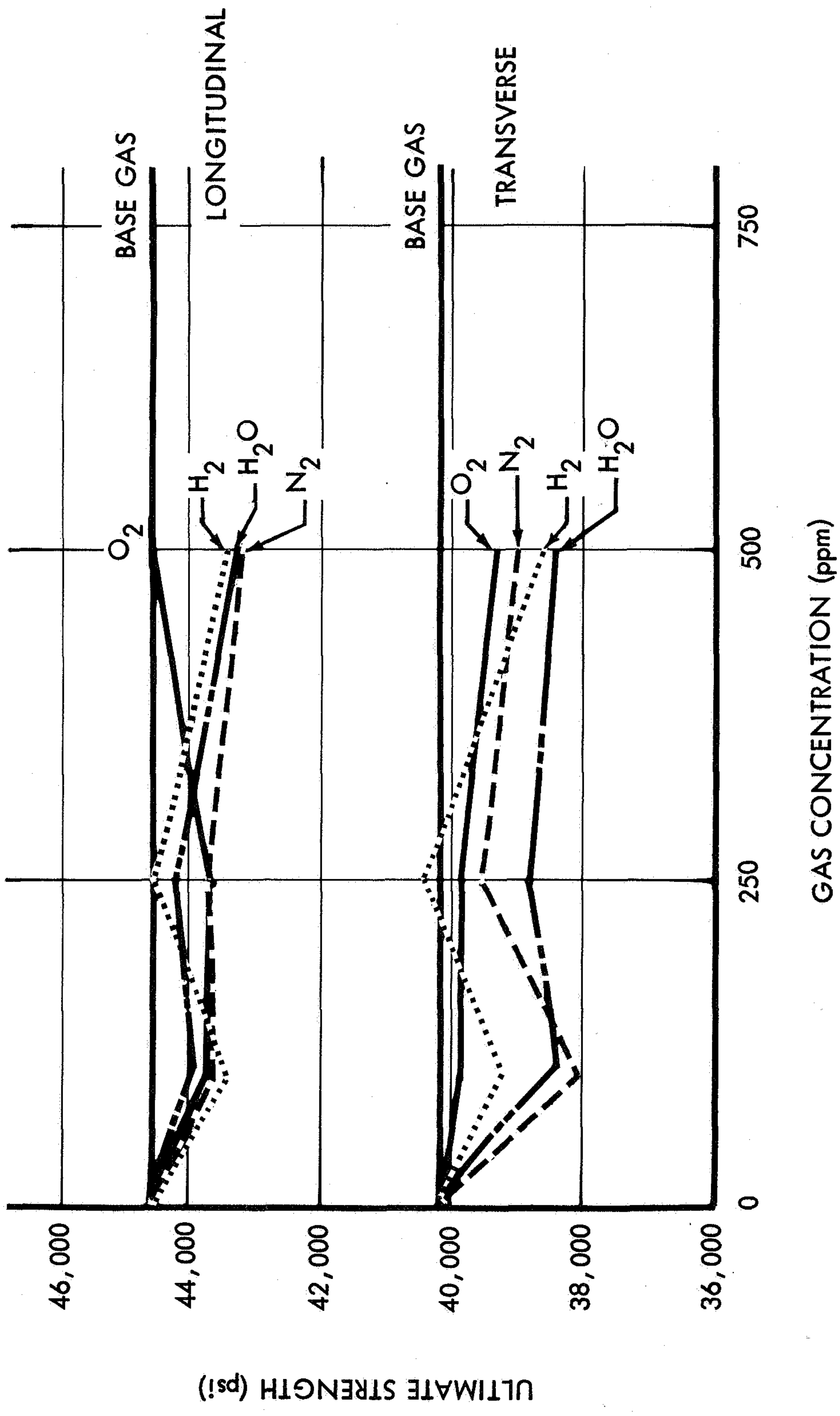

Figure 47: EFFECT OF INDIVIDUAL CONTAMINANTS ON ULTIMATE TENSILE STRENGTH (ALL OTHERS AT 5 PPM)

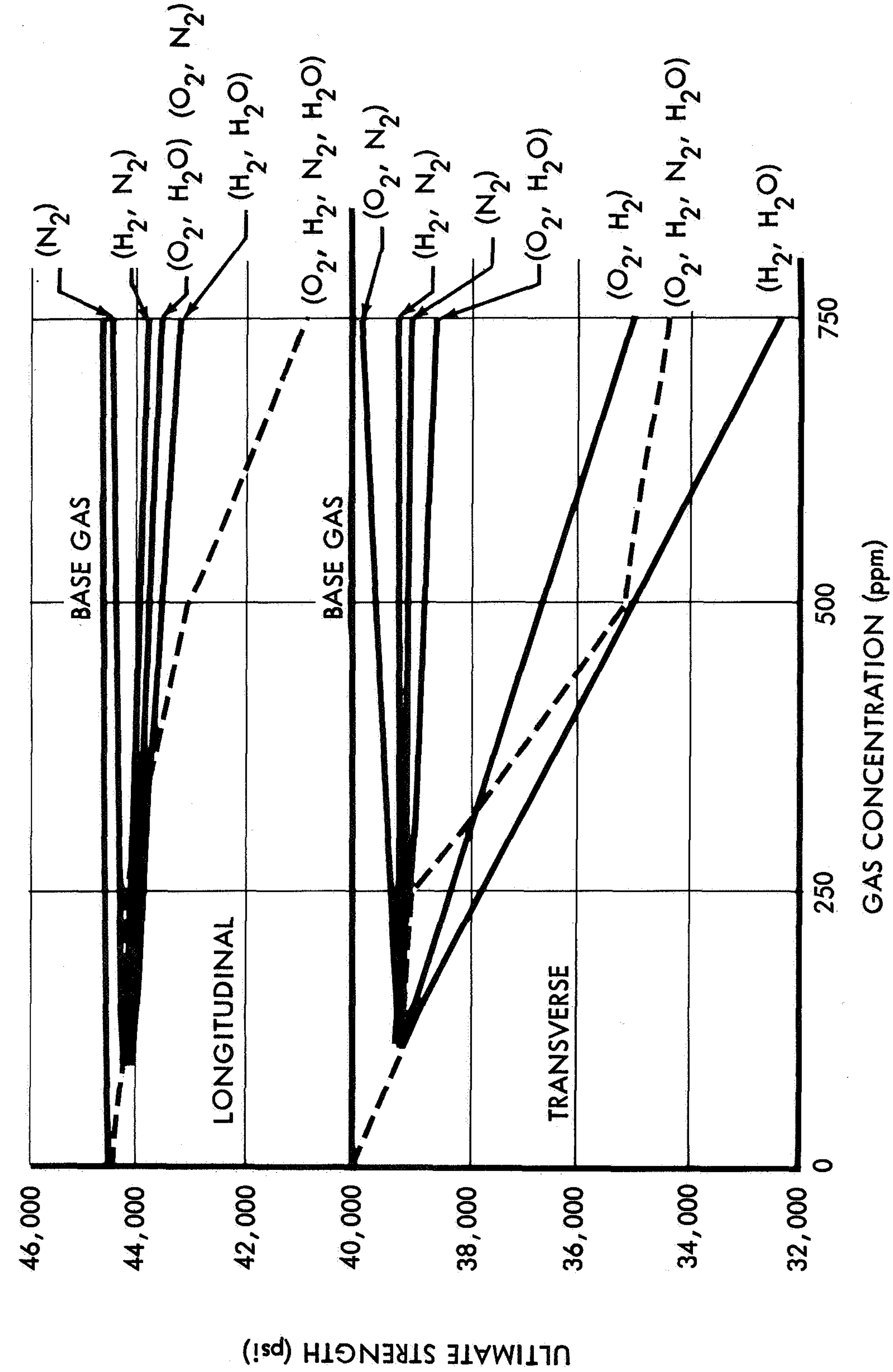

Figure 48: EFFECT OF CONTAMINANTS ON ULTIMATE TENSILE STRENGTH (ALL OTHERS AT 100 PPM)

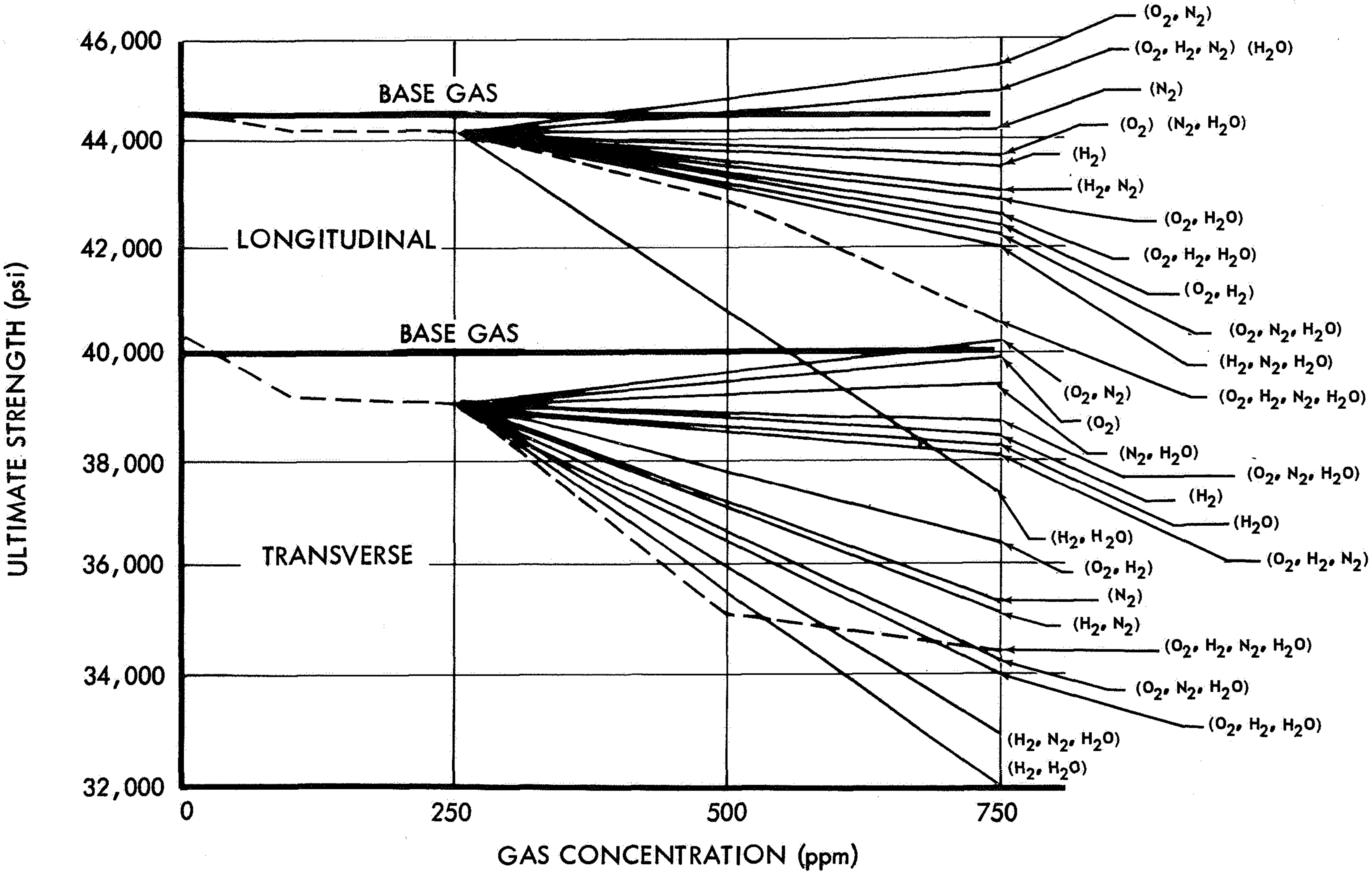

Figure 49: EFFECT OF CONTAMINANTS ON ULTIMATE TENSILE STRENGTH (ALL OTHERS AT 250 PPM)

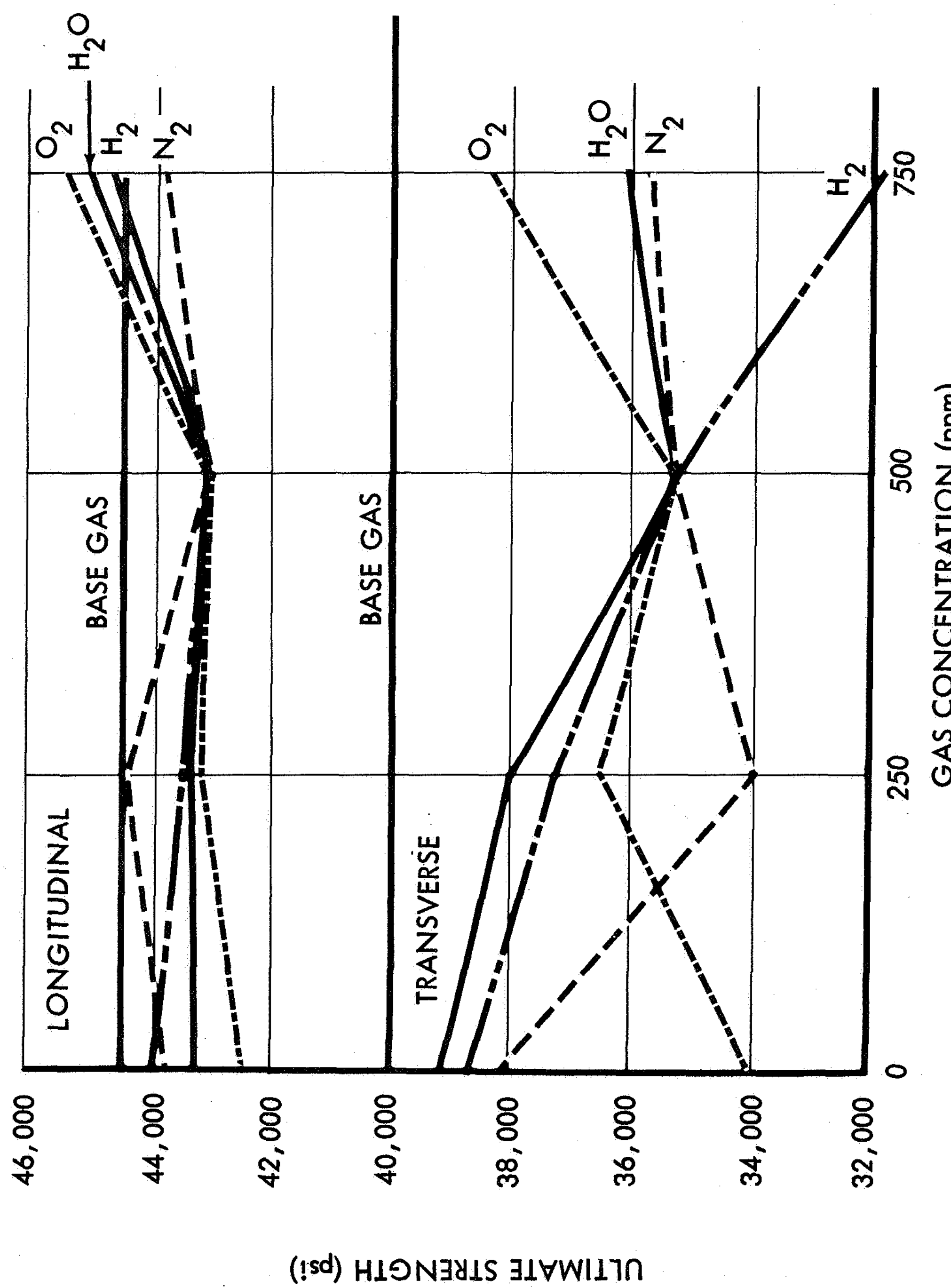

Figure 50: EFFECT OF CONTAMINANTS ON ULTIMATE TENSILE STRENGTH (ALL OTHERS AT 500 PPM)

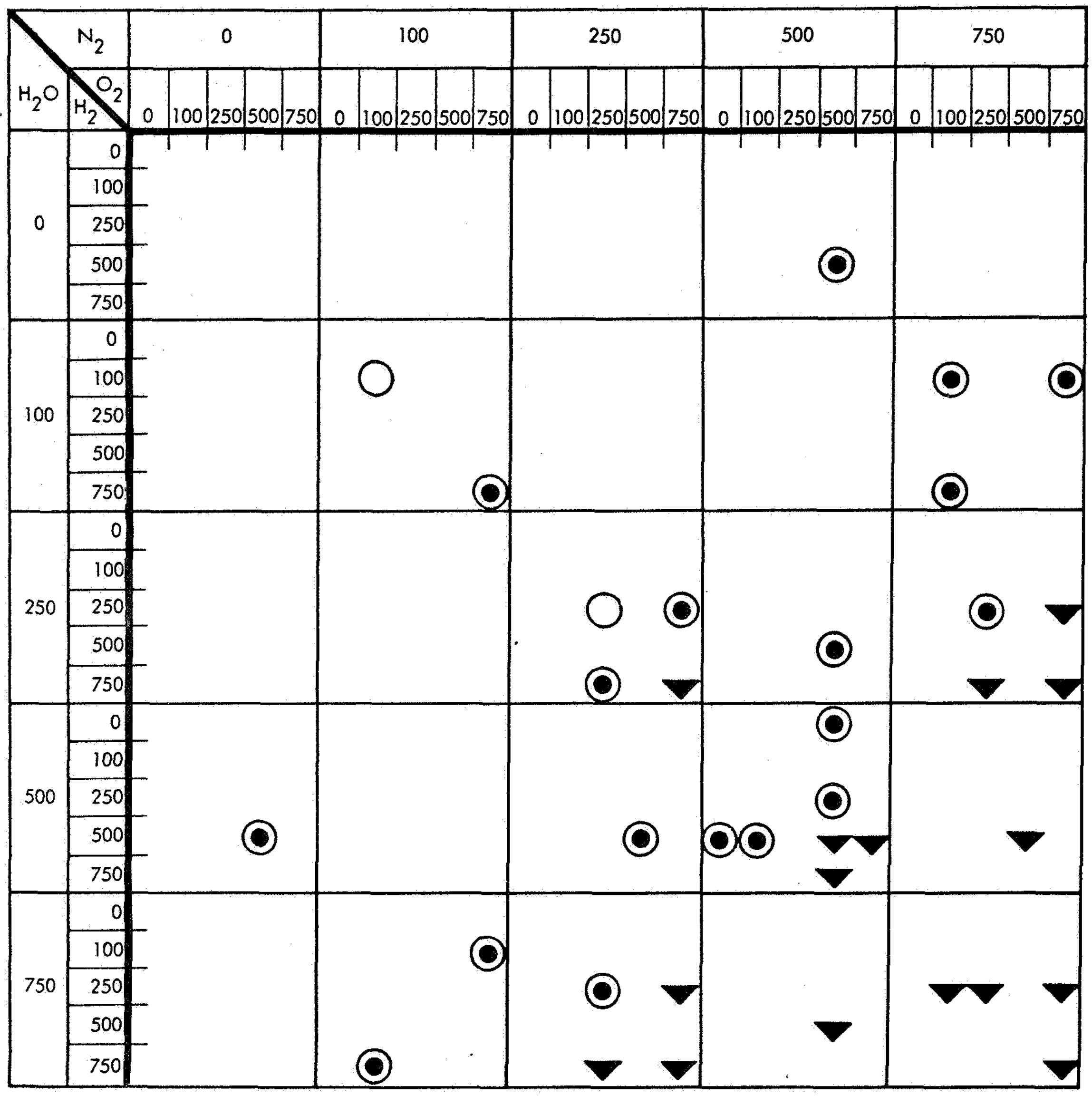

○ 0-1000 PPM Total Contamination
◉ 1000-2000 PPM Total Contamination
▼ 2000-3000 PPM Total Contamination

Figure 51: STATISTICAL PLAN FOR SAMPLE DISPLAY

BASE GAS	C - LT. GREY, SHINY S - SMOOTH U - NONE P - NORMAL A - STABLE				
H_2O VAPOR	100 ppm C - SHINY S - SMOOTH U - NONE P - NORMAL A - STABLE	100 ppm	250 ppm C - LT. GREY, SHINY S - SLIGHT RIPPLE U - NONE P - NORMAL A - STABLE	250 ppm	500 ppm C - DULL, OXIDE SPOTS S - SCALY U - SOME P - NORMAL A - STABLE
O_2	100 ppm C - SHINY GREY S - SMOOTH U - SLIGHT P - NORMAL A - STABLE	250 ppm C - SHINY WITH OXIDE S - RIPPLED U - YES, SLIGHT P - NORMAL A - STABLE	250 ppm	500 ppm C - SHINY GREY S - SCALY U - YES P - NORMAL A - STABLE	500 ppm
N_2	100 ppm C - SHINY GREY S - SMOOTH U - NONE P - NORMAL A - STABLE	250 ppm C - SHINY YELLOW S - RIPPLED U - NONE P - LAST 10" IRREGULAR A - STABLE	250 ppm	500 ppm C - YELLOW, BROWN S - SCALY U - SOME P - NORMAL A - STABLE	500 ppm
H_2	100 ppm C - SHINY GREY S - SMOOTH U - NONE P - NORMAL A - STABLE	250 ppm C - SHINY GREY S - SMOOTH U - NONE P - LIGHT A - STABLE	500 ppm	500 ppm C - SHINY GREY S - RIPPLED U - NONE P - NORMAL A - STABLE	2500 ppm
BACKUP ONLY	C - BROWN S - ROUGH U - SOME P - EXCESSIVE A - STABLE H_2/He TO BACKUP 11,500 ppm H_2	C - SHINY S - SMOOTH U - NONE P - NORMAL A - STABLE H_2O/He TO BACKUP 100 ppm H_2O	C - SHINY S - SMOOTH U - NONE P - NORMAL A - STABLE AIR TO BACKUP 100% AIR	C - SHINY S - SMOOTH U - NONE P - NORMAL A - STABLE H_2O/AIR TO BACKUP 1000 ppm H_2O	
MIDPOINT 500 ppm O_2, N_2, H_2, H_2O	C - DULL S - SCALY U - SOME P - NORMAL A - STABLE				

Figure 52: VISUAL CHARACTERISTICS IN SINGLE GAS, BASE GAS, MIDPOINT AND BACKUP STUDY

N_2		0	100		250			500
H_2O	H_2 \ O_2	500	100	750	250	500	750	0
0	500							
100	100		C - YELLOW S - RIPPLED U - NONE P - NORMAL A - STABLE					
				C - DULL GREY S - SCALY U - NONE P - NORMAL A - STABLE				
250	250				C - RAINBOW, YELLOW S - RIPPLED U - SLIGHT P - EXCESSIVE A - WAVER		C - YELLOW S - SCALY U - HEAVY P - NORMAL A - WANDER	
	500							
	750				C - RAINBOW S - RIPPLED U - SOME P - NORMAL A - STABLE		C - BLUE, YELLOW S - RIPPLED U - SLIGHT P - NORMAL A - STABLE	
500	0							

Figure 53: VISUAL CHARACTERISTICS OF WELDMENT

H_2O	N_2	0	100		250			500
	O_2 / H_2	500	100	750	250	500	750	0
500	250							
	500	C - SHINY, OXIDE SPOTS S - SCALY U - HEAVY P - EXCESSIVE A - SHORT OUTS				C - BLUE S - SCALY U - NONE P - EXCESSIVE A - SHORT OUTS		C - BLUE, BLACK S - SCALY U - NONE P - EXCESSIVE A - WANDER
	750							
750	100			C - DULL GREY S - SCALY U - SOME P - NORMAL A - SHORT OUTS				
					C - RAINBOW S - SCALY U - NONE P - NORMAL A - WAVY		C - SHINY GREY S - SCALY U - SOME P - EXCESSIVE A - WANDER	
	500							
	750		C - DULL GREY S - SCALY U - NONE P - NORMAL A - SOME WAVER		C - DULL GREY S - SCALY U - NONE P - EXCESSIVE A - SHORT OUTS		C - DULL GREY S - SCALY U - HEAVY P - EXCESSIVE A - SHORT OUTS	

Figure 54: VISUAL CHARACTERISTICS OF WELDMENT

H_2O	N_2	500			750			
	H_2 \ O_2	250	500	750	100	250	500	750
0	500		C - SHINY S - RIPPLED U - SOME P - NORMAL A - WANDER					
100	100				C - YELLOW S - SCALY U - NONE P - NORMAL A - STABLE			C - YELLOW S - SCALY U - NONE P - NORMAL A - STABLE
	750				C - YELLOW S - SCALY U - NONE P - NORMAL A - STABLE			
250	250					C - RAINBOW S - SCALY U - NONE P - NORMAL A - WANDER		C - YELLOW S - SCALY U - SLIGHT P - NORMAL A -
	500		C - RAINBOW S - SCALY U - SLIGHT P - NORMAL A - WANDER					
	750					C - RAINBOW, YELLOW S - SCALY U - NONE P - NORMAL A - SLIGHT WANDER		C - BLUE, YELLOW S - SCALY U - SOME P - NORMAL A - STABLE
500	0		C - BLUE S - SCALY U - SOME P - EXCESSIVE A - WAVER					

Figure 55: VISUAL CHARACTERISTICS OF WELDMENT

H_2O	N_2 → H_2 ↓ O_2 →	500: 250	500: 500	500: 750	750: 100	750: 250	750: 500	750: 750
500	250		C - BLUE S - SCALY U - SLIGHT P - NORMAL A - WAVER					
	500	C - BLUE S - SCALY U - SOME P - NORMAL A - STABLE	500 LEVEL C - DULL, OXIDE SPOTS S - SCALY U - YES P - NORMAL A - NORMAL	C - BLUE, YELLOW S - SCALY U - NONE P - NORMAL A - STABLE			C - BLUE, OXIDE SPOTS S - SCALY U - NONE P - NORMAL A - WANDER	
			C - SHINY, DULL SIDES S - SANDPAPER U - NONE P - NORMAL A - SOME WAVER					
750	100							
	250					C - RAINBOW S - SCALY U - SOME P - SOME LT. AREAS A - ELECTRODE BUILDUP		C - BLUE S - SCALY U - SOME P - EXCESSIVE A - STABLE
	500		C - BLUE, YELLOW S - SANDPAPER U - SOME P - NORMAL A - STABLE					
	750					C - DULL, OXIDE SPOTS, YELLOW S - SCALY U - SLIGHT P - NORMAL A - ERRATIC		C - DULL S - SCALY, ROUGH U - SOME P - EXCESSIVE A - ERRATIC

Figure 56: VISUAL CHARACTERISTICS OF WELDMENT

BASE GAS	P - .3 D - 2.84298	L - 43,600 T - 38,900 F - 576,000	P - .3 D - 2.84326	L - 45,000 T - 41,000 F - 161,000	P - .3 D - 2.84401	L - 45,600 T - 40,800 F - 59,600	P - .3 D - 2.84405	L - 43,600 T - 39,600 F - 827,000		
H_2O VAPOR	P - .18 D - 2.84066	L - 43,700 T - 38,000 F - 1,016,000	P - .18 D - 2.83953	L - 44,100 T - 38,600 F - 528,000	P - .27 D - 2.83486	L - 43,400 T - 38,200 F - 412,000	P - .27 D - 2.83555	L - 44,900 T - 39,300 F - 711,000	P - 1.47 D - 1.1345	L - 44,100 T - 38,300 F - 214,000
O_2	P - 0 D - 2.84452	L - 43,700 T - 39,800 F - 729,000	P - .99 D - 2.84822	L - 43,400 T - 39,700 F - 401,000	P - .99 D - 2.83011	L - 44,000 T - 39,900 F - 366,000	P - .18 D - 2.85233	L - 44,000 T - 39,100 F - 648,000	P - .18 D - 2.84884	L - 45,000 T - 39,400 F - 642,000
N_2	P - .29 D - 2.84212	L - 43,600 T - 38,000 F - 644,000	P - .74 D - 2.84173	L - 43,400 T - 39,400 F - 163,000	P - .74 D - 2.84230	L - 44,000 T - 39,500 F - 192,000	P - .41 D - 2.84205	L - 44,000 T - 38,800 F -403,000	P - 1.46 D - 2.84166	L - 42,500 T - 39,100 F - 1,359,000
H_2	P - .12 D - 2.84308	L - 43,400 T - 39,100 F - 551,000	P - .24 D - 2.84819	L - 44,400 T - 40,300 F - 391,000	P - 12.5 D - 2.82397	L - 43,000 T - 38,000 F - 126,000	P - 12.5 D - 2.82192	L - 43,700 T - 39,100 F - 148,000	P - D - 2.75590	L - 37,400 T - 27,200 F - 8,000
CONTAMI-NATION IN BACKUP ONLY	D - 2.83798	L - 43,800 T - 39,900 F - 255,000	D - 2.83810	L - 43,800 T - 39,900 F - 600,000	D - 2.84197	L - 43,500 T - 38,400 F - 106,000	D - 2.84274	L - 43,500 T - 38,400 F - 164,000		
MIDPOINT OF FACTORIAL	P - 26.71 D - 2.80402	L - 42,700 T - 32,500 F - 122,000	P - 26.71 D - 2.82330	L - 42,900 T - 35,200 F - 221,000	P - 26.71 D - 2.81019	L - 43,200 T - 32,500 F - 193,000	P - 26.71 D - 2.82275	L - 43,100 T - 36,100 F - 105,000	P - 26.71 D - 2.82041	L - 43,400 T - 37,500 F - 254,000

P - POROSITY   L - LONGITUDINAL
D - DENSITY   T - TRANSVERSE
F - FATIGUE

Figure 57: POROSITY AND DENSITY, FATIGUE AND TENSILE DATA OF SINGLE GASES

H_2O	N_2 / O_2 / H_2	0	100		250			500				750			
		500	100	750	250	500	750	0	100	500	750	100	250	500	750
0	500									.89 2.83301					
100	100		.06 2.84115									.12 2.84180			09 2.83637
	750			3 2.82220								4 2.83060			
250	250				12 2.82742		.77 2.83605						9 2.82610		.03 2.83416
	500									9 2.83039					
	750				7 2.82778		.15 2.83235						20 2.82416		.38 2.83362
500	0									4 2.83505					
	250									6 2.82144					
	500	.59 2.82700				15 2.81812		40 2.80253	6 2.82862	26.71 2.81734	.60 2.82306			100 2.79564	
	750									50 2.80432					
750	100			2.18 2.82870											
	250				10 2.81588		14 2.82416						20 2.81696		6 2.82844
	500									50 2.82302					
	750		14 2.84516		.38 2.83362		20 2.79879						29 2.82148		91 2.80388

DEFECTS/INCH
DENSITY

Figure 58: STATISTICAL DESIGN SHOWING POROSITY AND DENSITY

H_2O	N_2 → / O_2 → / H_2 ↓	0	100		250			500				750			
		500	100	750	250	500	750	0	250	500	750	100	250	500	750
0	500									L - 43,300 T - 39,000 F - 198,000					
100	100		L - 44,300 T - 39,200 F - 178,000									L - 44,400 T - 39,000 F - 483,000			L - 43,700 T - 39,700 F - 190,000
	750			L - 43,700 T - 35,900 F - 121,000								L - 43,700 T - 39,100 F - 184,000			
250	250				L - 43,400 T - 39,000 F - 198,000		L - 43,800 T - 40,200 F - 235,000						L - 44,300 T - 35,400 F - 285,000		L - 45,500 T - 40,300 F - 346,000
	500									L - 43,300 T - 37,900 F - 134,000					
	750				L - 43,600 T - 38,500 F - 306,000		L - 42,500 T - 36,500 F - 267,000						L - 43,100 T - 35,300 F - 393,000		L - 45,000 T - 38,200 F - 357,000
500	0									L - 44,100 T - 38,700 F - 291,000					
	250									L - 43,500 T - 37,300 F - 184,000					
	500	L - 43,900 T - 38,300 F - 395,000				L - 44,300 T - 33,900 F - 185,000		L - 42,500 T - 34,000 F - 76,900	L - 43,200 T - 36,400 F - 93,700	L - 44,100 T - 33,400 F - 216,000	L - 45,400 T - 38,200 F - 231,000			L - 43,800 T - 35,600 F - 155,000	
	750									L - 44,700 T - 31,800 F - 98,700					
750	100			L - 43,500 T - 38,500 F - 340,000											
	250				L - 45,000 T - 38,400 F - 207,000		L - 43,000 T - 34,300 F - 103,000						L - 43,800 T - 39,500 F - 415,000		L - 42,400 T - 38,800 F - 294,000
	500									L - 45,100 T - 36,100 F - 163,000					
	750		L - 43,100 T - 32,400 F - 106,000		L - 37,400 T - 32,000 F - 78,800		L - 42,700 T - 34,200 F - 218,000						L - 42,000 T - 33,000 F - 108,000		L - 40,800 T - 34,300 F - 72,600

L - LONGITUDINAL WELD STATIC TEST
T - TRANSVERSE STATIC TEST
F - FATIGUE CYCLES TO FAILURE

Figure 59: FATIGUE AND STATIC TEST DATA

variations in density, which could be mistaken for porosity. This is caused by the agglomeration of incipiently melting constituents, primarily copper.

No attempt was made to correlate the porosity data from the three methods although similar trends were apparent. Each method is considered complementary to the other. The metallographic examination is most useful in obtaining a visual appreciation of the level of porosity experienced with the specific contamination conditions. Polaroid photographs of each of the weldments for ready reference are incorporated in Figures 37 through 46. The photos show the polished and etched condition for each contamination treatment.

STATIC TENSILE TESTS

The static tensile tests proved to be the most consistent and reliable of mechanical analyses. The tensile test data are shown in Figures 17, 18, and 19. The statistical analyses are graphically plotted in Figures 47, 48, 49, and 50 and are summarized as follows:

1) Figure 47 shows that the addition of the individual gases except oxygen decreases in the longitudinal and transverse ultimate strengths, approximately 2 percent. The addition of oxygen shows no significant effect;

2) At 100 ppm of the individual gases, the strength decreases and then increases at 250 ppm. This observation is of interest because all of the points follow similar trends. Each point generally represents two weldments and two test specimens per weldment.

Figures 48, 49, and 50 show the factorial results. The curves basically indicate decreases in strength with increased contamination. Hydrogen and water vapor combinations were generally most detrimental causing 20-percent decreases in strength in some instances. In contrast, oxygen and nitrogen addition increased strength about 1 percent higher than the base gas reference under some contamination conditions. Further intensified study of these curves will be of importance when production contamination conditions are defined.

VISUAL EFFECTS

One of the most significant effects of contamination was changes in surface condition forming undercut, discoloration, and roughness. Because it is difficult to place a numerical value on surface condition, two weldment sample displays have been prepared for reference. The displays include: (1) the mixed gas weld samples mounted in the configuration shown in Figure 51; and (2) the individual gas weld samples mounted in order of increasing contamination. To provide a ready reference of a particular sample characteristic, the analysis and visual observations have been described in Figures 52 through 56 in the same basic configuration as the mounted samples in the display. The porosity and mechanical data are shown in a similar manner in Figures 57, 58, and 59. Surface variations caused by the individual gases are summarized as follows:

1) 500 ppm total contamination is necessary to cause a significant change in appearance, which could be considered cause for weldment rejection;

2) 100 ppm H_2O caused yellowish surface appearance fading to grayish, with roughening of the surface at 500 ppm;

3) Oxygen gave a silvery to grayish appearance and increased the undercut with increasing concentration;

4) Nitrogen gave a blackish appearance along the edge of the weld bead. This discoloration increased in intensity with increasing contamination from 100 to 500 ppm; the surface in the center of the bead began to yellow at 500 ppm;

5) Hydrogen gave a grayish rough appearance and decreased undercut was observed as concentration was increased; at 250 ppm the undercut was eliminated.

Increased surface effects were noted with the mixed gases, because for most of the conditions, the total contamination was in excess of 500 ppm. Between 750 and 1000 ppm total contamination, the arc begins to wander leaving a wavy bead. At 1500 ppm total contamination, the arc becomes erratic and unstable.

FATIGUE EVALUATION

Two fatigue specimens were analyzed for each weldment panel, except where weldments received duplicate contamination treatment, and then only one specimen was analyzed from the second panel. Five fatigue specimens were prepared from a base gas panel and were used to establish an S/N (stress/cycles to failure) curve. The stress level chosen was 26,000 psi. Above 26,000 psi, excessive necking down was experienced in the weld bead region indicating that the elastic limit had been exceeded. Below 26,000 psi, the cycles to failure were in excess of 1,000,000 and were unrealistic from the standpoint of time required to test the samples.

The fatigue analysis data is given in Figures 17, 18, and 19. Extreme amounts of variation in results occurred with specimens from the same weldment or with similar contamination treatment. Even with the high degree of variability, definite positive trends were evident when log averages of the fatigue specimens were compared. The great amount of variability does limit the extent to which quantitative values for this physical property can be defined. Graphic plots of the fatigue test data are shown in Figures 60, 61, 62, and 63 and are summarized as follows:

1) The plot of individual gas effects, Figure 60, was of special interest for comparison with the tensile results, Figure 47. For example, at 100 ppm, tensile values decreased for all contamination conditions, while it was observed that the average fatigue life increased for samples. At the 250-ppm level, tensile values increased and the fatigue values decreased. Above 250 ppm, decreases in tensile strength are generally observed, while fatigue life increased with nitrogen and oxygen at 500 ppm and decreased with water vapor and hydrogen at 500 ppm. This observation is significant in that both test methods complemented the other in identifying the mechanical property change.

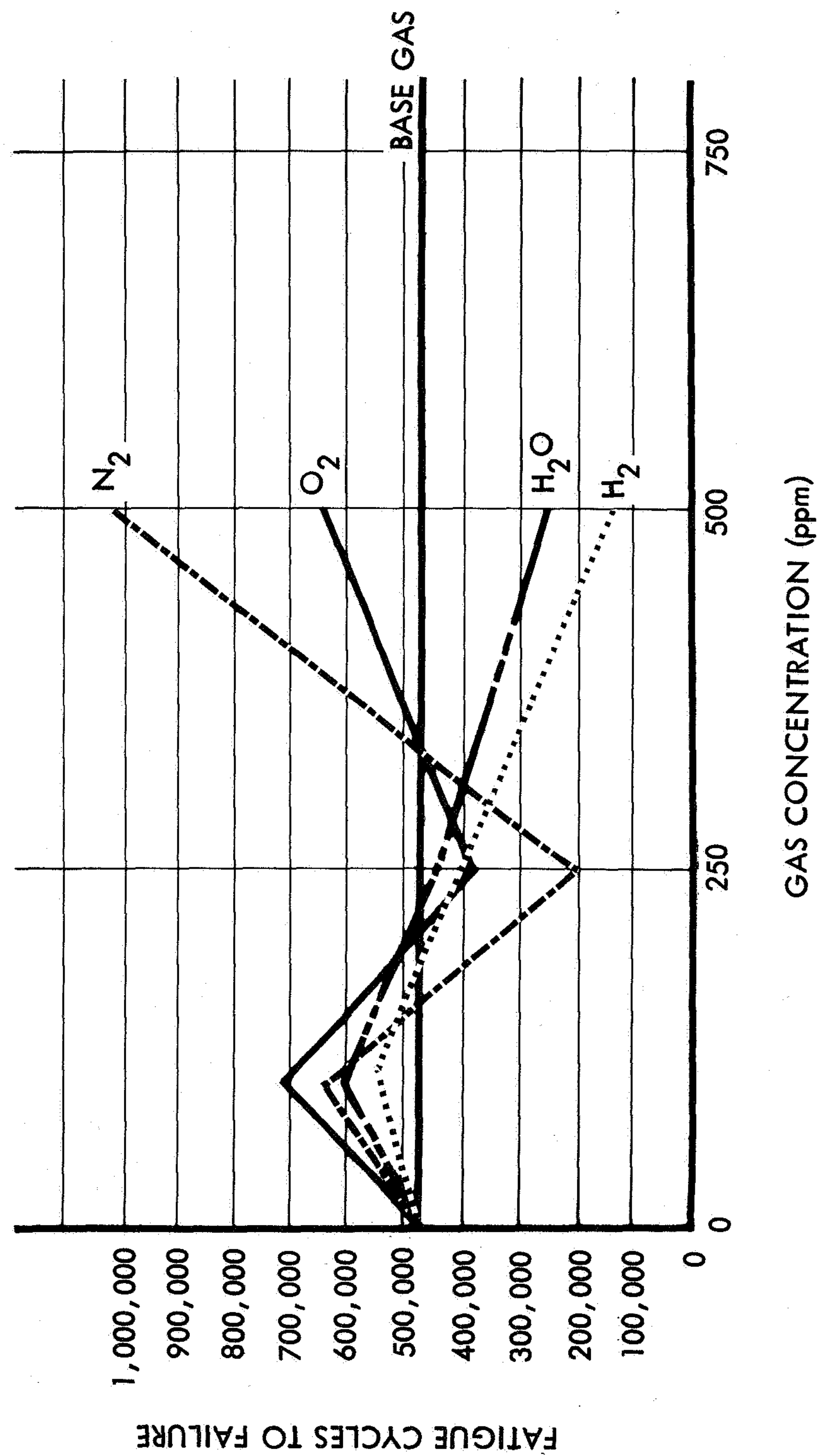

Figure 60: EFFECT OF INDIVIDUAL GASES ON FATIGUE LIFE (ALL OTHERS AT 5 PPM)

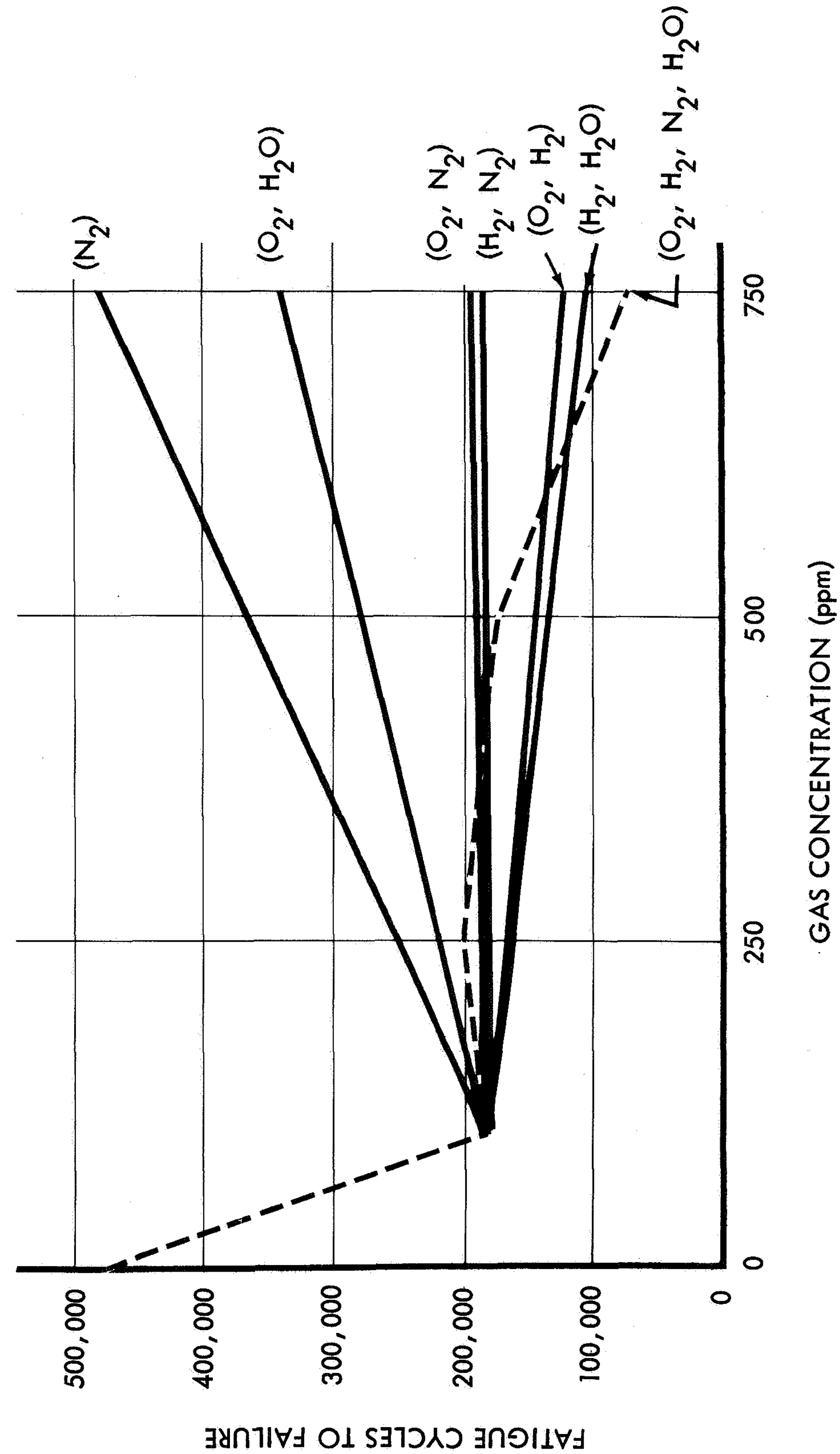

Figure 61: EFFECT OF GAS CONCENTRATION ON FATIGUE LIFE (ALL OTHERS AT 100 PPM)

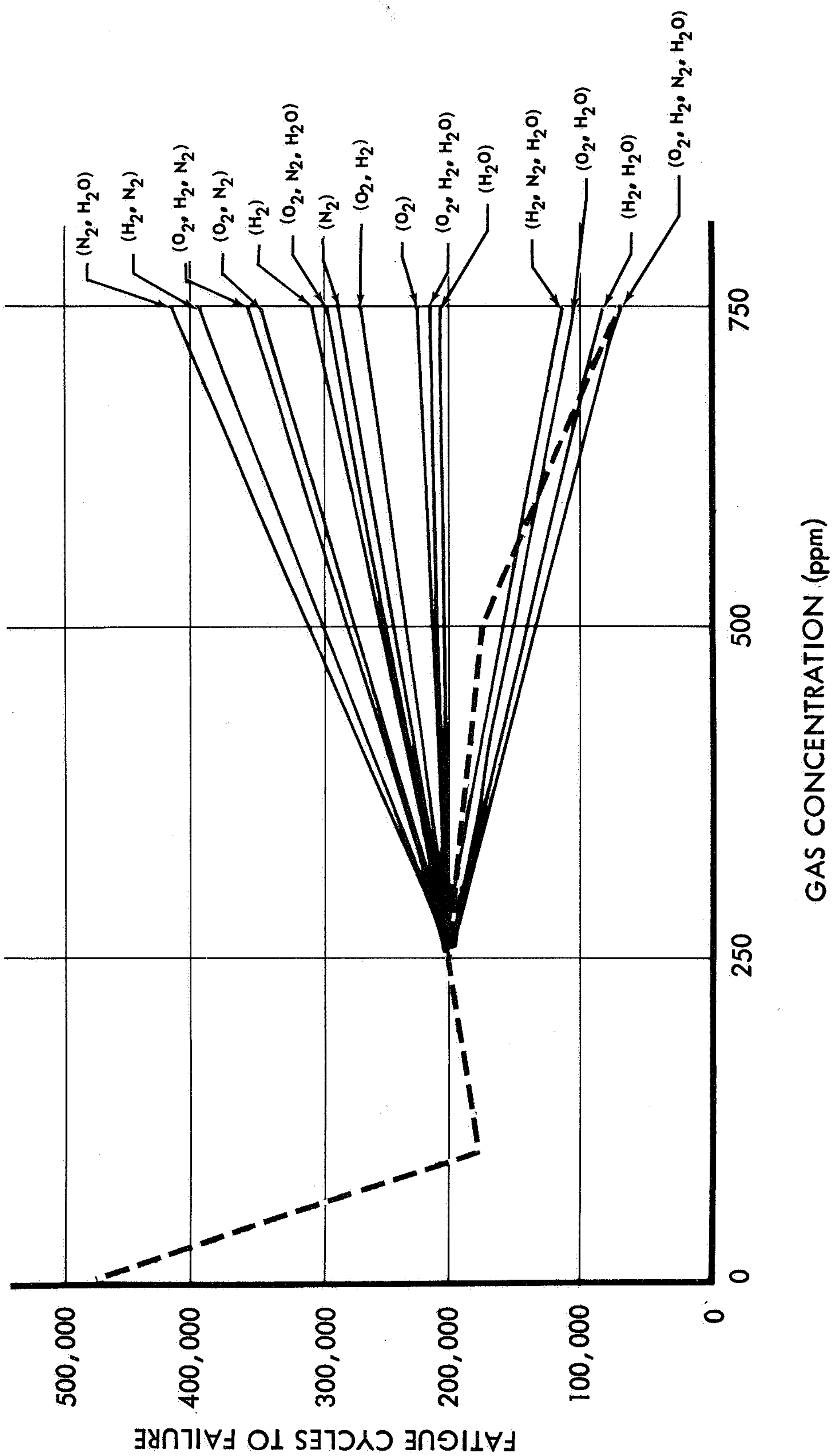

Figure 62: EFFECT OF GAS CONCENTRATION ON FATIGUE LIFE (ALL OTHERS AT 250 PPM)

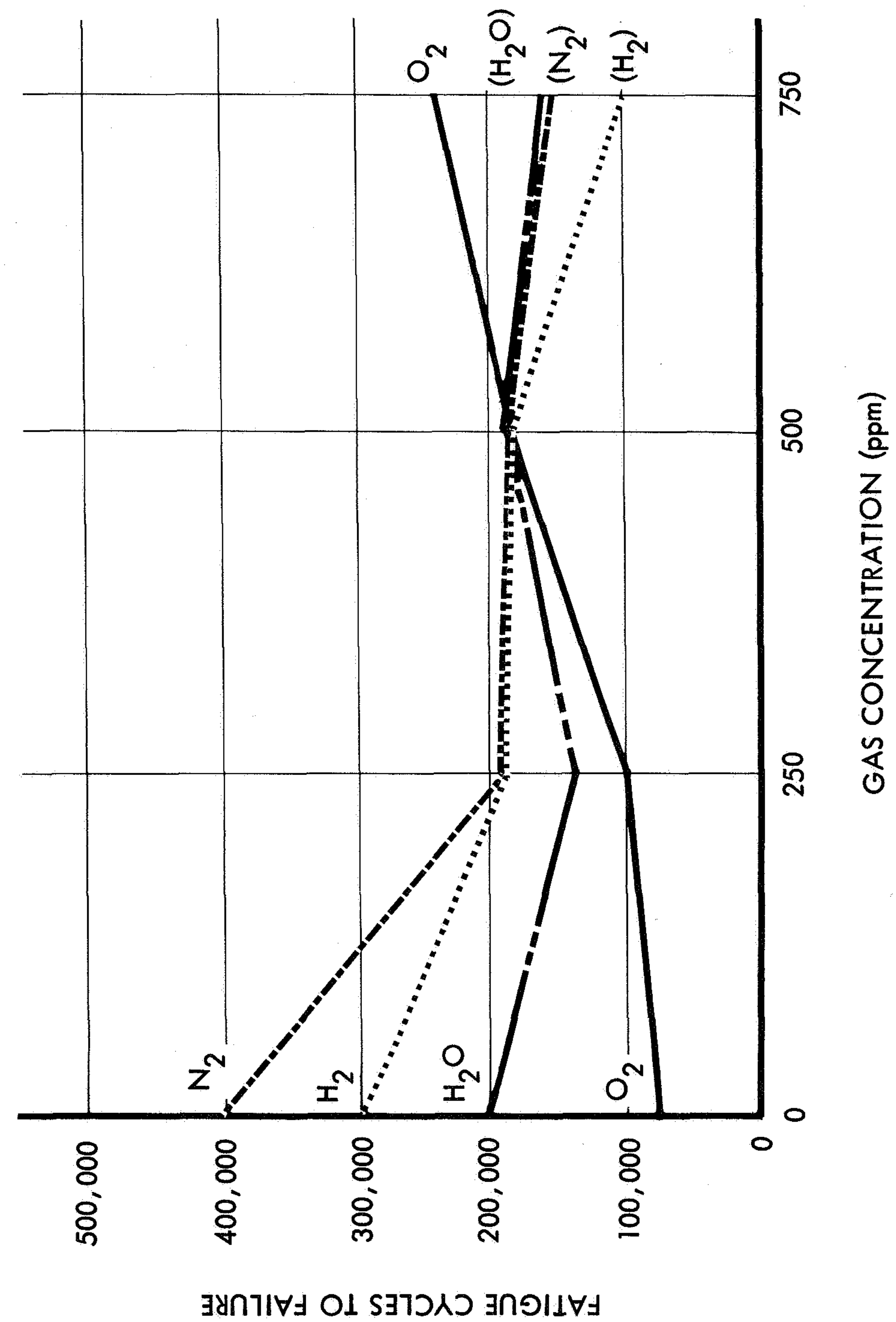

Figure 63: EFFECT OF GAS CONCENTRATION ON FATIGUE LIFE (ALL OTHERS AT 500 PPM)

2) Figure 61 shows the results of the factorial analysis varying contaminants to 750 ppm, with the level of the other gases at 100 ppm. Fatigue life with all contaminants at 100 ppm was significantly reduced. At this level of contamination, 750 ppm nitrogen addition increased fatigue life to near the base gas level. Oxygen and water vapor showed an increase. However, the cycles to failure were still significantly below the base gas level.

3) Figure 60 shows the interactions observed with all other contaminants held at 250 ppm. At this level, nitrogen in combinations is predominantly occurring, when increases in cycles to failure are observed. Hydrogen and water vapor decrease predominantly.

4) Figure 61 shows the effects of varying contaminants with all others held at the 500-ppm level. In this case, nitrogen and hydrogen addition decreases fatigue life. Water vapor had very little effect and oxygen showed a general increase. It should be emphasized that fatigue life is reduced with increase in shielding gas contamination and this reduction becomes quite significant with concentrations above 500 ppm total contamination.

ADDITIONAL STUDIES INCLUDED IN THE PROGRAM

Two exploratory surveys were included in the program as an addition to the original scope of work. These investigations were performed to further identify the contamination problem and possible sources of weld porosity. Following is a brief discussion of the problem and results of the tests performed.

HELIUM FLOW EFFECTS

The determination of the effect of helium flow rate variation on weld quality is obviously quite important to establish that weld property changes are being caused by the contaminant additions. To perform this evaluation, a test panel was prepared having the same basic configuration of panels used in the program. The panel was marked at three points along the surface to divide it into four separate sections. Welding was initiated with a flow rate of helium of 80CFH and decreased to 60, 40, and 20CFH at each of the marks. Flow was terminated 2 inches before the end of the weld for comparison with the no-flow condition. The results of this test showed that the weld bead configuration and appearance remained uniform with no visual changes occurring until the flow was terminated. The residual chamber contaminants in the atmosphere control chamber entered the arc area when flow was stopped, causing increased undercut and penetration. Radiographic analysis showed no change for the different flow conditions. It was concluded from the test that:

1) Large variations in helium flow rate have insignificant effects on weldment quality or weld bead configuration while welding in a confined area without atmospheric disturbances;

2) Contamination effects were not influenced by small changes in flow of the helium shielding gas;

3) Flow rates for production shielding can be determined by the rate necessary to maintain contamination within an acceptable limit.

CONTAMINATION IN THE BACKUP BAR

Throughout the program, contamination concentration in the backup bar was maintained at the same level as the shielding gas. It is considered important to determine the amount of contribution the backup gas makes to a specific weld quality change. This information is also important from a production standpoint because weldments are often prepared without shielding the root side of the weld. This presents the problem of contamination effects on weldment quality by influx through the weld joint. The contamination introduced along the backup included: (1) air; (2) 2-percent hydrogen; (3) 100 ppm H_2O in helium; and (4) 1000 ppm H_2O in helium. The test data is shown in Figure 64. Figure 65 shows the metallographic photographs. The results compared to base gas samples are summarized as follows:

1) Porosity levels did not increase even at 2-percent hydrogen in the backup;

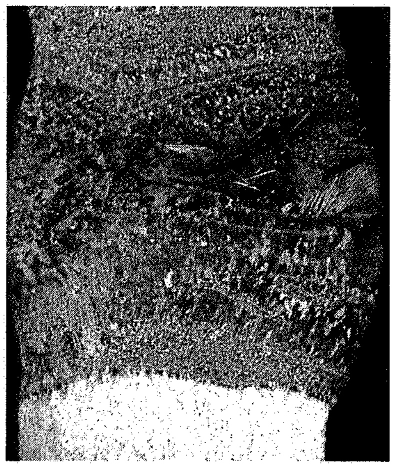

11,500 PPM H_2

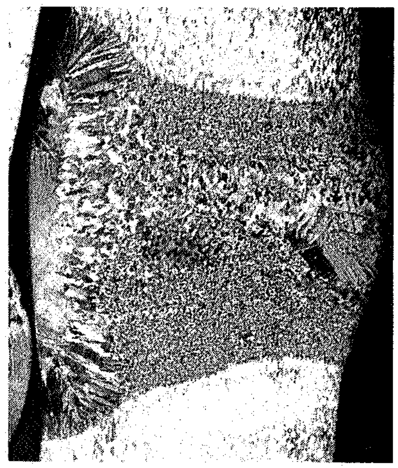

100 PPM H_2O IN He

100% AIR

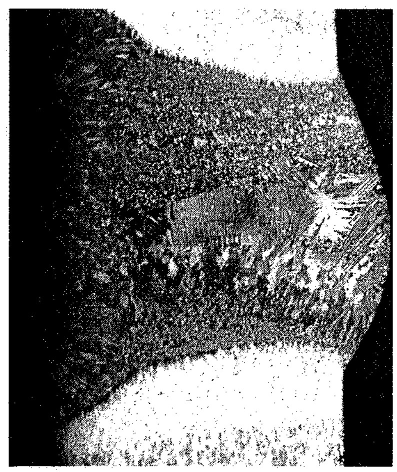

1000 PPM H_2O IN AIR

Figure 64: CONTAMINATION IN BACKUP ONLY (ETCHED)

SAMPLE NO.	TOP			CENTER			BOTTOM			D/ INCH	METAL. POROSITY	BEAD	DENSITY BASE	g/IN
511	1/34	0	1/34	6/34	2/34	1/34	13/34	8/34	4/34	1	NONE	2.83798	2.83614	3.71782
512	7/34	2/34	0	6/34	3/34	0	0	0	0	18/34	NONE	2.83810	2.85701	3.99157
1311	0	0	0	0	0	0	0	0	0	0	NONE	2.84197	2.83985	4.16009
1412	0	0	0	0	0	0	0	0	0	1/34	NONE	2.84274	2.83955	4.28732

POROSITY DATA

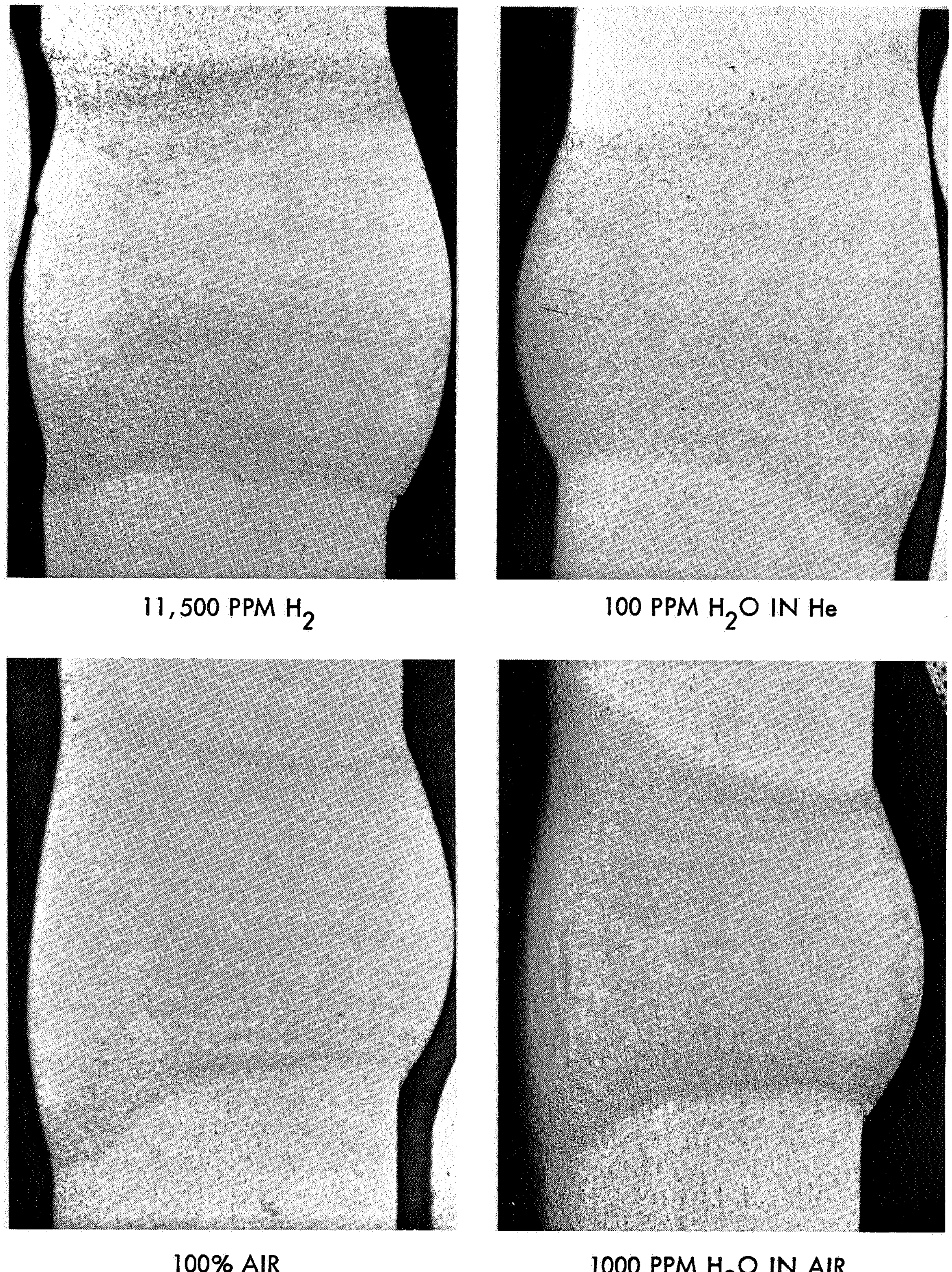

Figure 65: CONTAMINATION IN BACKUP ONLY (POLISHED)

2) The undercut was slightly increased for all contamination conditions;

3) The surface appearance with 2-percent hydrogen added, showed discoloration equal to panels having 500 ppm or more contamination. No perceptible difference was noted between surface appearance of base gas samples and the air and helium moisture conditions in the backup.

It was concluded relative to test conditions used in this program that:

1) The contribution of contaminants in the backup to changes in weldment quality is relatively insignificant;

2) Contaminants entering the arc zone are the major factor in a quality change;

3) In general, production welding would not require shielding along the root of the weld.

CONCLUSIONS

DEFINITION OF CONTROL LIMITS

Weld shielding-gas contamination is directly related to the weld quality requirements of a particular production part. Once the requirements are defined, the data accumulated in the study can be used to establish the control limits. As a potential guide for generating control parameters, some of the significant contamination effects have been combined in chart form (Figure 66). The concentration points, relative to a contamination effect, indicate where occurrence of a weld quality change is initially observed. In using this chart, shielding gas flow rate must be considered in setting weld contamination limits, because changes in flow at a given contamination level vary the quantity of contamination introduced to the welding arc per unit length.

SOURCE OF CONTAMINATION

The determination of the quantitative effects of gases on weldment quality provides an insight into the sources of contamination. High-quality weldments would generally be expected with the present shielding gas purity level if commercially purchased gas were the only consideration. However, contamination originates from many sources (such as residual impurities in the shielding gas, dirty or old connecting line from the cylinder to the torch, atmosphere influx, airborne particles, oil, water or atmosphere leaks, and surface contamination), and the combination of these determines the absolute level of the impurities introduced to weldment. As demonstrated in the program, 250 ppm of any of the contaminants studied was necessary before significant quality changes were observed. Should a 250-ppm limit be required for a production process, exceptionally tight control would be necessary on the various sources of contamination. To illustrate, Figure 67 shows a plot relating grams of surface hydrocarbon to level of hydrogen generated. Although this curve is only an estimate and will vary depending on the type of hydrocarbon, it does serve to illustrate the amounts that may be tolerated. As shown, less than one milligram per inch would be necessary to continuously generate 250-ppm hydrogen in the shielding envelope. Also shown is the estimated level of hydrogen generated by welding through a single fingerprint. The results would be 750-ppm hydrogen increase in the area contaminated and a significant increase in porosity. These estimates have been based on the assumption that hydrocarbons on the surface of the weld joint would have the same effect as an equivalent amount of hydrogen being introduced as a contaminant in the shielding gas. However, hydrocarbons on the surface are expected to be more detrimental because they enter directly into the arc area without dilution, while only a portion of the shielding gas comes in contact with the molten puddle, permitting adsorption into the weld metal.

Water vapor or hydrocarbons from atmosphere influx appear to be an unlikely major source of hydrogen contamination. To illustrate this, Figure 68 shows

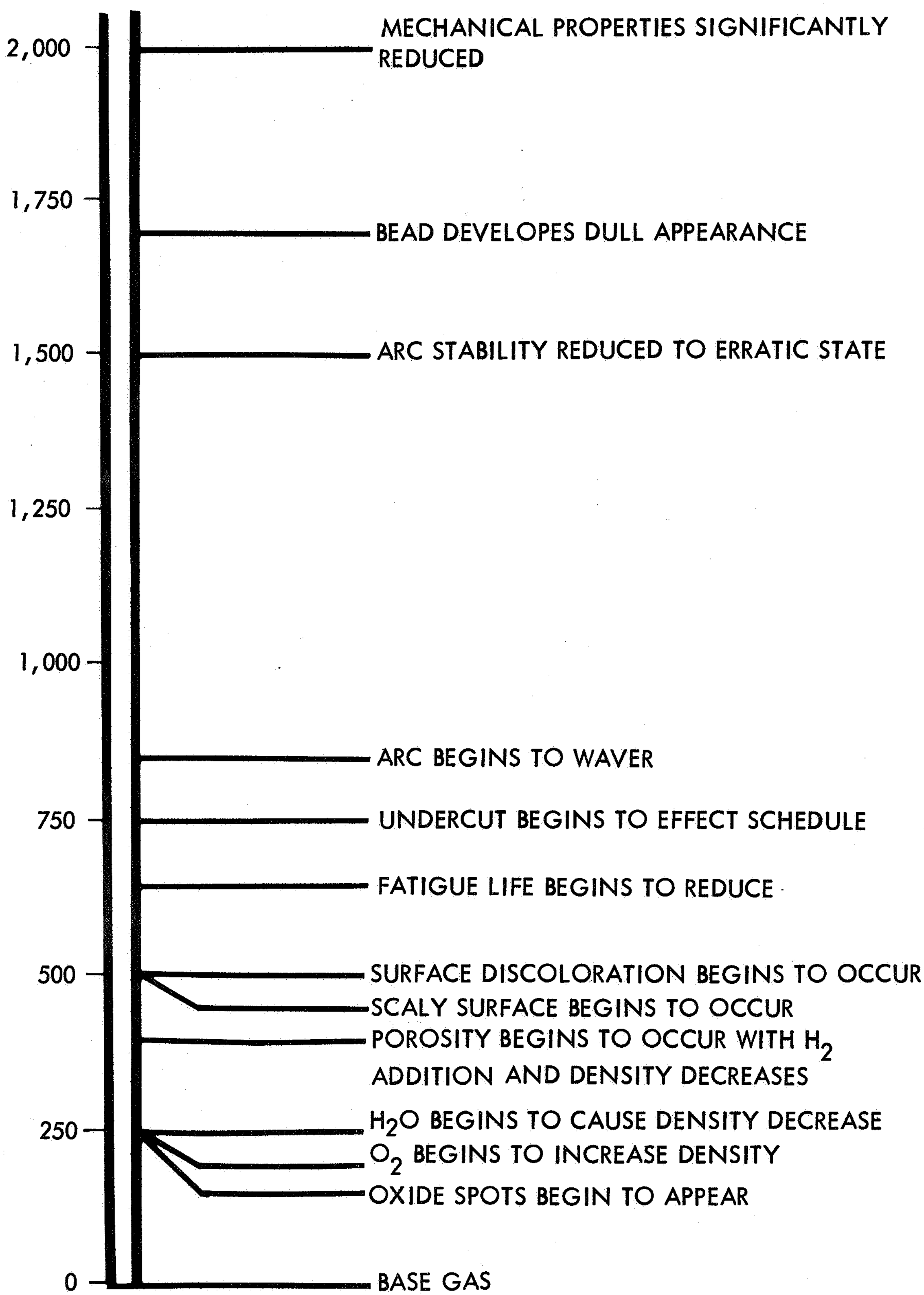

Figure 66: CONCENTRATION LEVELS WHERE SIGNIFICANT CHANGES OCCUR

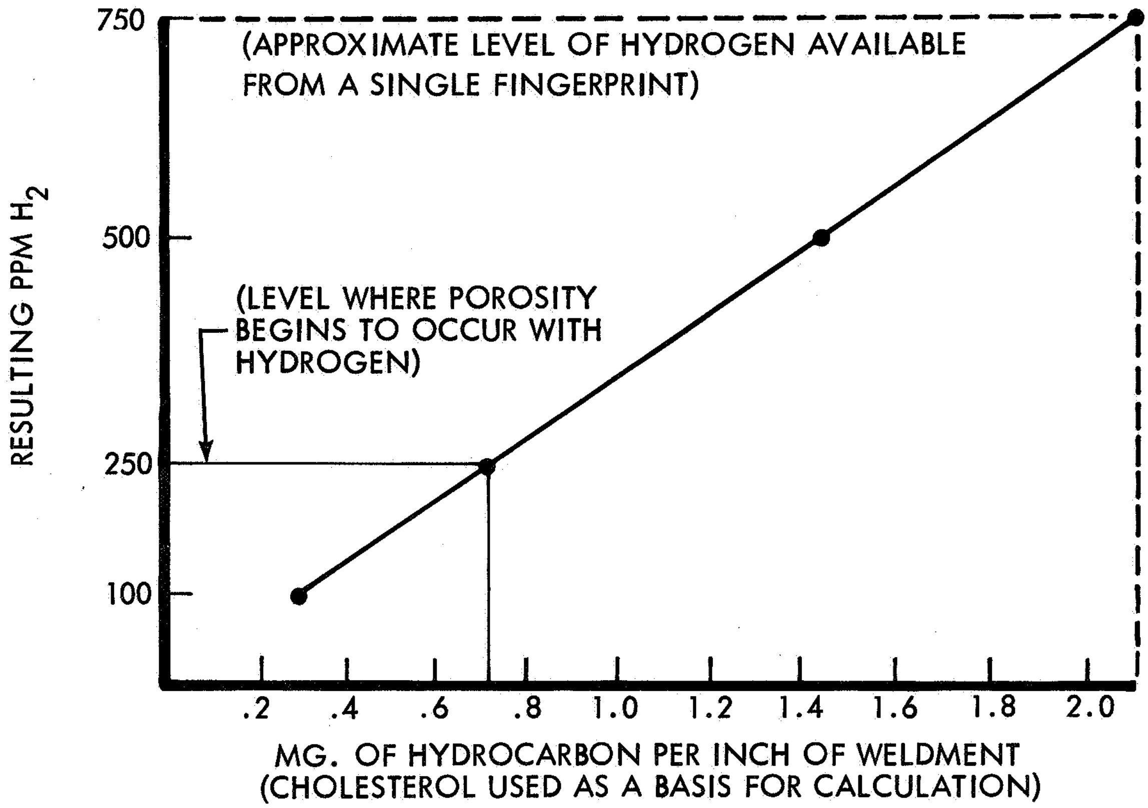

Figure 67: CALCULATED VOLUME OF HYDROGEN AVAILABLE TO WELDMENT FROM HYDROCARBON CONTAMINATION

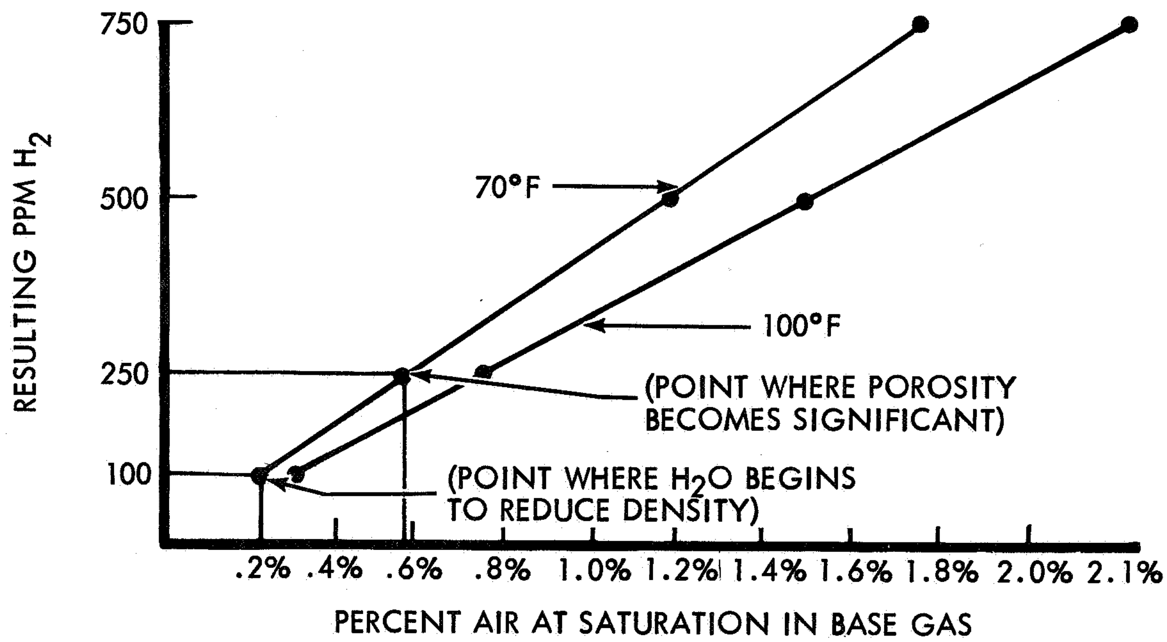

Figure 68: VOLUME OF WATER AVAILABLE TO WELDMENT FROM SATURATED AIR CONTAMINATION

the amount of atmosphere influx necessary to provide a continuous level of 250-ppm water vapor into the shielding envelope.

Extension of the above comparison can be made for many different situations to further define the contamination problem. Therefore, the results of this program will provide visibility on the sources of contamination, which in turn places emphasis on the more important areas requiring control.

INDIVIDUAL AND MIXED GAS EFFECTS

This study shows that the optimum contamination condition for highest weldment quality would be to maintain impurities in the arc below the levels achieved with a 250-ppm addition to shielding gas. A definition of the actual production contamination levels would establish the feasibility of maintaining such a low maximum limit.

In the case of porosity, addition of a contaminant, such as oxygen, could improve weldment quality under certain conditions. It should be emphasized that improved characteristics could be obtained only in isolated circumstances and that the quality would generally be lower than the optimum low-contamination condition.

In the case of undercut, due to weld-bead sag, the addition of hydrogen decreases the tendency for formation of this condition. Undercut is essentially eliminated at 250-ppm hydrogen in the shielding gas without any perceptible change in mechanical properties or porosity levels. The necessity to conduct a second pass weld, which causes a significant decrease in weld strength, might feasibly be eliminated by hydrogen addition if environmental conditions could be sufficiently controlled. It is highly questionable at this time whether the high degree of control necessary for hydrogen addition could be accomplished in a production application.

As previously discussed, the program will be of significant value in arriving at shielding gas control levels required for various production situations. In Saturn V welding it would be desirable to establish the optimum control limit below 250 ppm. However, when welding under field conditions, where contamination cannot be carefully controlled, additions of specific contaminants might feasibly be used to improve general quality. The data accumulated would be of value in identifying the particular addition and control limits necessary to improve a weld characteristic.

STATISTICAL TREATMENT OF DATA

The statistical evaluation was a key factor for the successful correlation and definition of quantitative contamination effects on weldment quality. Mathematical relationships were established for calculation of a specific quality effect when contamination levels are known. The mathematical formula is limited in that the equation does not provide a universal fit for all points within the ranges studied. More effort is necessary to improve the mathematical expressions.

As expected, the statistical treatment of the radiographic and density data yielded the best correlation. The tests were extremely sensitive to the small changes in weldment defects caused by the gas contamination. The mechanical tests were not expected to differentiate between small changes in defects, but did define significant variations in the fatigue and tensile properties due to contamination.

METHODS OF EVALUATION

All of the methods used to evaluate the weld quality provided some useful definition of the weldment characteristics. The radiographic and density analyses proved most sensitive to determination of porosity change, while the metallograpic analysis provided a visual indication of the porosity levels. The fatigue analysis had a great deal of variability between specimens of the same general quality, which indicates that future evaluation of fatigue life should be based on more samples than were used for this study. The tensile analysis did not show any appreciable change until large amounts of porosity occurred. However, a good definition of mechanical properties related to porosity has been made in this study, and future efforts would not require these tests unless a better fatigue life correlation is required.

REVIEW OF PROGRAM OBJECTIVES

The basic objective, which was to quantitatively establish the relationship between contamination in the shielding gas envelope and porosity in 2219-T87 weldments, has been achieved. The mathematical equation describing this relationship is shown on Page 29 of this report. In view of the complexity of the welding process and the many variables that could effect weld quality, excellent and repeatable results were obtained regarding effects of shielding gas contamination. The accumulated data provides a better insight into the contamination problem, and it is felt that the program results can be an important factor in defining the corrective action necessary to resolve the problem of porosity in weldments.

RECOMMENDATION FOR CONTINUED INVESTIGATION

This study of shielding gas contamination effects on 2219-T87 aluminum has emphasized the need to control the levels of various gases within the shielding gas envelope. However, there are a number of weld schedule conditions, commonly encountered in the production process, lacking sufficient definition for general shielding gas control. These areas are summarized below and are recommended for continued study.

CONTAMINATION EFFECTS AT VARIOUS VOLTAGES AND AMPERAGE LEVELS

During welding it has been observed that small variations in the voltage and/or amperage at a specific contamination level would markedly change the weld characteristic (especially surface condition). In some cases it was noted that a detrimental surface condition could be completely eliminated by changes of the voltage and/or amperage. In two instances (see Figure 11, sample pairs (1002 and 1103) and (1004 and 1303)) the surface condition was markedly improved while the porosity level increased ten-fold over the weldment produced with the initial weld setting.

In production welding, it is expected that contamination influx could change surface appearance sufficiently to require a weld schedule compensation to maintain a desired weld bead characteristic. Frequent schedule changes also occur in production due to the large variety of material configurations and joint preparations. Whatever the cause for deviation in schedule, it would be desirable to establish or predict weldment quality, at a given contamination level, resulting from the new set of weld parameters. Because there are positive indications from this study that the corrective action could improve or degrade the weld properties, a study program is necessary to evaluate the weld quality in terms of contamination, with variations in voltage-amperage, travel speed, and other weld parameters. The program would result in definition of the contamination problem for different weld schedule conditions providing increased control flexibility associated with actual production situations. Specifically, the study would provide information to: (1) establish the feasibility of correcting for effects of contamination by weld schedule change; (2) determine the contamination limits for various weld schedule conditions; and (3) establish the contamination control criteria for production fabrication conditions.

SURFACE CONTAMINATION

A recent request for proposal by NASA defined the need to conduct a study of surface contamination as related to weld quality. This program has emphasized the importance of such a study in that, surface and organic matter plus airborne particles appear to be a probable source of high hydrogen concentrations causing high porosity levels experienced in production. The investigation would result in definition of surface contamination control limits, a significant step in ultimate production control leading to increased weldment reliability.

CONTAMINATION EFFECTS WHEN WELDING WITH HELIUM AND ARGON MIXTURES

Because significant gas mixture relationships are involved in achieving a specific weldment quality, the introduction of still another gas (such as argon) is also expected to influence the weldment properties. A preliminary study at Boeing indicated that argon would in fact play an important role in affecting a specific welding characteristic at a given contamination level. In the preliminary investigation it was found that high quality weldments (equivalent to the best welds made in this study) could be produced using mixtures of helium and argon up to 50 percent. This was accomplished by varying the weld schedule, basically increasing amperage, and lowering voltage as the argon concentration was increased. However, it was also found that contamination levels (approximately 100 ppm), which could be tolerated using the helium shielding, would create extreme undercut and arc interruption resulting in completely unacceptable weldments. It was concluded that the mixture increased the sensitivity to contamination and that the results given in this report would not apply when using different shielding mediums. Therefore, it would be beneficial to conduct a study to establish the contamination control limits using mixtures of helium and argon. The result of such a program would be to obtain additional information necessary for production contamination control using a He/Ar shielding mixture.

ADDITIONAL DEVELOPMENTS

In addition to the extension of the contamination effects studies, this investigation has emphasized the need to improve production control of contamination, particularly hydrogen and hydrogen-bearing constitutents, to maintain weldment porosity within acceptable limits. Essentially, the purity of the helium shielding gas and the cleaning procedures used in this program were adequate to effect high-quality weldments; however, it is important to note that an inert gas control chamber is not the normal environment for the majority of the production fabrication processes. Such factors as atmosphere influx into the shielding envelope, impurities in the shield gas, and part contamination following cleaning will play an important role in production weld quality. Ultimately, it would be desirable to measure the various levels of contamination just prior to welding to provide a means of corrective action before an unexceptable weld is made. To accomplish this objective, it is necessary to develop instrumentation for measurement of contaminants in the shielding gas envelope and on the part surface.

Developmental programs have been conducted at Boeing that have established the feasibility of an in-process shielding gas contamination control system, and laboratory models of monitors capable of being integrated into production process have been developed and successfully demonstrated.

It would be very desirable at this point to conduct a program for the purpose of developing in-process production control instrumentation for ensuring that contamination is within acceptable limits. A realistic approach to this program would be to construct a single control system capable of preweld and in-process control by: (1) miniaturization and adaptation of state-of-the-art measurement tools; and (2) development of new measurement instrumentation where required. This development would result in improved weldment reliability and maximum utilization of accumulated contamination data.

ADDITIONAL ANALYSIS OF DATA

Considerably more information can be obtained by further analysis and reduction of data from this study. The statistical evaluation of: (1) size and distribution of porosity; and (2) comparison of the different analytical methods are examples of work yet to be performed. A continuation study would therefore be valuable in converting the information into the most useful form for the production application.